UNIVERSITÀ DEGLI STUDI DI TRIESTE

XXVIII CICLO DEL DOTTORATO DI RICERCA IN

BIOMEDICINA MOLECOLARE

DISSECTION OF THE ROLE OF CALPAIN IN THE REGULATION OF AUTOPHAGY

Settore scientifico-disciplinare: **BIO11**

DOTTORANDA
ELENA MARCASSA

COORDINATORE
PROF. GUIDALBERTO MANFIOLETTI

SUPERVISORE DI TESI
PROF. CLAUDIO SCHNEIDER

COSUPERVISORE
DR. FRANCESCA DEMARCHI

ANNO ACCADEMICO 2014 / 2015

RIASSUNTO:

Le calpaine appartengono alla famiglia delle proteasi calcio-dipendenti, coinvolte in diversi processi cellulari, tra i quali la regolazione delle dinamiche di adesione cellula-cellula, il processo di proliferazione e migrazione cellulare, e infine il controllo del processo autofagico e apoptotico.

Nelle cellule sono espresse diverse isoforme di calpaina, ma quelle più studiate e conosciute sono le ubiquitarie micro e milli-calpaina (CAPN1 e CAPN2 rispettivamente). Per la loro attivazione, entrambe hanno bisogno della subunità regolativa chiamata *calpain small subunit 1* (CAPNS1). Nel nostro laboratorio è stato dimostrato che le calpaine ubiquitarie, sono indispensabili per il normale progresso del processo autofagico.

In questo studio Bif-1 è stato identificato come substrato della micro-calpaina, e come possibile fattore di collegamento tra l'attività proteolitica di queste proteine e l'autofagia.

All'inizio del progetto sono state studiate le dinamiche di formazione degli autofagosomi in cellule U2OS, dove è stato silenziato stabilmente il gene che codifica per la subunità regolativa, CAPNS1. Come fattore di stress si è scelto di utilizzare la tapsigargina, un inibitore dell'ATPasi del reticolo sarco-endoplasmatico, che in primo luogo, causando stress del reticolo, induce l'attivazione del processo autofagico. In secondo luogo, il blocco di questa ATPasi provoca un aumento della concentrazione di Ca^{2+} citoplasmatico, in grado di promuovere l'attivazione delle calpaine.

Risultati preliminari hanno dimostrato che in cellule senza calpaina è presente un livello maggiore della proteina LC3 lipidata (LC3-II) rispetto alle cellule di controllo. Risultati simili sono stati osservati mediante microscopia confocale, utilizzando il costrutto pH-sensibile GFP-RFP-LC3. Questo marker permette di decorare tutte le strutture vescicolari che caratterizzano il processo autofagico, dal fagoforo all'autolisosoma. Di fatto, in cellule senza calpaina è stato riscontrato un aumento di strutture positive per LC3-II che non rappresentano autolisosomi ma strutture precedenti, suggerendo una connessione tra l'attività regolativa di calpaina e le prime fasi di formazione dell'autofagosoma.

In seguito è stata valutata la distribuzione dell'apparato del Golgi, che rappresenta una delle risorse lipidiche necessarie per la formazione e la maturazione

dell'autofagosoma. Nelle cellule in cui è stata silenziata calpaina la localizzazione del Golgi appare completamente differente dalle cellule di controllo. Di fatto, in quest'ultime, le cisterne circondano il nucleo, mentre nelle cellule senza calpaina, la struttura è raggruppata a un lato del nucleo. L'assenza di calpaina comporta quindi una differente localizzazione del Golgi, che potrebbe in qualche modo provocare alterazioni nel processo di formazione e maturazione degli autofagosomi.

ATG9 è l'unica proteina trans-membrana che regola le fasi iniziali del processo autofagico e che è in parte localizzata nel trans-Golgi network.

Per studiare il comportamento di ATG9 in relazione ad LC3 e ai suoi interattori, Vps34 e il recettore per la transferrina (TfR), sono state usate tecniche di microscopia confocale, e saggi d'interazione.

Nelle cellule silenziate per CAPNS1 si nota chiaramente una differenza nelle dinamiche di movimento delle strutture positive per ATG9. Nelle cellule di controllo, vescicole positive per ATG9 si muovono distintamente verso vescicole positive per LC3. Nelle cellule senza calpaina invece, dopo induzione di autofagia, si è evidenziata una situazione più stabile, quasi di blocco del traffico di ATG9.

Una delle proteine chiavi per la regolazione delle dinamiche degli organelli, tra cui il Golgi, è Bif-1. Questa proteina è coinvolta, grazie ai suoi domini strutturali, nel processo di fissione del Golgi; inoltre interagisce indirettamente con Beclin1, componente importante del complesso PI3K di classe III, la cui attività è essenziale nella fase di nucleazione dell'autofagosoma.

Inizialmente abbiamo verificato se la presenza o meno di calpaina potesse in qualche modo interferire con le normali attività di Bif-1. Mediante immunofluorescenza abbiamo dimostrato che nelle cellule di controllo, una volta indotta autofagia, la proteina Bif-1 co-localizza con ATG9, lontano dalle membrane del Golgi. Al contrario, nelle cellule senza calpaina, Bif-1 e ATG9 rimangono sul Golgi. Questo dato rivela un'attività diretta di calpaina su questa fase di trasporto, guidata da Bif-1, di vescicole positive per ATG9 dal Golgi verso il sito dove si forma l'autofagosoma.

Grazie all'utilizzo di un software bio-informatico, abbiamo identificato nella sequenza amminoacidica di Bif-1, due ipotetici siti di taglio di calpaina. Il primo situato subito dopo l'alfa-elica presente al N-terminale della proteina, che è responsabile del legame di Bif-1 alle membrane. Il secondo sito di taglio si trova invece alla fine del dominio N-BAR. Saggi di taglio *in vitro* hanno rivelato che il taglio avviene in prossimità del N-terminale di Bif-1. Nuove analisi, come

spettrometria di massa e studi funzionali, saranno in seguito effettuate, con lo scopo finale di identificare esattamente il sito di taglio e l'attività della forma processata di Bif-1.

In conclusione abbiamo identificato Bif-1 come nuovo substrato di calpaina, coinvolto nella regolazione del trasporto di vescicole dall'apparato del Golgi verso il sito di formazione degli autofagosomi. Questi risultati, non solo aggiungono nuove informazioni a quanto fino ad ora si conosce sull'attività delle calpaine, ma rappresenta anche un ottimo punto di partenza per lo sviluppo di strategie terapeutiche basate sulla regolazione del processo autofagico.

UNIVERSITA' DEGLI STUDI DI TRIESTE

Graduate School in MOLECULAR BIOMEDICINE

PhD Thesis

Dissection of the role of calpain in the regulation of autophagy

Student: **ELENA MARCASSA**

Supervisor: **PROF. CLAUDIO SCHNEIDER**

Co-supervisor: **DR. FRANCESCA DEMARCHI**

Academic year 2014 / 2015

TABLE OF CONTENTS:

LIST OF ABBREVIATIONS:

AMBRA: Autophagy/Beclin-1 Regulator 1

AMP: adenosine monophosphate

AMPK: AMP-activating protein kinase

APAF1: apoptotic protease activating factor 1

AR: androgen receptor

ATF6: activating transcription factor 6

ATG: autophagy-related gene

ATP: adenosine triphosphate

BAX: Bcl-2 associated x protein

BCL-2: B-cell lymphoma 2

BIF-1: Bax interacting factor 1

CaMKKβ: Calcium-activated calmodulin-dependent kinase kinase-β

CAPN1: calpain 1 or micro-calpain

CAPN2: calpain 2 or milli-calpain

CAPNS1: calpain small subunit 1

CAST: calpastatin

CCCP: carbonyl cyanide m-chlorophenyl hydrazone

COP-I: coat protein 1

CDK5: cyclin-dependent kinase 5

DFPC1: double FYVE-containing protein 1

ER: endoplasmic reticulum

ERGIC: ER-Golgi intermediate compartment

FAK: focal adhesion kinase

FCCP: carbonyl cyanide-4-(trifluoromethoxy)phenylhydrazone

FIP200: FAK family kinase-interacting protein of 200 kDa

FOXO: Forkhead box protein O

GAS2: grow arrest-specific 2

GAPR1: Golgi-associated plant pathogenesis-related protein 1

GLUT4: insulin-responsive glucose transporter 4

HER-2: human epidermal growth factor receptor 2

HIF1: hypoxia inducible factor 1

HSP70: heat shock cognate protein of 70 kDa

IBD: inflammatory bowel disease

IKBα: nuclear factor of kappa light polypeptide gene enhancer in B-cells inhibitor, alpha

IRE1: inositol-requiring enzyme 1

IRS 1/2: insulin receptor substrate 1/2

JNK: c-Jun NH(2)-terminal kinase

LAMP1/2: lysosome-associated membrane protein 1/2

LC3: microtubule-associated protein 1a/1b light chain 3

LGMD2A: limb-girdle muscular dystrophy type 2A

LSDs: lysosomal storage disorders

MAPK: Mitogen-activated protein kinases

MEF: mouse embryonic fibroblast

MFN 1/2: mitofusin 1/2

MVB: multivesicular body

N-BAR: N-bin-amphiphysin-Rvs domain

NF-Kβ: nuclear factor- κB

PDB: Paget disease of bone

PDK1: phosphoinositide-dependent protein kinase-1

PE: Phosphatidyl-ethanolamine

PERK: RNA-dependent protein kinase-like ER kinase

PI3P: Phosphatidyl-inositol 3-phosphate

PINK1: PTEN-induced putative kinase 1

PI3K: Phosphatidylinositol-4,5-bisphosphate 3-kinase

PKA/B/C: protein kinase A, B, C

PP2A: protein phosphatase 2A

RAB: Ras superfamily of monomeric G proteins

RE: recycling endosome

RHEB: Ras homolog enriched in brain

ROS: reactive-oxygen species

SH3: Src-homology 3 domain

SNARE: hairpin-type-tail anchored soluble N-ethylmaleimide-sensitive factor Attachment Protein receptor

SNP: single nucleotide polymorphism

TBC1D25: tubuling folding cofactor D 25

TGN: trans-Golgi network

TOM: translocase of the outer membrane

TOR: target of rapamycin

TSC1/2: tuberous sclerosis 1/2

ULK1/2: unc-51 like autophagy activating kinase 1/2

UPR: unfolding protein response

USP1: ubiquitin-specific peptidase 1

UVRAG: UV Radiation Resistance Associated protein

VAMP: vesicle-associated membrane protein

VMP1: vacuole membrane protein 1

VPS34: vacuolar protein sorting 34

WIPI 1-4: WD-repeat protein Interacting with Phospho-Inositides 1-4

THESIS ABSTRACT

Calpains are a family of calcium dependent intracellular proteases implicated in a variety of cellular processes, from cell adhesion to cell proliferation and migration, and also autophagy. Cells express different isoforms of calpain, among which the best studied are the ubiquitous micro and milli-calpain (CAPN1 and CAPN2), that share a common regulatory subunit called calpain small subunit 1 (CAPNS1). Our lab demonstrated that ubiquitous calpains are important for the proper progression of the autophagic process; in this scenario calpain could be a promising target for the development of anti cancer treatment.

In this study we identified Bif-1 as a calpain substrate, implicated in the early stages of the autophagosome formation. Firstly, we studied autophagosomes formation kinetics in U2OS cell line stably depleted for CAPNS1. As a stressor factor we choose thapsigargin that blocks the sarco/endoplasmic reticulum Ca2+-ATPase (SERCA), causing endoplasmic reticulum stress and autophagy induction. In addition, the blocking of the pump increases the cytoplasmic levels of calcium, thus activating calpain. Cells lacking for calpain showed a higher level of lipidated LC3 as compared to control cells. Similar results were obtained with a confocal microscope, using the pH sensitive RFP-GFP-LC3 baculovirus reagent, able to stain all the structures that characterize the autophagic pathway, from the phagophore to the autolysosome. Indeed, in CAPNS1 depleted cells we saw an increase in the amount of RFP-GFP-LC3 suggesting a role of calpain in the early stages of autophagy. Then, we focused our attention on Golgi distribution, since this organelle is one of the membrane sources indispensible for the nucleation of the autophagosome. Interestingly, in CAPNS1 depleted cells the distribution of this structure is completely different from the distribution of control cells. This indication led us to hypothesize that without calpain, the Golgi membranes are not delivered properly to the site where the autophagosome starts to form. One of the proteins responsible for the fission of the Golgi network is the autophagy-related protein 9 (ATG9), the only trans-membrane protein of the process. Live cell imaging techniques and biochemical assays were applied to study the dynamics of ATG9 positive vesicles together with LC3 and with its interactors, Vps34 and Transferrin Receptor. The depletion of CAPNS1 clearly affects the behaviour of this protein, underlining again its involvement in the early stages of autophagy, and in particular in the process of delivery of Golgi membranes toward the site where phagophore forms. At this point we focused our attention on Bif-1, an

important protein that regulates membrane dynamics of organelles, such as Golgi, mitochondria and autophagosomes. We verified whether the activity of calpain on Bif-1 could play an important role in this dynamics. By immunofluorescence, we found that in U2OS control cells, overexpressing ATG9, Bif-1co-localized together with ATG9 and away from the Golgi membranes after induction of autophagy with thapsigargin; on the opposite, in CAPNS1 depleted cells, Bif-1 and Atg9 remain on the Golgi. At this point, we checked by means of a bio-informatics tool, whathever the Bif-1 aminoacid sequence contains putative calpain cleavage sites. Interestingly, two hypothetical sites were found: one after the N-terminal helix responsible for Bif-1 binding to membranes, and the other one at the end of the N-BAR domain. In-vitro cleavage assays revealed that the cleavage occurs at the very N-terminal of Bif-1. Further works, including mass spectrometry analysis and functional studies of Bif-1 mutants, are going on, in order to exactly identify the aminoacid cleaved by calpain and the activity of the Bif-1 cleaved form.

In conclusion, we identified Bif-1 as a calpain substrate, possibly implicated in the delivery of Golgi membranes towards the sites where autophagosomes start to form. These findings not only increase the nowadays knowledge about calpain implication in the progression of autophagy, but represent a starting point for the development of therapeutic strategies that seek in the regulation of autophagy a possible treatment.

AIM OF THE PROJECT

Calpains are cysteine proteases involved in numerous physiological and pathological phenomena. They are considered as a *bio-modulator*, indeed their proteolytic activitity generate new functional proteins known to be directly or indirectly implicated in a variety of cellular processes with cancer development and progression being one of them. The most intensely studied are the ubiquitous micro and milli-calpain that share a common regulatory subunit called calpain small subunit 1. Several studies have linked different types of cancers to an altered expression of different members of the calpain system. For instance high expression of milli-calpain in basal-like or triple-negative diseases is associated with adverse breast cancer-specific survival, underling the importance of calpain in tumor growth and progression. Interestingly our group identified the role of calpain in the regulation of breast cancer stem cells proliferation, highlighting the implication of these proteins also in cellular architecture and cell fate decision. The results are contained in the following paper (enclosed at the end of this thesis):

Raimondi, M., Marcassa, E., Cataldo, F., Arnandis, T., Mendosa-Maldonado, R., Benstagno, M., Schneider, C., Demarchi, F., (2016). Calpain restrains the stem cells compartment in breast cancer. Cell Cycle; 15(1):106-16.

These observations led us to investigate in details the role of the ubiquitous micro and milli-calpain in cells survival processes, such as apoptosis and autophagy, both phenomena that closely overlap with signalling pathways regulating tumorigenesis.

Autophagy is an extremely complex network, regulated by a system of different proteins that respond to intra and extra-cellular signals. In literature, there are fews works that well demonstrated how the pleiotropic activity of this protease is linked both to a positive and a negative regulation of autophagy. Indeed, as a bio-modulator, calpain acts on different substrates, controlling in different ways the autophagic process and as a consequence tumor growth and progression. Therefore we wanted to dissect the role of the ubiquitous calpains in the regulation of macroautophagy, focusing our attention on the identification of the mechanism in which calpain is involved.

1. INTRODUCTION

1.1 THE CALPAIN SYSTEM

1.1.1 The Calpain superfamily: overview

Calpains are a well-conserved family of calcium-dependent cysteine proteases that are implicated in a variety of calcium-regulated processes such as signal transduction, cell proliferation, cell cycle progression, cell differentiation, apoptosis, and membrane fusions (Suzuki et al., 2004). Alterations in the activity of these proteins are connected to a series of diseases such as neuronal degeneration, Alzheimer, cancer, and multiple sclerosis (Zatz and Starling, 2005).

Calpains were firstly identified in 1964 as cytosolic proteases, showing calcium-dependent proteolytic activity at neutral pH (Guroff, 1964). Nowadays they are defined as *modulator proteases;* theirs activity is not dependent on a particular aminoacid sequence but they recognize bonds between domains. As a result the substrates are transformed into new functional proteins with new activities within cells (Sorimachi et al., 2011).

The name "calpain" was chosen to underline calcium dependence and the homology with the cysteine-protease papain. Indeed, calpains belong to the papain superfamily of cysteine proteases, but their similarities to papains and cysteine cathepsins are less significant than the similarities between different calpains (Sorimachi et al., 2011).

Calpain proteins are found in all eukaryotes and in few bacteria; currently there are 15 known human calpain isoform genes (Table 1.1) which are defined by the presence of a protease domain similar to that found in the two most well studied isoforms micro and milli-calpain (CAPN1 and CAPN2).

1.1.2 Proprieties and structure of calpains

Micro and milli-calpain are heterodimers consisting of a catalytic subunit (80 kDa) encoded by CAPN1 and CAPN2 genes respectively, and a common regulatory subunit (28 kDa), called calpain small subunit 1, encoded by CAPNS1 gene (Storr et al., 2011).

X-rays analysis of calpain's crystals well elucidated the topology of these proteins; thanks to these data different domains were identified within the aminoacid sequences (Blanchard et al., 1997; Hosfield et al., 1999). Micro and milli-calpain, together with their regulatory subunit, belong to the group of the conventional calpain, characterized by a well-conserved aminaocid structure. On the other hand there are unconventional calpains that share with the other members of the family, only the presence of a protease domain (DII).

The catalytic subunits of micro and milli-calpain, are formed by four domains (DI to DIV; Fig. 1.1). The DI is the N-terminal domain, characterized by a short α-helix that is autolysed at the moment of the activation of calpains by calcium. The DII possesses the conserved protease domain that represents the core of the enzyme activity. It is made by two subdomains IIa and IIb, which bind calcium ions forming the catalytic cleft. In particular the active site is forming between the Cys-105 on the IIa and His-262-Asn-286 on the IIb subdomain (Suzuki et al., 2004). The DIII has no apparent sequence homology to other proteins; it has an orderly structure similar to the C2 domain (a structural domain that is involved in membrane targeting) of the phospholipase C; for this reasons it is also called C2 like domain. This domain is also able to bind calcium ions that are responsible of the interaction with phospholipids (Tompa et al., 2001). The carboxyl-terminal DIV domain contains the five EF hands motifs (EF-hand unit consist of two helix linked by a calcium-binding loop), responsible for calcium binding. The last EF hand region cannot bind calcium but it is important for the interaction with the EF hand of the regulatory subunit allowing their dimerization.

CAPNS1 is composed only by two domains: DV and DVI. The DV, also called glycine-rich domain, is characterized by a string of glycine residues responsible for the interaction with the plasma membrane (Imajoh et al., 1986). During calpain activation most of the glycine cluster is autolysed. The carboxyl-terminal domain DVI of CAPNS1 is characterized by five EF hands motifs.
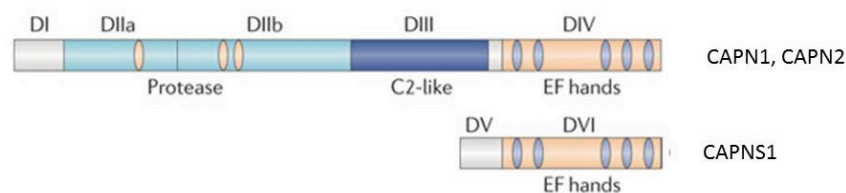

Figure 1.1: Schematic structure of μ-, milli-calpain and the regulatory subunit (CAPNS1) (Modified by Storr et al., 2011).

Micro and milli-calpains (μ-calpain and m-calpain) are 62% identical at the aminoacid level; however they differ in terms of the Ca^{2+} concentration (μM versus mM) required for their proteolytic activity in vitro. Calpain normally exists as an inactive enzyme in the cytosol where it is in direct contact with other proteins; indeed it remains structurally inactive in the absence of calcium. But when this is present, calpain translocates to membranes where ions can bind both IIa and IIb of the DII domain, causing a conformational change that allows the formation of the catalytic cleft. Autocatalytic hydrolysis of DI takes place during activation, and dissociation of the regulatory subunit from the catalytic subunit occurs as a result (Sorimachi et al., 2004). In addition to their structural features, calpains are also categorized according to their tissue and organ distribution (Table 1.1); there are ubiquitously expressed calpains and others that are expressed only in specific tissues or organs (Sorimachi et al., 2011).

Calpain Product	Gene	Other Names	Tissue Distribuition	Association with the regulatory subunit
Calpain 1	CAPN1	μ-calpain large subunit	Ubiquitous	+
Calpain 2	CAPN2	m-calpain large subunit	Ubiquitous	+
Calpain 3	CAPN3	P94, nCL-1	Skeletal Muscle	-
Calpain 5	CAPN5	hTRA-3, nCL-3	Ubiquitous	-
Calpain 6	CAPN6	CANPX	Placenta, Embryonic Muscle	-
Calpain 7	CAPN7	PalBH	Ubiquitous	-
Calpain 8	CAPN8	nCL-2	Stomach	-
Calpain 9	CAPN9	nCL-4	Digestive Tract	+
Calpain 10	CAPN10		Ubiquitous	ND
Calpain 11	CAPN11		Testis	ND
Calpain 12	CAPN12		Hair Follicle	ND
Calpain 13	CAPN13		Ubiquitous	ND
Calpain 14	CAPN14		ND	ND
Calpain 15	SOLH	SOLH	Ubiquitous	ND
CAPNS1	CAPNS1	CAPN4/Calpain Small Subunit 1	Ubiquitous	+
CAPNS2	CAPNS2	Calpain Small Subunit 2	Ubiquitous	+

Table 1.1: Human calpain family members: for each protein gene name, alternative names, distribution and possible association with the regulatory subunit were reported.

1.1.3 Calpain regulation

The mechanisms by which calpains are activated and identify their protein targets are complex and poorly understood. An intricate strategy for the regulation of calpain activity seems to be necessary because calpain is an abundant cytoplasmic protease that can cleave many intracellular signaling and structural proteins (Zatz, M., Starling, A., 2005).

Calpastatin is the ubiquitously expressed endogenous inhibitor of μ-calpain and m-calpain; it seems to be present only in vertebrate tissues. Calpastatin is released from intracellular storage aggregates into the cytosol following calcium influx to allow the interaction with calpain.

By a structural point of view it consists of an N-terminal XL domain, a L region and four repetitive inhibitory domains (I-IV) (Wendt et al., 2004). Each inhibitory domain inhibits one calpain molecule and is characterized by four subdomains (A, B, C and D). The inhibitory action of calpastatin requires calcium-induced structural changes in calpain to allow the A, B and C regions to bind. Region B blocks the active site of calpain (Hanna et al., 2008; Moldoveanu et al., 2008) (Fig. 1.2).

A single gene (CAST) encodes for calpastatin and it has multiple promoters that generate different isoforms; these promoters can be differentially regulated in a tissue-specific manner. Both, type I and type II, calpastatin contain the L domain but have different N-terminal sequences generated from tandem promoters that are associated with exons 1xa and 1xb. Type III calpastatin is the product of a promoter that is associated with the untranslated exon 1u resulting in a protein in which the XL region is absent from the L domain; type IV
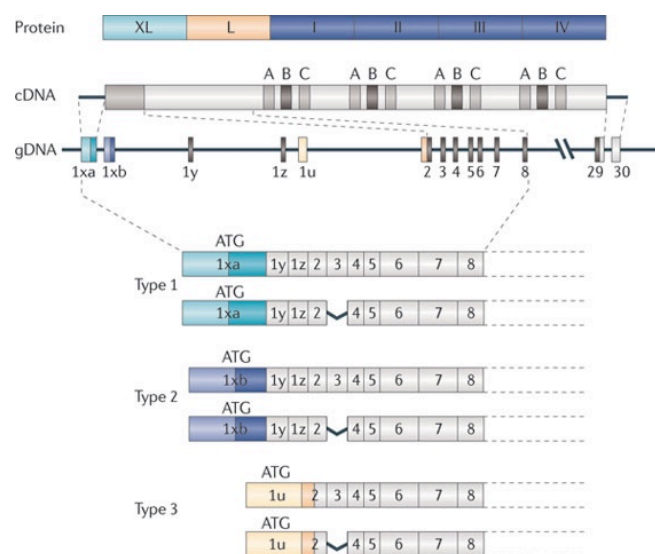

Figure 1.2: Schematic structure of Calpastatin (Storr et al., 2011)

calpastatin is a testis-specific isoform that is generated from a promoter between exons 14 and 15 and lacks the L domain and the inhibitory domain I.

The activity of calpastatin is predominantly regulated by post-translational modifications; indeed it was demonstrated that calpastatin derived from rat skeletal muscle and from rat brain is subjected to in vitro phosphorylation by protein kinase C (PKC) and protein kinase A (PKA), and this modification can modulate calpastatin specificity (Salamino et al., 1994) or inhibitory efficiency (Salamino et al., 1997). More recently, it was shown that in human neuroblastoma cells, PKA triggers calpastatin phosphorylation, and this event leads to aggregation of calpastatin, while calcium influx leads to disaggregation, through a protein phosphatase activity. This reversible phosphorylation event regulates the amount of soluble calpastatin available to bind and inhibit calpain (Averna et al., 2001).

Membrane localization of calpains is another important mechanism for the regulation of their activity; the binding to phospholipids decreases the Ca^{2+} requirement for calpain activation (Suzuki et al., 1992). Once calpain is activated, autolyzed fragments appear; this mechanism replaces the need for high Ca^{2+} levels. This cleavage eliminates respectively the first 18 and 26 aminoacids from the N-terminal of the catalytic subunits (micro and milli-calpain). It has also been proposed that the dissociation of the large subunit from the regulatory subunit is a mechanism of activation; moreover other proteins can act as co-activator. For example the acyl-CoA-binding protein has been identified as an activator of m-calpain in rat skeletal muscle (Melloni et al., 2000).

Most recently, phosphorylation has been proposed as being involved in activating μ- and m-calpain; indeed there are three sites each of phosphotyrosine, phosphoserine and phosphothreonine within calpains (Kuo, et al., 1994).

A gene product with a specific calpain inhibitory activity has been characterized at Laboratorio Nazionale CIB: the growth arrest specific gene 2 (Gas2) (Benetti et al., 2001). The expression of this gene is specifically induced during the G0 arrest phase of the cell cycle in NIH3T3 fibroblasts, (Schneider et al., 1988). Gas2 is a component of the microfilament system and co-localizes with actin fibers (Brancolini et al., 1992). Gas2 binds domain III and IV of m-calpain through its amino-terminal domain, while its carboxyl-terminal region exerts the inhibitory function. The isolated amino-terminal region has been demonstrated to act as a dominant negative form of Gas2 (Gas2DN), being able to bind, but not to inhibit, calpain activity and to rescue the effects of Gas2 on calpain function in vivo (Benetti et al., 2001).

1.1.4 Cellular functions of ubiquitous calpains

The calpain family catalyses the proteolysis of a large number of specific substrates; many of these have been identified and characterized in vivo and in vitro; nevertheless the physiological roles of the calpains remain unclear. The presence of conserved μ- and m-calpain in almost all mammalian cells, suggests that these enzymes are essential in a cellular environment, but the absence of specific inhibitors has so far prevented unambiguous proof of a particular physiological role.

To understand their activities, calpain transgenic mouse models were used. Homozygous disruption of CAPNS1 in mouse cells eliminates both μ- and m-calpain activities, but they grow and divide apparently normally. CAPNS1 +/- mice are viable, fertile, and phenotypically normal but the CAPNS1 double knockout is embryonic lethal, indicating the essential role of calpains in embryogenesis (Arthur et al., 2000). In the same way, also CAPN2 -/- mice, which lack the m-calpain catalytic subunit, die at the pre-implantation stage of development (Dutt et al., 2006). On the other hand, CAPN1 knockout mice show no apparent phenotype, indicating that m-calpain compensates for μ-calpain in this scenario (Azam et al., 2001). Their Ca^{2+} dependence suggests a connection to signal transduction, and the common assumption that the calpains become membrane bound on exposure to Ca^{2+} suggests that cytoskeletal proteins may be among the favored substrates. The list of proposed calpain substrates is very long and they suggest that calpain may be involved in different cellular processes such as cell adhesion, spreading, and migration, myoblast fusion, cell cycle control, and mitosis. Moreover its function and the biological outcome of calpain activity are strictly dependent on the cellular context.

1.1.4.1 Calpain and cell migration

The localization of calpains to integrin-associated focal adhesion structures indicates a clear action of these proteases in the regulation of cell migration (Huttenlocher et al., 1997) (Fig 1.3). Focal adhesions are clustered integrins that mediate cell adhesion and signalling in association with numerous proteins (Lebart and Benyamin, 2006).

The formation of the focal adhesion complex is a calpain-dependent mechanism and it is characterized by the presence of β3 integrin subunit and spectrin, both cleaved by calpain (Bialkowska et al., 2000; Bialkowska et al., 2005).
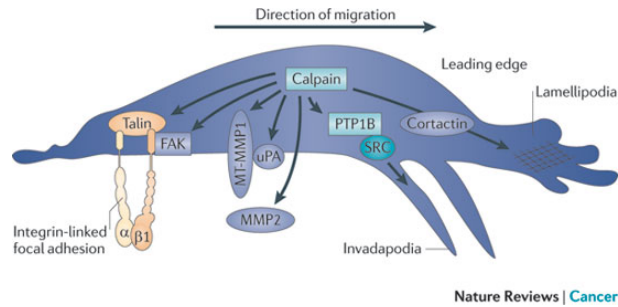
Figure 1.3: Calpain and cell migration (Storr et al., 2011)

m-calpain mediated cleavage of the focal adhesion component, talin, promotes the disassembly of cell-substratum adhesions (Beckerle et al., 1987); this specific effect suggests that the linking of integrins to the actin cytoskeleton made by this protein is important for regulating the integrity of adhesive contact sites (Franco et al., 2004). Another important component involved in the regulation of cell-cell adhesion through talin is the focal adhesion kinase (FAK). FAK promotes cell migration, orchestrating the signalling cascade between integrins and growth factors receptors. Calpain-mediated limited proteolysis of FAK affects talin dynamics and as a result they together regulate the turn-over of the adhesions (Chan et al., 2010). Besides the cleavage of FAK and talin, calpain can cleave numerous other substrates to promote cellular motility, such as paxillin (Yamaguchi et al., 1994), fodrin (Sato et al., 2004), ezrin (Wang et al., 2005), vinculin (Serrano and Devine, 2004), and alpha-actinin (Selliah et al., 1996).

On the other hand, there are also cases where the proteolytic activity works as a negative regulator, reducing cellular migration. Paxillin is an adaptor protein that localizes to focal adhesions and has been implicated in cell motility; normally it promotes cell migration, but interestingly calpain activity generates also an inhibitory fragment of paxillin that reduces the motility of cells (Cortesio et al., 2011).

It seems now clear that calpain proteases not only act on the destabilization of adhesion to the extracellular matrix, but also play an important role in the formation and turnover of new adhesion complexes.

1.1.4.2 Calpain, cell death and survival

As mentioned before, the activity of calpain proteases is dependently on the localization, on the level of expression, and also on the cellular context.

Calpain has been implicated in both pro-survival and pro-apoptotic processes; it is considered as the leading factor of a degradation pathway that is parallel but completely independent from the proteasomal degradation process.

Calpain is able to cleave wild-type p53, regulating protein stability to prevent p53-dependet apoptosis (Kubbutat and Vousden, 1997). In addition to this mechanism, m-calpain can physically interacts with GAS2 protein, preventing p53 cleavage (Benetti et al., 2001). Calpains play also an important role in the regulation and activation of the systemic inflammatory response. Once the cytokine tumor necrosis factor α (TNF-α) have bound its receptor followed the activation of the signaling cascade that also activates cytosolic m-calpain. The protease degrades the cytoplasmic inhibitor nuclear factor of kappa light polypeptide gene enhancer in B-cells inhibitor alpha (IκBα), allowing the translocation of the transcription factor nuclear factor κB (NF-κB) in the nucleus and the activation of the transcription (Han et al., 1999). In the same way calpain degrades in vivo the transcription factor c-Myc; indeed inhibition of calpain activity using cell-permeable inhibitors leads to c-Myc accumulation (Small et al., 2002). Moreover in certain cellular context, calpain cleaves at lysine 298 of Myc generating Myc-nick, a cytoplasmic form of the transcription factor that promotes α-tubulin acetylation, activating changes in cell morphology and accelerating muscle differentiation (Conacci-Sorrell et al., 2010).

Calpain activity can also affect cell cycle progression, through mechanisms that include cleavage of cyclin E to a more active low-molecular mass form in breast cancer (Wang et al., 2003), and altered cellular location of m-calpain during mitosis (Schollmeyer, 1988).

In addition, calpain can interfere with the interaction between protein phosphatase 2A (PP2A) and serine/threonine-specific PKB to prevent forkhead box O (FOXO)-mediated cell death (Bertoli et al., 2009). Interestingly, PP2A can also negatively regulate calpain during cell migration (Xu and Deng, 2006).

Several studies have shown that calpains cooperate with the caspase cysteine protease machinery for the induction of apoptosis (Storr et al., 2011). Caspase 7, 9, 10 and 12 are all subjected to calpain-mediated cleavage (Gafni et al., 2009; Chua et al., 2000). During endoplasmic reticulum stress calapin can activate caspase 12, resulting in c-Jun N-terminal kinases-dependent apoptosis (Tan et al., 2006).

Calpain can facilitate apoptosis through the cleavage of various members of the apoptosis regulating B-cell lymphoma 2 (BCL-2) family, including promoting apoptosis through Bcl-2-associated X protein (BAX) and BH3 interacting-domain death agonist-mediated cytochrome

c release (BID), and cleavage of BCL-2 to allow BAX translocation into the mitochondria (Wood et al., 1998).

Calpain is able to activate several other substrates that are involved in promoting apoptosis, such as the cyclin-dependent kinase 5 (CDK5; Lin et al., 2006), the apoptotic protease activating factor 1, (APAF1; Fettucciari et al., 2006), the c-Jun N-terminal kinases (JNK; Tan et al., 2006), JUN and FOS (Pariat et al., 2000).

1.1.4.3 Calpain and autophagy

Autophagy is a process involved in the maintenance of cellular homeostasis; in a physiological context, damaged organelles and proteins are delivered to the lysosomes for degradation. There is a clear cross-talk between autophagy and apoptosis; in this context conventional calpains play an important role (Moretti et al., 2014). In melanoma cells, the inhibition of conventional calpains enhances the basal autophagic response, which acts as a protective mechanism against cisplatin cytotoxicity (Del Bello et al., 2013).

Calpains can inhibit autophagy through the cleavage of $G_{s\alpha}$ (α-subunit of heterotrimeric G-proteins); the resulting increase of adenylyl cyclase activity produces high levels of cyclic AMP, which, in turn, inhibits autophagy. Indeed μ- and m-calpain knockdown by siRNA and calpain inhibitors cause an increase in the level of production of microtubule-associated protein 1a/1b light chain 3 (LC3) -positive vesicles, together with an increase in the autophagosomes number (Williams et al., 2008).

Calpain knockdown in Drosophila protects against the aggregation and toxicity of proteins, like mutant huntingtin, in an autophagy-dependent fashion. Furthermore the overexpression of the calpain inhibitor, calpastatin, increases autophagosome levels (Menzies et al., 2015). Several Atg (Autophagy-related gene) proteins involved in different phases of autophagy are proteolytic targets of Calpain-1 in vitro (Norman et al., 2010). For example calpain-mediated Atg5 cleavage provokes apoptotic cell death; indeed truncated Atg5 translocated from the cytosol to mitochondria, associated with the anti-apoptotic molecule Bcl-xL and triggered cytochrome c release and caspase activation. This proteolytic process represents again a molecular link between autophagy and apoptosis (Yousefi et al., 2006).

Moreover, the calpain-mediated degradation of p62 contributes to the abrogation of the pro-survival function of autophagy in tumor cells and in cancer stem cells (Colunga et al., 2014). Calpain localized predominantly near the endoplasmic reticulum and Golgi membranes, that represent sites where the autophagosome stars to form; different cellular and extracellular stimuli and various treatments, such as tunicamycin, an inhibitor of N-glycosylation and

thapsigargin, an inhibitor of the SERCA pump, are able to induce ER stress, activating autophagy (Ogata et al., 2006). In this scenario, the cytoplasmic level of calcium increases and calpain becomes active.

Our group demonstrated that in mouse fibroblast cells that are deficient in calpain, autophagy is impaired with a resulting dramatic increase in apoptotic cell death. Indeed in CAPNS1-depleted cells, ectopic LC3 accumulates in early endosome-like vesicles that may represent a salvage pathway for protein degradation when autophagy is defective (Demarchi et al., 2006).

1.1.5 Calpain in human diseases

A number of pathologic conditions have been associated with disturbances of the calpain system. They include type 2 diabetes, cataracts, Duchenne's muscular dystrophy, Parkinson's and Alzheimer's disease, rheumatoid arthritis, ischemia, stroke and brain trauma, various platelet syndromes, hypertension, liver dysfunction, and some types of cancer.

Several studies show that the conventional calpain system is differently expressed in human tumor tissues (and/or in tumor cell lines) compared to normal counterparts (Moretti et al., 2014). Aberrant expression of calpain has been implicated in tumorigenesis. Increased expression of μ-calpain is observed in schwannomas and meningiomas (Kimura et al., 2000). There is a correlation between higher μ-calpain mRNA levels with increased malignancy in renal cell carcinoma (Braun et al., 1999).

The role played by calpains in prostate cancers, where calpains have been show to be over-expressed under basal conditions (Rios-Doria et al., 2004) and after androgen deprivation (Liu et al., 2014), is of particular interest. Androgen receptors (AR), which play a pivotal role in prostate cancer cell proliferation and viability, undergo a calpain-mediated breakdown during chemotherapy-induced apoptosis. However, AR can also undergo calpain-mediated processing, which generates a constitutively active truncated receptor. This post-translational modification contributes to the transition from hormone-sensitive to hormone-refractory state, the latter condition being not curable by androgen-ablation therapy (Libertini et al., 2007).

Interesting findings with therapeutic implications were shown in Human Epithelial growth factor Receptor 2 (HER2) -positive breast cancer cells. Acquired-resistance to anti-HER2 Trastuzumab therapy occurs commonly in HER2-positive breast cancer, and involves over-activation of HER2 and its crosstalk with other HER family members. In Trastuzumab-resistant cells suppression of CAPNS1, which is up-regulated in all HER2-positive breast

cancers, decreases cell survival and restores Trastuzumab-response (Kulkarni et al., 2012). Further calpain family members are implicated in cancer, including increased expression of calpain 6 in uterine sarcomas and carcinosarcomas (Lee et al., 2007), as well as in uterine cervical neoplasia (Lee et al., 2008); decreased expression of calpain 3 variants in melanoma (Moretti et al., 2009); and decreased expression of CAPN9 in gastric cancer (Yoshikawa et al., 2000).

Mutation in CAPN3 gene, that codifies for skeletal muscles calpain 3 causes the limb-girdle muscular dystrophy type 2A (LGMD2A), a progressive disorder of the skeletal muscles (Zazt et al., 2003). CAPN3 mutations lead to a deficiency in the protein production and a subsequent death of muscle-cell nuclei (myo-nuclear apoptosis) together with a perturbation of IκBα pathway (Baghdiguian et al., 1999). A ubiquitous calpain involved in the onset of type 2 diabetes is calpain 10; a polymorphism within intron 3 in the CAPN10 gene affects its translation to mRNA. Low levels of calpain 10 mRNA were observed in association with the up-regulation of PKC essential for the phosphorylation of insulin receptor (Baier etal., 2000). Calpain 10 may have a role in the actin reorganization that is required for insulin-stimulated translocation of insulin-responsive glucose transporter 4 (GLUT4) to the plasma membrane in adipocytes (Paul et al., 2003).

The principle feature of the Alzheimer's disease is the deposit of β-amyloid peptides in extracellular amyloid plaques. Calpains are not directly related to this phenotype, however calcium and m-calpain levels are elevated in this scenario, together with autolysis of μ-calpain (Grynspan et al., 1997; Saito et al., 1993). In addition in patients with Alzheimer's disease, calpain cleaves p35 protein, essential for the development of neuronal tissues. The cleavage product p25 activates CDK5 (Kusakawa et al., 2000).

The insurgence of numerous diseases is connected to a disturbed calcium homeostasis within muscles cells, caused by different factors. For example in Duchenne's muscular dystrophies, the absence or a deficiency of dystrophin, causes an increased Ca^{2+} level in muscle and inappropriate calpain activity (Tidball, J., G., Spencer, M.,J., 2000). In the myocardial infarction Ca^{2+} homeostasis is lost, triggering inappropriate calpain activity.

In cataracts, a sight disturb, calcium influx activates m-calpain that cleaves α- and β-crystalline but not γ-crystalline; the crystalline fragments aggregate causing this illness (Shearer et al., 2000).
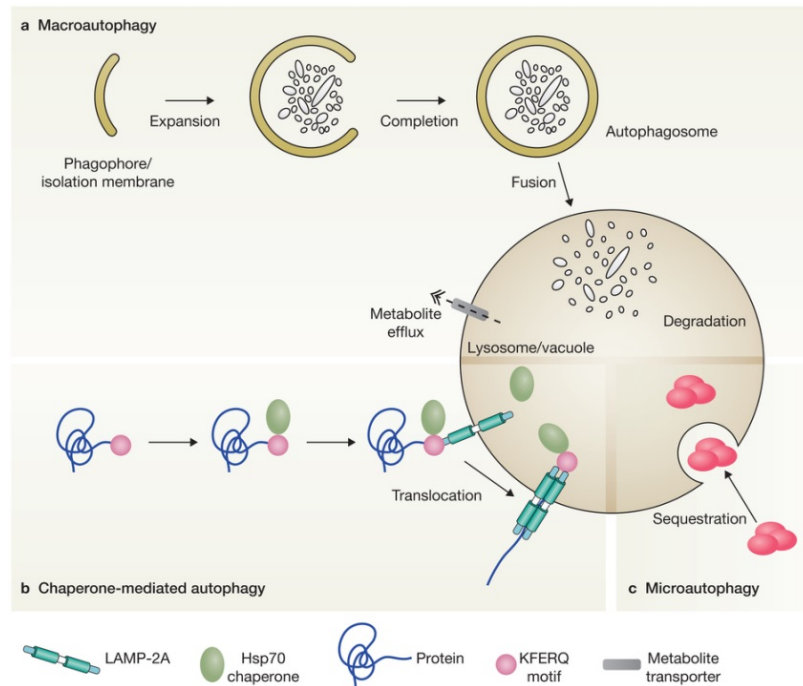
1.2 THE AUTOPHAGIC PROCESS

Figure 1.4: Three different types of autophagy (Boya et al., 2013)

Autophagy is a lysosome-mediated degradation pathway for non-essential or damaged cellular components that plays an important homeostatic role in cell survival, differentiation and development (Mizushima N., 2007).

There are three types of autophagy (Fig. 1.4): macroautophagy allows the degradation of damaged organelles and proteins through the activity of an intermediate vesicular structure called autophagosome; microautophagy concerns to a degradation process where only small molecules can be directly engulfed by the lysosome. The last one is the chaperone-mediated autophagy, where proteins that have to be degraded, are firstly recognized by a chaperone and then delivered to the lysosome. Indeed, proteins carrying the penta-peptide KFERQ-like sequence are recognized by the Heat Shock cognate protein 70 (Hsp70) chaperone which then associates with the integral lysosome associated membrane protein 2A (LAMP-2A), triggering its oligomerization. This event leads the translocation of the bound protein into the lysosome interior through a process that requires Hsp70 (Boya et al., 2013).

Recent studies have clearly demonstrated that autophagy has a great variety of physiological and pathophysiological roles, such as starvation adaptation, intracellular protein and organelle clearance, development, anti-aging, elimination of microorganisms, cell death, tumor suppression, and antigen presentation (Mizushima N., 2005).

1.2.1 Macroautophagy

Macroautophagy, hereafter autophagy, is a multistep process that allows the degradation of entire parts of cytoplasm, thanks to a double-membrane structure, the autophagosome.

Under physiological condition (basal condition) autophagy is important for the constitutive turnover of cytosolic components; in particular situation such as starvation, hypoxia and other stress stimuli, this process can be induced (Mizushima N., 2007). Several signaling molecules and cascades modulate autophagy in response to numerous cellular and environmental cues (Boya et al., 2013).

Autophagosome formation represents the initial of the process, also called nucleation step; at this level, the cytoplasmic constituents including organelles, are sequestered by a unique membrane called phagophore or isolation membrane, which is a very flat organelle like a Golgi cisterna. Complete sequestration by the elongating phagophore results in the formation of the autophagosome, which is typically a double-membraned organelle. The origin of the autophagosome membranes has been a major question in the field and at present, there is much controversy about the organelle from which the membranes originate. Recent studies suggest that there may be contributions from multiple sources.

Under conditions in which autophagy is induced by various forms of starvation, autophagosomes appear to be formed at the endoplasmic reticulum (ER) in phosphatidylinositol 3-phosphate (PI3P) enriched regions, via structures called omegasomes (Axe et al., 2008; Hayashi-Nishino et al., 2010; Hamasaki et al., 2013; Ylä-Anttila et al., 2009) and at mitochondria (Hailey et al., 2010). Moreover also plasma membrane and the Golgi network contribute to nascent autophagosomes under both basal and autophagy induction conditions (Ravikumar et al., 2010; Geng, J. and Klionsky, D., J. 2010).

Once tha autophagosome is formed it goes toward the process of its maturation; this phase consists in different events including the fusion with multi-vesicular bodies (MVBs) and endosome vesicles. This step is fundamental because endosomes and MVBs provide to the nascent autophagosome the machinery (lysosomal membrane proteins and proton pumps) required for the final step: the fusion with lysosomes (Tooze et al., 1990; Berg et al., 1998). During the fusion process, the inner membrane of the autophagosome and the cytoplasm-derived materials contained are degraded by lysosomal hydrolases. These degradation structures are called "autolysosomes" or "autophagolysosomes". Once macromolecules have been degraded monomeric units, such as amino acid are transported back to cytoplasm where they can be reused for biosynthesis or energy production (Mizushima N., 2007).

1.2.2 The regulation of autophagy

Basal-level autophagy is very low under normal conditions; therefore, an efficient mechanism to induce autophagy is crucial for organisms to adapt to stress and extracellular signals. During nutrient deprivation, autophagy is induced through two major signaling cascades that sense nutrient status, activate cell division and growth, and negatively regulate autophagy. These are the target of rapamycin (TOR) and Ras-cAMP-PKA pathways (Fig.5; He, C., and Klionsky, D., J., 2009).

In mammal cells, in nutrient-rich conditions TOR (mTOR) interacts with, phosphorylates and inactivates the Unc-51 like autophagy activating kinases 1 and 2 (ULKs), and the autophagy-related protein 13 (ATG13), suggesting a negative regulative role for mTOR in the process. During starvation mTOR is inactivated and autophagy is activated. Currently there are three theories that could describe how the signal cascade works. The first one suggests that mTOR directly senses and is phosphorylated in response to nutrient signal (Long et al., 2005). However evidence in *Drosphila* and mammals proposed that the Ras-related small GTPases activates mTOR in response to aminoacids, mediating the translocation of the complex to subcellular compartments that contains the Ras homolog enriched in brain (Rheb), the activator of mTOR (Sancak et al., 2008). Other studies indicated that mTOR activation can depend also by the vacuolar protein sorting protein 34 (Vps34); indeed this protein is stimulated by the presence of amino acids, which leads to the activation of mTOR (Nobukuni et al., 2005).
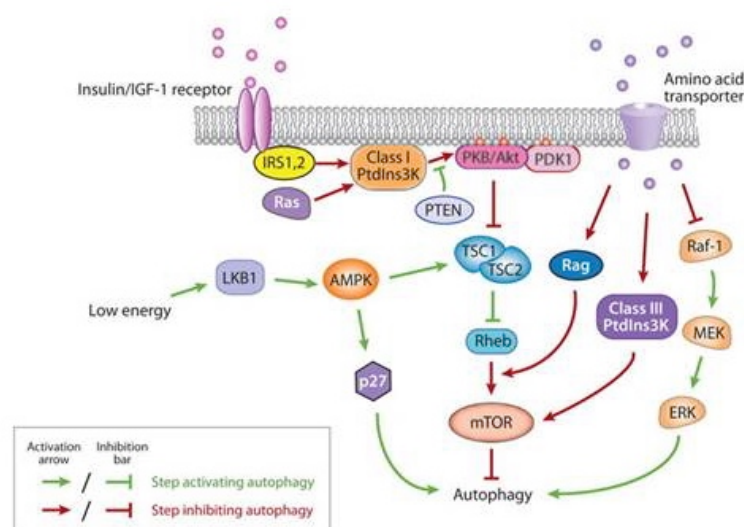

Figure 1.5: Regulatory pathways of autophagy, in response to aminoacid, hormones and energy stimuli (He C., and Klionsky, D., J., 2009)

All these three mechanisms have as a final result the activation of the downstream proteins ULK1 and ULK2; these proteins are responsible for the phosphorylation of the Atg13 and the focal adhesion kinase family-interacting protein of 200 kD (FIP200), and finally the activation of autophagy (Hosokawa et al., 2009).

The Ras/cAMP-dependent PKA signalling pathway is important for glucose sensing within cells. In nutrient rich condition, the small GTPases, Ras1 and Ras2, are active and enhance the production of cAMP. High levels of cAMP bind to the regulatory subunit of PKA releasing its inhibitory effect. The activation of Ras/PKA axis leads to autophagy inhibition probably mediated by the directly regulation of ULK1 (Budovskaya et al., 2004; Schmelzle et al., 2004).

Autophagy can also be activated by growth factors that regulate the pathway through a different signaling cascade compare to that one of nutrients, but again at the end converge on mTOR. Insulin and insulin like growth factors bind and phosphorylated theirs receptors, inducing the recruitment of the insulin receptor substrate 1 and 2 (IRS1 and IRS2). These two proteins allow the binding of other adaptor molecules, including p85 that belongs to the class I PtdIns3K. p85 is important for the generation of phosphatidyl-inostiol 3-phosphate (PIP3) that induces the activation of Protein Kinase B (PKB) signaling through phosphoinositide-dependent protein kinase 1, (PDK1) (Alessi et al., 1997; Stokoe et al., 1997). Also Ras signaling play a role in autophagy regulation by growth factors. Indeed Ras represents a negative regulator for nutrient deprivation-induced autophagy through the class I PI3-kinase signaling pathway (Furuta et al., 2004).

A reduction in the cellular energy, in terms of adenosine triphosphate (ATP), is considered another signal to induce autophagy in mammals. A decrease of the ATP/AMP ratio activates 5'-AMP-activated protein kinase (AMPK) that phosphorylates the tuberous sclerosis complex (TSC1 and TSC2), which inhibits mTOR activity through Rheb (Inoki et al., 2003) (Fig.1.5).

Different intracellular and extracellular stress signals lead to the induction of autophagy. A low level of oxygen (at or below 1%) is considered as a hypoxia; this particular condition is presented in physiological developing embryo and in different pathological conditions including also cancer. Little is known about the pathway involved in the hypoxia response; hypoxia-inducible factor 1 (HIF1) is the primary transcription factor activated by low level of oxygen. In general this factor controls a set of genes that regulate mitochondrial autophagy (mitophagy) (Zhang et al., 2008). Another signal that activates overall mitophagy is the oxidative stress. Indeed, the generation of reactive-oxygen species (ROS) within mitochondria induces the activation firstly of mitophagy that allows the elimination of

damaged mitochondria and also the program of autophagy cell death. In normal condition, some ROS target the conserved Cys81 on Atg4 that is responsible for the cleavage of LC3 before the autophagosome-lysosome fusion. The oxidation of the cysteine inhibits the protease activity of Atg4 and promotes the lipidation of LC3 (Scherz-Shouval et al., 2007).

The last important consideration has to be done with regard to the connection of autophagy signaling with the endoplasmic reticulum and its activity. In this cellular compartment newly synthesized proteins are folded and they are delivered to other subcellular structures and vesicles. Moreover it is the major Ca^{2+} reservoir of the cell. Different cellular stimuli such as hypoxia, glucose deprivation, calcium efflux and so on, lead to the accumulation of unfolded proteins and to the activation of the unfolding protein response (UPR) (Fig. 1.6; Bernales et al., 2006). The UPR signals in mammals involved three different downstream pathways, headed by three distinct proteins: inositol-requiring kinase 1 (IRE1), activating transcription factor 6 (ATF6) and RNA-dependent protein kinase-like ER kinase (PERK). These factors signal misfolded protein levels in the ER and activate the transcription of different target genes. JNK is the downstream target of IRE1 and it is essential for the lipid conjugation of LC3 induced by tunicamycin of by accumulation of misfolded protein in the cytoplasm due to proteasome inhibition (Ding et al., 2007b; Ogata et al., 2006). ER stress also induces release of luminal Ca^{2+} to the cytosol, activating a series of proteins such as the Calcium-activated calmodulin-dependent kinase kinase-β (CaMKKβ) that activates AMPK inducing autophagy (Hoyer-Hansen et al., 2007).
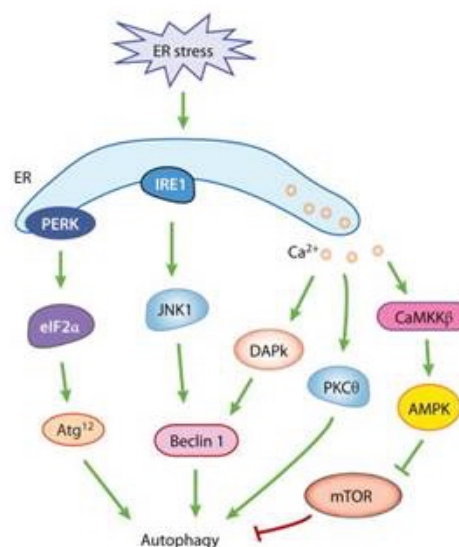

Figure 1.6: ER pathways activating autophagy, in response to ER stress (He C., and Klionsky, D., J., 2009)

These numerous ways to induce or inhibit autophagy show how this process is important to sustain cellular homeostasis. At the end it is possible that autophagy plays dual roles in determining cell fate, depending on specific cell types, stimuli and conditions (Ding et al., 2007a).

1.2.3 The Autophagy-related (ATG) proteins

The autophagic process is tightly regulated by a set of specific Autophagy-related Genes (ATG). The first yeast genetic screening revealed the activity of 15 different ATG genes (Tsukada, M. and Oshumi, Y., 1993). Currently, 27 ATG genes have been identified in *S. cerevisiae*. Most are gathered together into three large groups by their function: non-selective autophagy (17 genes), selective autophagy (7 genes), and degradation of autophagic bodies (2 genes) (Wang, C., W. and Klionsky, D., J., 2003). Several mammalian homologues of yeast ATG genes have been identified (Table 1.2 and Figure 1.7), and the mechanisms of yeast autophagy are largely conserved in mammals. Starting from now only mammalian autophagy will be discussed.

Once autophagy is activated the constitutively active ULK complex, made by ULK1, ULK2, Atg13 and FIP200, can moved toward the site of formation of the autophagosome. ULK1 phosphorylates FIP200 and Atg13 to allow the formation of this complex (Mizushima, N., 2010). The ULK complex resides in the cytoplasm and is normally inactivated by mTOR (Hosokawa et al., 2009).

One of the main components of autophagosomal membranes is the PI3P; this phospholipid is found in all types of cellular membranes where it helps to recruit different proteins. Vps34 produces PI3P for autophagy and is one of the members of the Class III phosphatidylinositol 3-kinase complex (Class III PI3K complex) together with Vacuolar protein sorting protein 15 (Vps15), Beclin1 and Atg14 (Itakura et al., 2008). The localization of this complex near the ER in proximity of the site of formation of the phagophore, is driven by the N-terminal region of Atg14 (Matsunaga et al., 2010). The kinase activity of ULK1 is essential for Atg14 activity.

Mammals have at least other two Class III PI3K complexes that play roles in endosomal transport and autophagosome-lysosome fusion. One of these include UV irradiation resistance-associated gene (UVRAG) instead of Atg14 (Zhong et al., 2009). Beclin1 binds

also other proteins such as Bcl-2, the Autophagy/Beclin-1 Regulator 1 (AMBRA1) and vacuole membrane protein 1 (VMP1) (Funderburk et al., 2010).

The third component of the process that participates to the formation of the isolation membrane is the "Atg12 Conjugation System". This complex is made by: Atg12, Atg16 and Atg5 together with two enzymes Atg7 and Atg10. This is presented as a dimer (2:2:2) on the outer membrane of the phagophore and is essential for proper elongation of the membrane (Mizushima et al., 2011). Immediately after the completion of autophagosome formation it dissociates from the membrane. This system is necessary for the formation of the "LC3 Conjugation System". LC3 is an ubiquitin-like protein, synthesized as a precursor (LC3 I) with additional sequence at the C-terminal, which are processed by the cysteine protease Atg4 (Kabeya et al., 2004). The resulting C-terminal glycine-exposed form of LC3 is activated by Atg7, transferred to Atg3 and finally covalently linked to an amino group of phosphatidylethanolamine (PE), a major membrane phospholipid. Both these conjugation systems are good markers for the detection of membrane structures during autophagy; the first one (Atg12-Atg5-Atg16) localizes specifically to the isolation membrane, whereas the second one tracks the full process (Kabeya et al., 2000; Kirisako et al., 1999).

In addition to these well-defined complexes there are single proteins that play alone different roles along the process. VMP1 is an ER- and Golgi complex-associated transmembrane protein, firstly discovered in pancreatic exocrine cells (Dusetti et al., 2002); later it was shown to localize to the site of formation of the autophagosome and to interact with Beclin1 (Itakura E., Mizushima, N., 2010; Repolo et al., 2007). The precise role of VMP1 is not well defined; recent data suggest that this protein transiently localizes to early autophagic structures and dissociated from them in a PI3K-dependent manner (Itakura E., Mizushima, N., 2010).

Another ER-localized protein is the Double FYVE Containing Protein 1 (DFCP1). DFCP1 was identified as a PI3P binding protein; indeed it binds to PI3P thanks to its FYVE domain (Axe et al., 2008). Upon starvation, DFCP1 co-localizes with isolation membrane and autophagosome markers, underling the idea that the ER may provide components for autophagosome formation; one of this is DFCP1 that provides phospholipid to the nascent membrane.

Mammalian cells have four Atg18 homologs, which are known as WD-repeat protein interacting with phosphoinositides (WIPI) 1–4 (Jeffries et al., 2004). Their activity is again related to the initial step of autophagy: similar to DFCP1, they translocate from membranes or ER to autophagosome formation site upon induction of the process.

The only transmembrane autophagy related protein is ATG9 that is involved in the delivery of membrane to the initiation site of autophagy (Noda et al., 2000); normally it is localized on the Golgi cisternae and in late endosome vesicles; upon autophagy induction ATG9 co-localized with LC3 (Yamamoto et al., 2012; see paragraph 1.3.4)

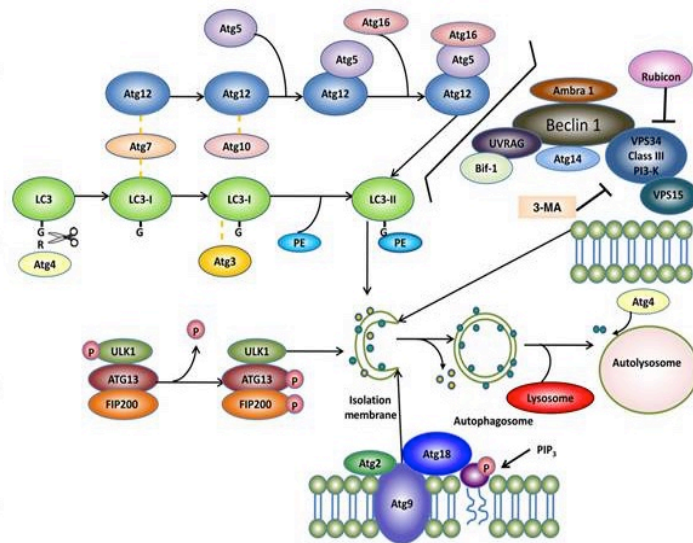| YEAST	MAMMALS	Complex
ATG1	ULK1/2	ATG1/ULK complex
ATG13	ATG13	
ATG17	-	
ATG29	-	
ATG31	-	
-	FIP200	
Vps34	Vps34	Class III PI3K complex
Vps15	Vps15	
ATG6	Beclin 1	
ATG14	ATG14	
-	AMBRA 1	
UVRAG	UVRAG	
ATG12	ATG12	ATG12 conjugation system
ATG7	ATG7	
ATG10	ATG10	
ATG5	ATG5	
ATG16	ATG16	
ATG8	LC3 I/II	ATG8/LC3 conjugation system
ATG4	ATG4	
ATG7	ATG7	
ATG3	ATG3	
ATG2	ATG2	Others
ATG9	ATG9	
ATG18	WIPI 1/2/3/4	
-	DFCP1	
-	VMP1	

Table 1.2 and Figure 1.7: In the table there are listed the proteins involved in the regulation of autophagy and the complexes that they form, both for yeast and mammals. The figure represents the schematic roles of each components of the pathway (Modified by Ding et al., 2011).

1.2.4 Non-Atg Components required for autophagy

Autophagy is a process directly connected with other cytoplasmic processes, overall the secretory and endocytic pathways. Indeed, components of the latter processes fuse at different levels with structures of the autophagy machinery. In this scenario "non ATG" proteins involved in the trafficking of endosomes, exosomes and MVBs could be essential for the normal progression and conclusion of the autophagic pathway.

The hairpin-type-tail anchored soluble N-ethylmaleimide-sensitive factor Attachment Protein receptor (SNARE) Syntaxin 17 was identified as an autophagsomal SNARE protein necessary for the fusion event between the autophagosome and the endosome/lysosome. This

elegant study shows how the peculiar features of the tertiary structure of the protein are essential for its targeting to the membrane of the autophagosome (Itakura et al., 2012). Another SNARE protein implicates in this process is the Vesicle Associated Membrane Protein 7 (VAMP7) that is essential, together with other SNARE partners, to allow the maturation of the autophagosome. More in details, VAMP7 regulates the process of homotypic fusion between membranes positive for ATG16, but negative for LC3; this step is necessary to increase the size of the phagophore, therefore the formation of a mature autophagosome (Moreau et al., 2011).

The cytoskeleton, in particular microtubules, mediates an efficient protein trafficking during the autophagosome formation. The microtubule motor protein, dynein, is required for the autophagic clearance of protein aggregates in mammalian cells (Ravikumar et al., 2005); in the same context, it appears that autophagosomes are formed at random location in the cell, but transported toward the nucleus along microtubules after completion (Jahreiss et al., 2008). Ras superfamily of monomeric G proteins (Rab) are a key regulators of membrane trafficking and fusion events; in mammals there are almost 70 known Rab proteins, among which about 10 have a defined function in autophagy (Szatmari, Z., Sass, M., 2014). One example is Rab5, a well-known early endosome protein, involved in the early stages of autophagosome formation; it may have a role in the recruitment of the autophagic BECN1-PIK3C3 complex and subsequent PtdIns3P production on the phagophore membrane (Ravikumar et al., 2008).

1.2.5 Autophagy in human diseases

Since the discovery of Atg genes in the 1990s, there has been a proliferation of studies on the physiological and pathological roles of autophagy in a variety of autophagy cellular and animal models (Jiang, P., Mizushima, N., 2014).

A big part of the researches converge on the dissection of the role of autophagy during diseases associated with the accumulation of protein aggregates in cellular cytoplasm, such as Huntington's and Parkinson's diseases. Another big part of the work is trying to elucidate exactly in which way autophagy could help the prevention of tumorigenesis or, in an opposite way, it could help cancer cells to survive to anti-cancer treatments. Also muscles disorders, in particular cardio-myopathies have acquired a remarkable importance in this field.

The multi-step nature of the autophagic process makes it vulnerable to failure at different levels. Expression of ATG5 protein, a component of the ATG12 conjugation system,

essential for the initial step of the formation of the autophagosome, was found aberrant in different type of prostate cancers (Kim et al., 2011). Another protein involved in the initial step of the process connected to a series of cancers is Beclin1, a tumour suppressor protein. Indeed mono-allelic deletion of BECN1 has been detected in human breast, ovarian and prostate tumour specimens. In particular, the aberrant expression of Beclin1 was found in many kinds of tumour tissues correlates with poor prognosis (Liang et al., 1999; Han et al., 2014). Moreover latest data confirm another putative tumour suppressor protein involved at the beginning of autophagy. The Beclin1 interacting UVRAG is mono-allelically mutated at high frequency in human colon cancers. UVRAG-mediated activation of the Beclin1–PI3KC3 complex promotes autophagy and also suppresses the proliferation and tumorigenicity of human colon cancer cells (Liang et al., 2006).

Very recent data derived from mouse models knock-out for ATG5 or/and ATG7, together with preclinical investigations allow the developing of the first set of the autophagy inhibitor hydroxychloroquine (HCQ) clinical trials in patients with advanced cancer (Rebecca V., W., Amaravadi, R., K., 2015). Paget disease of bone (PDB) is a common disorder characterized by focal and disorganized increase of bone turnover. Two independent mutational events at the same position in p62 may be frequently associated with PDB (Laurin et al., 2002).

Genome wide association studies of non-synonymous of single nucleotide polymorphisms (SNPs) have linked ATG16L1 variants with susceptibility to Crohn's disease, a debilitating inflammatory bowel disease (IBD) that can involve the entire digestive tract (Hampe et al., 2006; Murthy et al., 2014). ATG16 is a key player during the initial step of autophagy; it forms a complex with the ATG12 conjugation system and it is essential for the lipidation of LC3. The Atg16L1 protein possesses a C-terminal WD repeat domain, and the Crohn's disease-associated mutation (T300A, also known as Ala197Thr) is within or immediately upstream of this domain. Unfortunately the precise effect of this mutation in the onset of the illness is still unknown (Murthy et al., 2014).

Regarding diseases connected to the latest step of the autophagic process, a big part of the studies has been done on lysosome dysfunction. Lysosomal storage disorders (LSDs), are a family of disorders caused by inherited gene mutations that perturb lysosomal homeostasis. These diseases are characterized by the accumulation of undigested macromolecules in the cell. As a result the lysosomal dysfunction is accompanied by impaired autophagic flux and accumulation of autophagy substrates such as p62, poly-ubiquitinated proteins, and damaged mitochondria (Lieberman et al., 2012). The first discovered LSD where autophagy is implicated is the Danon diseases, also called "Lysosomal glycogen storage disease with

normal acid maltase". This pathological condition is characterized by cardiomyopathy, myopathy and variable mental retardation; sequence analysis of LAMP2 derived from patience affected by this disease unveil the presence of eight different mutations that abolish the cytoplasmic and the transmembrane domain of the protein (Nishino et al., 2000).

A well-known neurodegenerative disease where two autophagic proteins are involved is Parkinson's disease that causes the reduction of the dopaminergic transmission in the basal ganglia (Fahn, S., 2003). PTEN-induced putative kinase protein 1 (PINK1) is a mitochondria-associated protein kinase that acts upstream of Parkin, an E3 ubiquitin ligase implicated in the selective degradation of damaged mitochondria by autophagy. Mutations in the genes that codify both these proteins lead to autosomal recessive or sporadic juvenile-onset Parkinson's disease (Kitada et al., 1998; Valente et al., 2004). Normally, when mitochondria is damaged and lose its membrane potential, PINK1 recruited Parkin which ubiquitin different proteins activating mitophagy. Excessive mitochondrial damaged could be linked to Parkinson's disease.

All these pathological conditions described until know are just a part of a long list of diseases connected to deregulation or dysfunction of autophagy (Table 1.3).

GENES	FUNCTIONS IN AUTOPHAGY	ASSOCIATED HUMAN DISEASE
ATG5	Autophagosome formation	Prostate Cancer
ATG16L1	Autophagosome formation	Chron's Disease
BECN1	Autophagosome formation	Breast, Ovarian and Prostate Cancer
p62	An adaptor protein for selective autophagy	Paget Disease of Bone
UVRAG	Autophagosme degradation	Colorectal Cancer
Parkin	Mitophagy induction	Parkinson's Disease
PINK1	Mitophagy induction	Parkinson's Disease

Table 1.3: List of the principal autophagic genes that are associated with a pathological condition in human.

1.3 NEW INSIGHTS ABOUT THE INITIAL STEPS OF AUTOPHAGOSOME FORMATION

The first crucial event in the autophagic process is the nucleation of the membrane that will become the autophagosome. The exact site where this process starts is not well understood and above all, the membrane sources forming the isolation membrane are not yet defined.

In the recent years, with the developing of new imaging techniques and fractionation
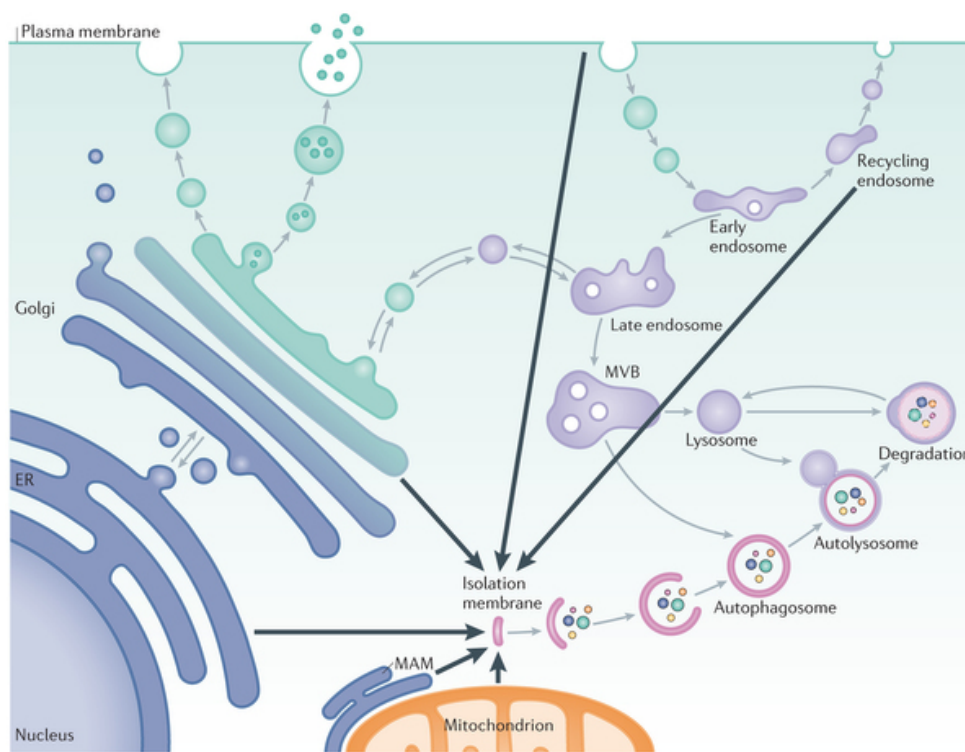
Figure 1.8: Schematic representation of the autophagic pathway and organelles that are involved in the process (Lamb et al., 2013)

protocols, it was possible to mark precisely all the compartments that participate to the initiation of autophagy. In addition the usage of electron tomography had helped understanding the organelles interplay. In this complex scenario, the ER plays a central role, together with mitochondria; during the progression of the process other cellular compartments like Golgi cisternae and vesicles such as endosomes, function as lipids sources (Fig 1.8). In addition, during starvation, other membrane origins may provide the site for the nucleation of the autophagosome.

1.3.1 The site where the autophagosome starts to form

In the 1960s electron microscopy studies identified the ER as the first membrane sources for autophagosome biogenesis (Novikoff, A., B., and Essner, E., 1962). Different ER-resident proteins are involved in the formation of the autophagosome among which DFCP1, a PI(3)P-binding protein localized on ER and Golgi membranes. In response to aminoacid starvation, DFCP1 translocates to the ER-associated membrane called "omegasome", where autophagosomal proteins reside (Axe et al., 2008). Here, for example, DFCP1 co-localizes with ATG14L, another ER protein necessary for the recruitment of the PI3-kinase complexes onto the ER surface (Matsunaga et al., 2010). Another study describes the involvement of the VMP1 in the initiation of the process. VMP1 is a trans-membrane protein localized on the ER and at the Golgi; upon autophagy activation its expression is induced (Vaccaro et al., 2008). In addition it was shown that VMP1 interacts with Beclin1, forming a complex essential for the recruitment and for the activation of the Class III PI3K complex on the site of autophagosome formation (Molejon et al., 2013). Finally also two elegant independent electron microscopy works had revealed the involvement of the ER in the formation of the phagophore (Yla-Anttila et al., 2009; Hayashi- Nishino et al., 2009).

Mitochondrial studies were also performed in order to validate the implication of this organelle. An artificial mitochondrial marker made by the sequence of the cytochrome b5 tagged to the fluorescent lipid NBD (7-nitro-2, 1, 3-benzoxadiazol-4-yl), was transferred from the outer membrane of the mitochondria to the autophagosome, upon starvation (Hailey et al., 2010). This event clearly suggests that autophagosomes could form also from the mitochondria. Moreover, the pro-apoptotic factor Bcl-2 localizes on mitochondria and its binding to the BH3 domain of Beclin1, prevents the formation of the Class III PI3K complex and subsequently the activation of the process (Pattingre et al., 2005). Following autophagy induction, Bcl-2 activity is inhibited by AMBRA1, that at the same time, induces the activity of Beclin1, finally activating autophagay (Strappazzon et al., 2011).

ER and mitochondria contact sites were also taken in consideration. In fact one model well explain by immunofluorescence and electron microscopy the collaboration between mitochondrial and ER proteins in the regulation of the nascent autophagosome. In particular it was found that the ER SNARE protein Syntaxin 17 (Stx17) binds and recruits ATG14L at these sites after autophagy induction (Hamasaki et al., 2013).

To summarize, a general consensus is emerging in the autophagy field. Autophagosomes membranes generate above all, from the ER but also mitochondria seem to play an important role; not less important, also de-novo synthesis has to be taken in account.

1.3.2 Autophagosome growing and maturation from the Golgi

After the step of nucleation, the phagophore starts to expand and to mature in a complete autophagosome. Golgi membrane, plasma membrane and endosomes contribute to this progression, delivering proteins and lipids that determine the final composition of the autophagosome. Regarding the Golgi dynamics, three molecular pathways participate to this step with the involvement of Golgi-resident proteins like Rab proteins, class III PI3K complex and ATG9. The Rab family of small GTPase regulates indirectly membrane fusion between different compartments. Rab1 and Rab33B are both involved in the progression of autophagy. Rab1 localizes in the ER-Golgi intermediate compartment (ERGIC) and in the Golgi stacks. It is necessary for the formation of DFCP1-positive omegasome (Mochizuki et al., 2013). Instead Rab33B is involved later in the process; it interacts with ATG16L1 (Itoh et al., 2008). More recently, the tubuling folding cofactor D 25 (TBC1D25) was identified as a Rab GAP of Rab33B; TBC1D25 binding LC3 controls autophagosome-lysosome fusion promoting GTP hydrolysis of Rab33B-GTP (Itoh et al., 2011). Autophagy can be negative regulated by the sequestration of Beclin1, a component of the class III PI3K complex, in the Golgi membrane; the Golgi-associated plant pathogenesis-related protein 1 (GAPR1) is responsible for the interaction and for the recruitment of Beclin1 towards the Golgi cisterna (Shoji-Kawata et al., 2012). The last protagonist of the maturation and growing of the autophagosome is ATG9 that is responsible for the proper delivery of Golgi membranes toward the site of formation of the autophagosome; details about this protein and its activity will be discussed in the paragraph 1.3.4.

1.3.3 The endocytic pathway contribution to autophagy

The convergence of the autophagosome and endocytic pathways was recognized in early morphological studies. In fact endosomes actively contribute to phagophore formation and expansion.

Endocytosis transports nutrients and grow factors from the outside of the cell within the cytoplasm, thanks to different types of vesicles. The process starts from the plasma membrane where specific proteins recognized molecules that have to be internalized. The pathway mainly consists of early endosomes, late endosomes and lysosomes. Endosomes function requires continuous vesicular budding and fusion events that are mediated by Rab proteins (Rink et al., 2005). Once the clathrin-coated vesicles are formed from the plasma membrane, these are converted in Rab5-early endosomes, which mature into Rab7-late endosome; these final structures can fuse with lysosome or directly with autophagosome. Therefore, the activity of endosomes is extremely important for autophagosome maturation. Indeed, once autophagosome is formed, it acquires proteins and enzymes that are normally
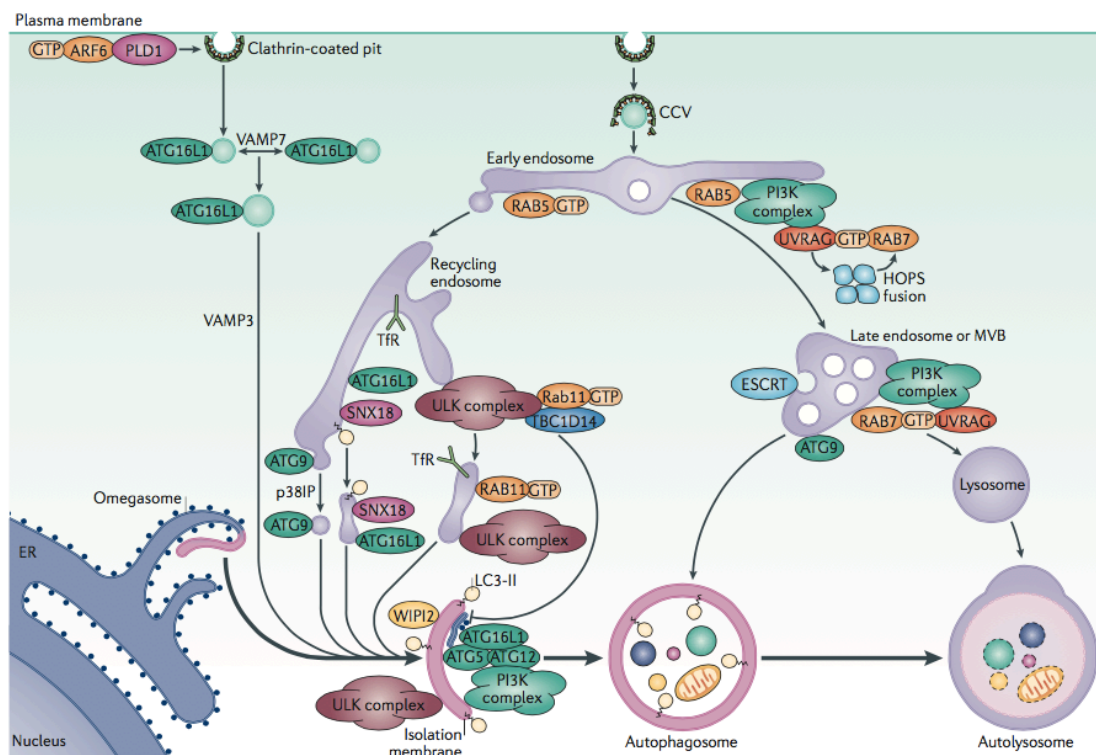

Figure 1.9: Schematic representation of the contribution of the endocytic pathway to autophagy (Lamb et al., 2013)

presented in early, late endosomes and MVBs (Dunn, 1990). EM studies detected endocytic markers in early and advanced autophagic vesicles (Punnonen et al. 1993; Liou et al. 1997). Clathrin-mediated endocytosis provides membrane that contributes to the formation of Atg16L1-positive, LC3-negative pre-autophagosomal structures (Fig.1.9). These precursors mature thanks to homotypic fusion, essential for the subsequent autophagosome formation; this fusion event depends on different SNARE proteins, including VAMP7 (Moreau et al., 2011). Rab11-positive recycling endosomes (RE) carry ULK1 and ATG9; upon autophagy induction, ULK1 complex together with transferrin and transferrin receptor are delivered in

Rab11-positive vesicles to forming autophagosome (Longatti et al., 2012). Finally the same work verified the presence of the RE/Endosome marker transferrin between the outer membrane of the autophagosome (Longatti et al., 2012), further affirming the connection between the endocytic pathway and autophagy.

1.3.4 The role of the autophagy-related protein 9

Atg9 was firstly identified in yeast genetic screening as the only transmembrane protein involved in the autophagic process (Lang et al., 2000). It is a multi-spanning protein with six highly conserved transmembrane domains and cytosolic NH_2 and COOH- terminal domains that are different in terms of length and aminoacid compositions (Noda et al., 2000).

Atg9 homologues exist in all species so far examined, and although its function is still unknown, it is required for autophagy in all species studied. In mammalian cells there are two functional orthologous: ATG9L1 and ATG9L2; the first one is ubiquitous while the second one is expressed only in placenta and pituitary gland. SiRNA-mediated knockdown of ATG9 impaired LC3 lipidation and protein degradation in HEK293 cells (Yamada et al., 2005), suggesting an involvement of this protein in the autophagic process; moreover it was demonstrated that ATG9 is essential for the survival of mice after birth, as described for ATG5 (Saitoh et al., 2009).

In nutrient rich conditions, ATG9 localizes in juxta-nuclear regions and is dispersed in the peripheral cytoplasm where it co-localizes with marker of late and early endosome, such as Rab5, Rab7 and Rab9. During starvation ATG9 moves towards the cytoplasm and co-localizes with LC3 protein alone, or together with Rab7, suggesting that ATG9 is present both in the immature and in the degradative autophagosomes (Saitoh et al., 2009). Additionally it was shown that ATG9 resides also in the recycling endosome that could represent the equivalent of the ATG9 reservoir found in yeast (Orsi et al., 2012).

The trafficking of ATG9 seems to be orchestrated by different cytoplasmic proteins. One study suggested that ULK1 controls the localization of ATG9 via a cascade involving myosin II. After induction of starvation the ULK1-Zipper-Interacting Protein Kinase (ZIPK)-Myosin II axis is activated and ATG9 is redistributed to the peripheral cytoplasm (Tang et al., 2010). Also the class III PI3K complex seems to be involved in the distribution of ATG9; indeed inhibitors of this complex or depletion of UVRAG or Beclin1 prevents its movement after induction of autophagy (Takahashi et al., 2011). All these data suggest an essential role of

ATG9 in the recruitment of the class III PI3K complex; this activity was well demonstrated in response to Salmonella infection (Kageyama et al., 2011). It could also be possible that this mechanism is efficient also for macroautophagy.

Another elegant work shows that ATG9 is indirectly involved in the recruitment of WIPI2 to the site where the autophagosomes start to form. Indeed, WIPI2 is thought to be recruited to phagophores by PI3P, the product of PI3K (Polson et al., 2010); here ATG9 may play a role in the recruitment of the class III PI3K complex in the context (Kageyama et al., 2011).

One interacting protein of ATG9 discovered in a yeast two-hybrid screening is the p38 interacting protein (p38IP) (Webber, J., L. and Tooze, S., A. 2010). In mammals p38IP contains a nuclear localization sequence, a peptide sequence rich in proline (P), glutamic acid (E), serine (S), and threonine (T) (PEST domain) and two serine rich domains. p38IP is essential for the redistribution of ATG9 upon starvation; indeed siRNA-mediated depletion of p38IP results in the loss of ATG9 dispersal and its retention at the juxta-nuclear pool. The interaction is mediated by the C-termini of each proteins and it is governed by p38α MAPK, which competes with ATG9 for p38IP binding. Thus, in nutrient-rich conditions, p38α is phosphorylated and thus activated, allowing it to bind p38IP with increased affinity, sequestering p38IP away from ATG9, and thereby preventing ATG9 dispersal and autophagy activation (Webber, J., L. and Tooze, S., A. 2010).

An additional regulator of ATG9 trafficking is the membrane curvature-driving protein Endophilin B1, also known as Bax-interacting factor 1 (Bif-1). Bif-1 is essential for the tabulation of the Golgi membranes and therefore for the movement of ATG9 toward the site of formation of the phagophore (Takahashi et al., 2011).

All these data suggest an essential role for ATG9 in the regulation and in the progression of autophagy, in particular during the step of formation of the autophagosome; moreover several proteins seems to be linked to this scenario; altough the precise mechanism by which ATG9 acts remains unknown.

1.3.5 The Bax-interacting factor 1 as a novel regulator of autophagy

Bax-interacting factor 1 (Bif-1) is a member of the endophilin protein family involved in the regulation of apoptosis, mitochondria morphology and autophagy; it was originally discovered as a Bax-binding protein (Pierrat et al., 2001; Cuddeback et al., 2001).

Endophilins are a well-conserved family of proteins involved in different membrane dynamics. Looking to the aminoacid sequence similarity, these proteins can be subdivided in two groups: the Endophilin A, involved in the formation of the endocytic vesicles and Endophilin B that includes Bif-1, important for membrane dynamics of organelles like Golgi and mitochondria, as well as autophagosomes (Pierrat et al., 2001).

This group of proteins is characterized by an amino-terminal N-Bin–Amphiphysin–Rvs (N-BAR) domain that is responsible for the binding to the lipid bilayers, inducing membrane curvature, and a carboxyl-terminal Src-homology 3 domain (SH3) that presents a proline-rich region essential for the formation of complexes with other proteins. More in details, the N – BAR domain has two α-helixes that form a coiled-coil structure responsible for the dimerization of the protein: the amphipathic helix (HO) and the amphipathic helix inserted helix 1(H1I). The HO region plays a crucial role in binding to membranes, while the H1I is inserted into the membrane driving the membrane curvature together with the BAR main body (Gallop et al., 2006).

Bif-1 was firstly identified in a yeast screening as a Bax-binding protein; Bax is a cytoplasmic protein that plays an important role in Bcl-2 dependent apoptosis. Normally Bax is localized in the cytoplasm but after induction of apoptosis, it binds to Bif-1 undergoing to a conformational change that allows its binding to the mitochondrial membrane, promoting apoptosis (Wolter et al., 1997).

Recently Bif-1 has acquired new importance in the autophagy field. Indeed it was published that Bif-1 interacts with Beclin 1 through UVRAG, activating autophagy and giving news insight the class III PI3K complex and the formation of the autophagosome (Fig.1.10; Takahashi et al., 2007). Upon starvation Bif-1 binds to UVRAG thanks to its SH3 domain; this interaction is essential for the

Figure 1.10: Schematic representation of the role of Bif-1 during autophagy (Takahashi et al., 2009).

activation of the class III PI3K complex. Moreover Bif-1 deficient cells are unable to form autophagosomes, suggesting an essential role of this protein in the process.

Bif-1 activity could also affect autophagy in other ways. For instance it has been demonstrated that Bif-1 plays a critical role in vesicle formation for coat protein I (COPI)-mediated retrograde transportation from the trans-Golgi network (TGN) to the endoplasmic reticulum (Yang et al., 2006). Therefore Bif-1 could be important for the delivery of COPI-vesicles membranes at the initiation site of formation of the phagophore.
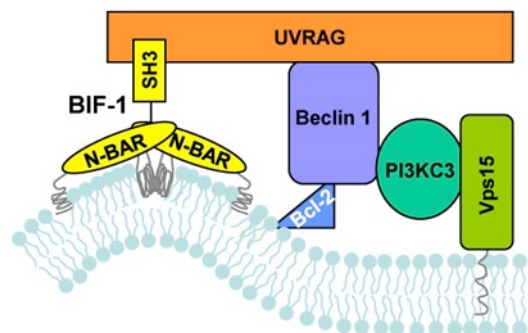
Another elegant work made by Hong-Gang Wang and his group, describes the importance of Bif-1 activity in the fission of Golgi membrane that are characterized by the presence of ATG9 proteins. It is well known that in physiological conditions ATG9 resides in the TGN and upon starvation, it moves towards cytoplasmic site where LC3 is also present. What is not completely clear is how ATG9 shifts from these two cellular locations. In this work it was demonstrated that Bif-1 plays an essential role for the trafficking of ATG9 from the Golgi membrane to the peripheral cytoplasm. Indeed, in response to nutrient starvation, Atg9-positive Golgi membranes were dispersed throughout the cytoplasm where they co-localized not only with Bif-1, but also with LC3 and Atg16. In this step it seems that both the α-helix (HO and H1I) are essential for the interaction with the Golgi membranes and for their fission (Takahashi et al., 2011).

1.4 CALPAIN AND MITOPHAGY

1.4.1 Autophagic clearance of damage mitochondria: mitophagy

Mitochondria produce energies in terms of ATP, through different metabolic pathways, using a series of cellular sources, such as lipids, aminoacids and carbohydrates. Mitochondrial metabolism is tightly regulated in order to meet cellular requirements. Among these regulative processes, the control of mitochondrial mass is determinant to maintain the metabolism of a cell (Melser et al., 2015).
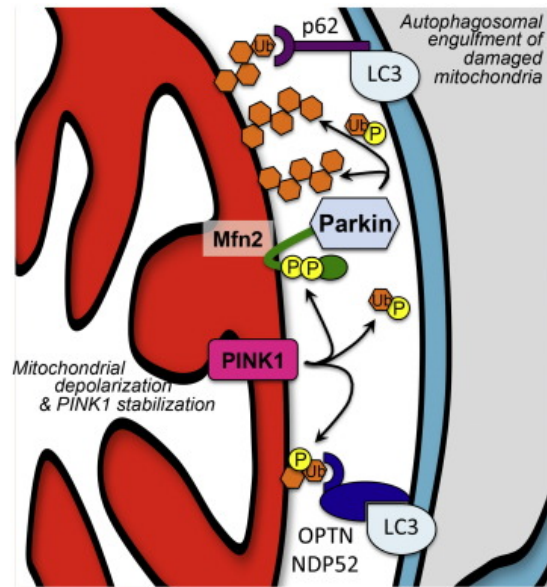
In physiological condition, a dynamic process of biogenesis and degradation sustains mitochondrial mass. The mechanism of degradation was characterized very recently and it is called mitophagy (Lemasters, 2005).

Mitophagy is a specific type of macroautophagy that allows the elimination of whole damaged mitochondria, passing through the autophagosome vesicle. It represents a crucial mechanism for mitochondrial quality control. Once the process is active, the phagophore recognize, tether and engulf the mitochondrion to form the autophagosome that at the end, fused with the lysosome. To this aim, cells need specialized molecules that sense damaged organelles and mark them with a signal for autophagic disposal (Eiyama A., & Okamoto, K., 2015).

Two main mitophagy mechanisms have been described in mammalian cells. The first one occurs during reticulocyte maturation where the autophagic protein ULK1 and ATG7 are mobilized during the early step of the process (Kundu et al., 2008). In addition also the mitochondrial protein BCL2/adenovirus E1B 19 kDa protein-interacting protein 3-like (BNIP3L or NIX) is involved (Schweers er at., 2007; Sandoval et al., 2008). NIX is a single pass membrane protein belonging to the BH3 family, imbedded in the outer membrane of the mitochondrion. Importantly, NIX contains an LC3-interacting region (LIR) at its N-terminal, facing the cytosol (Novak et al., 2010). With this domain NIX recognizes the pool of LC3 present on the phagophore surface and allow the formation of the autophagosome around the mitochondria.

The second mechanism is explained by the activity of two proteins: the E3 ubiquitin ligase Parkin, and PINK1 (Narendra et al., 2008; Fig.1.11). Normally, PINK1 is kept at an undetectable level in cells, by a mechanism that consists in two different post-translational cleavages that provoke the dissociation of the protein form the mitochondria. After the

depolarization of mitochondrial membrane and consequent lost of membrane potential, PINK1 is targeted to damage mitochondria, escaping from the post-translational modification. Here it stable associates with a translocase of the outer membrane (TOM) (Lazarou, et al., 2012). In this conformation, PINK1 homodimerizes and autophosphorylates, becoming active and capable to promote Parkin translocation to mitochondria (Okatsu et al., 2012). Once at the mitochondrion, PARKIN-mediated ubiquitination of mitochondrial substrates, including mitofusins (MFN1/2), leads to the recruitment of p62 and

1.11: Schematic representation of PINK/Parkin1 dependent mitophagy (Gerald W. Dorn II. 2015).

LC3. Then, mitochondria are engulfed into the autophagosome and eliminated through mitophagy.

1.4.2 Bif-1 and mitochondria

Bif-1 was firstly identified as a pro-apoptotic factor that binds to and activates Bax protein, in response to apoptotic stimuli (Cuddenback et al., 2001). Its membrane binding activity underling Bif-1 implication in the regulation of mitochondrial morphology; indeed its knockdown results in elongated mitochondria in HeLa cells (Karbowski et al., 2004). On the contrary in neuronal cells, Bif-1 knockdown attenuates apoptosis and promotes mitochondrial fragmentation (Wang et al., 2014). Loss of Bif-1 supresses mitophagy in MEF expressing Parkin, treated with the uncoupling reagent carbonyl cyanide *m*-chlorophenyl hydrazone (CCCP); in addition in this scenario, cells accumulate ER-associate immature autophagosome-like structures (Takahashi et al., 2013). The same work proposed a model in which Bif-1, together with Class III PI3K complex II, regulates the delivery of Golgi membranes positive for ATG9, to damaged mitochondria, to promote the formation of autophagosomes.

Until now there is no evidence about the involvement of calpain in the regulation of mitophagy; its connection with Bif-1 might indicate a possible role of this protease also in the control of this process.

2. MATERIALS AND METHODS:

2.1 Plasmids and reagents

The pAmCyan-N1-Bif1, pGEX-4T1-Bif-1, pEF6-Bif-1wt-Myc-HisA, pEF6-Bif-1dSH3-Myc and the pEF6-Myc-HisA-Bif-1S were a kind gift of Dr. Hong-Gang Wang. pHAGE-N-GFP-ATG9 and MSCV-Tet-FLAG-HA-IRES-PURO-ATG9 were generously provided by Dr. Ivan Dikic. HcRed-LC3 was constructed by inserting human LC3 in HcRed plasmid. Thapsigargin and Isopropil-β-D-1-tiogalattopiranoside (IPTG) were bought from Sigma. Antibodies were obtained from the following sources: rabbit anti-ATG9, mouse anti-Bif-1 and rabbit anti-pIRE from Novus Biologicals; mouse anti-Flag, rabbit anti-Actin, and mouse anti-CAPNS1 from Sigma; mouse anti-GM130 and mouse anti-p62 from BD Transduction Laboratories; mouse anti-Myc-Tag from Cell Signaling; goat anti-CAPN1 precursor and goat anti-CD71(TfR) from Santa Cruz; rabbit anti-active CAPN1 from Abcam; rabbit anti-Vps34 from ThermoFisher Scientific. LC3 antibodies were purified from rabbit serum after immunization with GST-LC3 according to standard procedures. siRNA targeting CAPNS1 was purchased from Eurofins MWG Operon (Germany): the pool of four siRNAs targeting CAPNS1 (1-GAG CAU CUC UAU AAC AUG AUU TT, 2-CCA CAG AAC UCA UGA ACA UUU TT, 3-UCA GGG ACC AUU UGC AGU AUU TT, 4-GAA GAU GGA UUU UGA CAA CUU TT). The Baculovirus reagents, RFP-GFP-LC3, GFP-Rab5a, RFP-KDEL-Calreticulin, and GFP-E1-alpha-pyrivate-dehydrogenase, were purchased from ThermoFisher Scientific. For the in-vitro transcription and translation of radio-marked proteins TnT T7 Quick Coupled Transcription/Translation System (Promega) was used.

2.2 Cell Culture, transfection and shRNA mediated silencing

U2OS cells were grown in Dulbecco's modified Eagle's medium (DMEM) low glucose, supplemented with 10% FCS, 1% penicillin/streptomycin (Lonza) and L-glutamine. U2OS pRS-control and pRS-shCAPNS1 were produced according to standard procedures. For cell infections: 293GP packaging cells were transfected with the calcium-phosphate method with pRetroSuper-shCAPNS1 or vector alone, after 72 hours the supernatant was harvested, filtered and added to U2OS cells. The infected cells were selected by the addition of puromycin and after 7 days the expression of CAPNS1 was checked by western blot. The same protocol was used to produce U2OS cells stably expressing HA-Flag-ATG9. For the production of the shCAPNS1 stable cell line with the reintroduction of calpain small subunit,

the U2OS cells describe above were infected with a pwzL vector expressing CAPNS1. 293T cells were grown in DMEM high glucose, supplemented with 10% FCS and 1% penicillin/streptomycin. Wild-type, CAPNS1-/- and *rescued* mouse embryonic fibroblasts (Arthur et al., 2000) were a kind gift of Dr. Peter A. Greer (Ontario, Canada); cells were grown in DMEM high glucose, supplemented with 10% FCS, 1% penicillin/streptomycin and Non-Essential Aminoacids solutions 100X (Sigma). For transient transfection and silencing, TransIT-LT1 transfection reagent (Mirus) and Lipofectamine RNAiMAX (Invitrogen) were used respectively, according to the manufacturer's instructions.

2.3 Western Blot analysis and immunoprecipitation

Western blotting was performed on cells lysates (50 mM Tris-HCl pH 7.5; 150 mM NaCl, 5 mM EDTA, 1% Triton X-100, supplemented with 0.5 mM NaF, 2 mM EGTA, 1 mM Sodium orthovanadate and complete protease inhibitor cocktail (Sigma)). Lysates were clarified by centrifugation for 10 min at 4°C and protein concentrations were assessed using Bradford protein assay (BioRad Laboratories). Samples containing equal amounts of proteins were boiled in SDS sample buffer, resolved using SDS-PAGE and transferred to nitrocellulose membranes. The blots were then probed with the appropriate antibodies. Before immunoprecipitation, U2OS cells stably expressing HA-Flag-ATG9 were transiently silenced for CAPNS1 for 3 days, and then treated for 1 h with 100 nM thapsigargin. Whole cell lysates (20 mM CHAPS, 125 mM NaCl, 50 mM TrisHCl, pH 7.5, supplemented with 0.5 mM NaF, 1 mM Sodium orthovanadate, complete protease inhibitor cocktail (Sigma)) were incubated for 2 h with anti-Flag antibody or with the anti-Myc antibody as a negative control. Protein G (GE Healthcare Life Sciences) was used to immunoprecipitate whole lysates for 2 h at 4°C. Samples were subjected to SDS-PAGE and immunoblotted.

2.4 Confocal Microscopy and live-cell imaging

Staining of U2OS cells transiently transfected with GFP and AmCyan tagged proteins or with Baculovirus reagents was performed after the cells were fixed on coverslips with 3% PFA for 20 min., washed with 0,1 M glycine in PBS and stained with Hoechst or Propidium Iodide for 5 min at room temperature. For immunofluorescence: after fixation with PFA, cells were permeabilized with 0,1% Triton-X100 in PBS for 5 min., and blocked in PBS containing 5% BSA for 30 min. at room temperature; then the slides were stained with the appropriate antibodies (antibodies dilution 1:100) and incubated for 2 h at 37°C. Following 3 washings with PBS, samples were stained with secondary antibody for 1 h at room temperature. Images

were acquired with LSM510 confocal microscope (Zeiss), and processed using ImageJ software. Imaging of live U2OS cells, grown on Nunc Glass Base dishes (Thermo Scientific) was performed on LSM510 confocal microscope (Zeiss), equipped with a cells incubator. During the 2 h time-lapse experiment, images were acquired every 2 min.

2.5 In vitro cleavage assay:

^{35}S-labelled in-vitro translated proteins were produced by standard procedures and incubated with micro-calpain on ice in 10 mM Tris, pH 7.5, 1.5 mM DTT, 750 μM $CaCl_2$. Reactions were terminated at the indicated time points by adding SDS-PAGE loading buffer and analysed on SDS-PAGE.

2.6 Electron Microscopy

Electron microscopy analysis was performed in collaboration with Eeva Liisa Eskelinen (University of Helsinki). In details, monolayers were fixed in 2% glutaraldehyde in 0,2 M Hepes buffer, pH 7.4, for 1 h at room temperature. Next the cells were incubated in 1% osmium tetroxide in 0,1 M sodium cacodylate buffer, pH 7.4, with the addiction of 15 mg/mL of potassium ferrocyanide, for 1 hour at room temperature. Then slides were dehydrated in a graded series of ethanol and embedded in Epon using routine procedures. Approximately 60-nm sections were cut and stained using uranyl acetate and lead citrate and were examined with a transmission electron microscope (Jeol JEM-1400). For autophagosome (AP) and autolysosomes (AL) quantification, sections were screened systematically at 4000x and pictures were acquired, in order to cover all the surface of the sections. Then the number of AP and AL was counted and reported as number of vacuoles per cell.

2.7 Expression and purification of GST-Bif-1

GST-Bif-1 wild type was expressed by pGEX-4T-1 plasmid in BL21de3 strain of *Escherichia coli*. Briefly, transformed cells were grown in Luria Bertani medium containing 100 μg/mL ampicillin at 37°C to an $A_{600\ nm}$ 0,8; then 1 mM IPTG was added to induce protein expression at 37°C for 3 h. Cells were lysed in PBS, pH 7.4, supplemented with 0.5 mM NaF, 2 mM EGTA, 1 mM Sodium orthovanadate and complete protease inhibitor cocktail, by sonication and centrifuged at 8000 xg for 30 min. The resulting supernatant was incubated with Glutathione Sepharose 4B (GE Healthcare) at 4°C for 1 h and then washed three times with PBS. The protein was eluted with 10 mM reduced glutathione in 50 mM Tris-HCl, pH 8.

2.8 FACS analysis

Cells were harvested and incubated with Mitotracker Orange CMTMRos (Invitrogen) or TMRE (Abcam), at room temperature for 45 min., then washed in PBS and resuspended in 500 μL of PBS. Unstained cells were used to set the threshold for FLH2 positive cells. 10.000 cells were analysed for each condition using a FACS Calibur flow cytometer (BD Biosciences); data were analysed using FlowJo software (Tree Star, Ashland, USA).

2.9 Statistical analysis

Results are expressed as means ± standard deviation of at least three independent experiments performed in triplicate, unless indicated otherwise. Statistical analysis was performed using Student's t-test. The p-value is indicated in the graph.

3. RESULTS AND DISCUSSION

Calpain represents a promising target for cancer therapy; the expression levels of micro-calpain and calpastatin are significantly associated with clinical-pathological criteria including tumour grade and oestrogens receptor expression. High expression of milli-calpain in basal-like or triple-negative disease is associated with adverse breast cancer-specific survival (Stoor et al, 2012). Recently, our group demonstrated that calpain small subunit 1 is involved in the switch from symmetric to asymmetric division of breast cancer stem cells (Raimondi et al., 2016). For these reasons, the principal interest of our laboratory is to study the roles of calpain, in cellular processes that function as a barrier against tumorigenesis. Autophagy is one of these processes. It was demonstrated that calpain activity is necessary for the proper progression of macroautophagy (Demarchi et al., 2006), indeed the depletion of CAPNS1 causes the accumulation of LC3 proteins in endosome like structures that could represent an alternative pathway, when autophagy is defective.

3.1 Autophagy studies after thapsigargin treatment

In order to characterize the role of calpain in the regulation of the autophagic pathway, we generated a U2OS cell line, where the regulatory subunit of the ubiquitous calpains, CAPNS1, is stably depleted and as a consequence also the activity of CAPN1 and CAPN2 are abrogated. Thapsigargin was utilized as an inducer of autophagy, since it inhibits the activity of the SERCA pump, that firstly causes endoplasmic reticulum stress (ER stress) and consequently autophagy induction (Ogata et al., 2006; Ding et al., 2007). In addition, the block of the SERCA pump causes an increase in the cytoplasmic levels of calcium, promoting calpain activation. For this study, 100 nM thapsigargin was added to shControl and shCAPNS1 U2OS cells. As shown in the western blot of the figure 3.1A, thapsigargin can rapidly and transiently induce an increase in active CAPN1 and a reduction in CAPN1 precursor. In order to monitor autophagosome formation kinetics, control and shCAPNS1 cells were incubated for 0, 30, 60 120 min. with 100 nM thapsigargin and lysates collected. In control cells, LC3 is converted to its lipidated form after 120 min, while in CAPNS1 depleted cells, the kinetics of LC3 lipidation appears faster (Fig. 3.1B). On the other hand p62

degradation couples LC3 lipidation in control cells; in contrast it is considerably reduced in shCAPNS1 cells (Fig. 3.1B and quantification in Fig. 3.1C).

Ultra-structural analysis made in collaboration with Eeva-Liisa Eskelinen from the University of Helsinki, demonstrate that a reduced number of autophagosomes are formed in CAPNS1 depleted cells, after autophagy induction, compared to control cells (Fig. 3.1D). Collectively these data suggest that CAPNS1 is involved in LC3-vesicles dynamics and autophagosome formation in response to thapsigargin treatment.
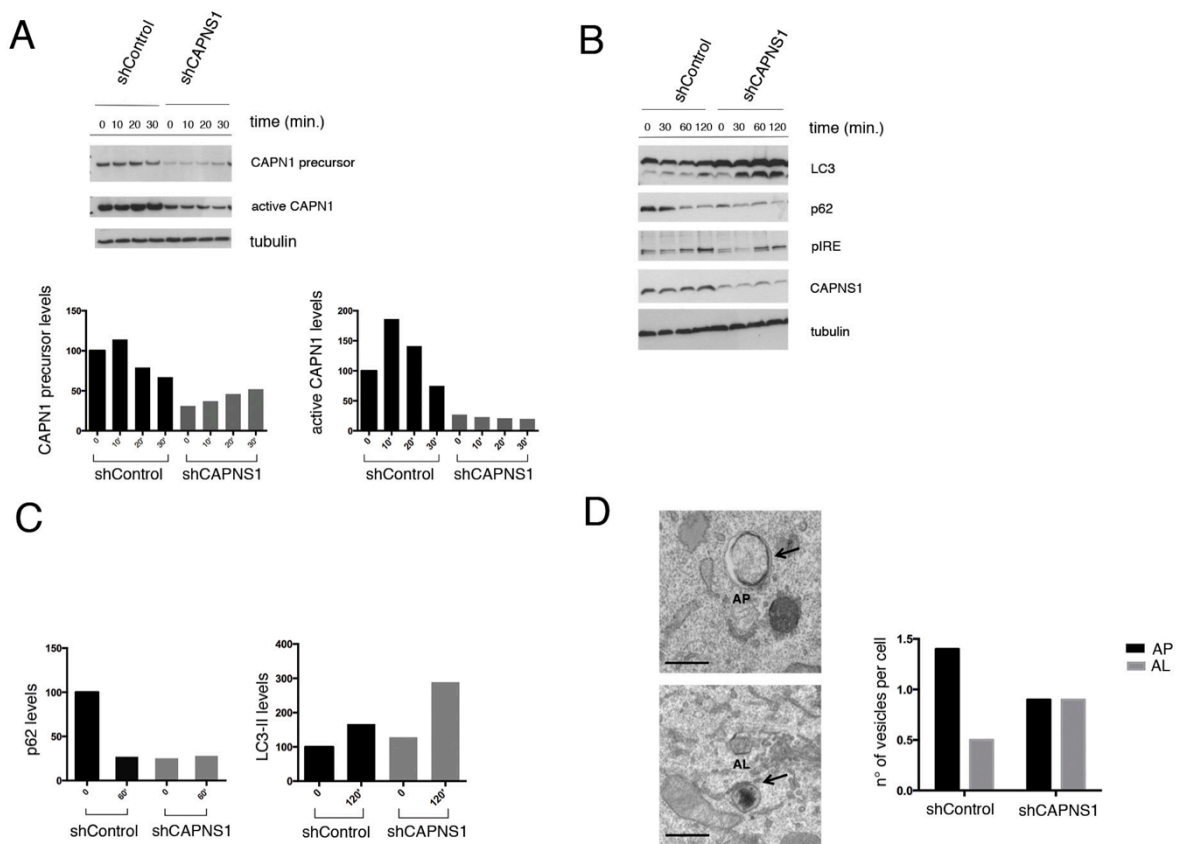

Figure 3.1 Thapsigargin treatment induces calpain activation and autophagy: A: Thapsigargin induces the activation of CAPN1. Control and shCAPNS1 cells were treated with 100 nM thapsigargin for 10, 20 and 30 min. and the lysates subjected to western blot analysis to quantify the precursor and the active form of CAPN1. The graphs represent the levels of precursor and active form normalized by tubulin. B: Control and shCAPNS1 cells were treated with 100 nM thapsigargin for 30, 60 and 120 min. and the lysates subjected to immune blot analysis to detect LC3, p62, pIRE, CAPNS1 and tubulin. C: Quantification of p62 and LC3-II levels of the figure B normalized by tubulin. D: Control U2OS and shCAPNS1 cells treated with 100 nM thapsigargin were analyzed by transmission electron microscopy. On the left representative pictures of autophagosome=AP and autolysosome=AL; scale bars correspond to 500 nM. The graph on the right shows the number of vesicles per cell.

3.2 Early endosomes dynamics are perturbed in CAPNS1 depleted cells

The endocytic pathway is strictly connected with the autophagic process, not only to deliver the degradative enzymes necessary to the lysosome, but also contributing at different stages to the progression of autophagy, from phagophore formation to autophagosome maturation (Tooze et al., 2014).

We previously reported that CAPNS1 depletion causes the impairment in autophagosome formation and ectopic LC3 accumulation in early endosome-like structure (Demarchi et al., 2006). To further characterize this phenotype live-cell imaging experiments were performed. Control and CAPNS1 depleted USO2 cells were stained with commercial baculovirus
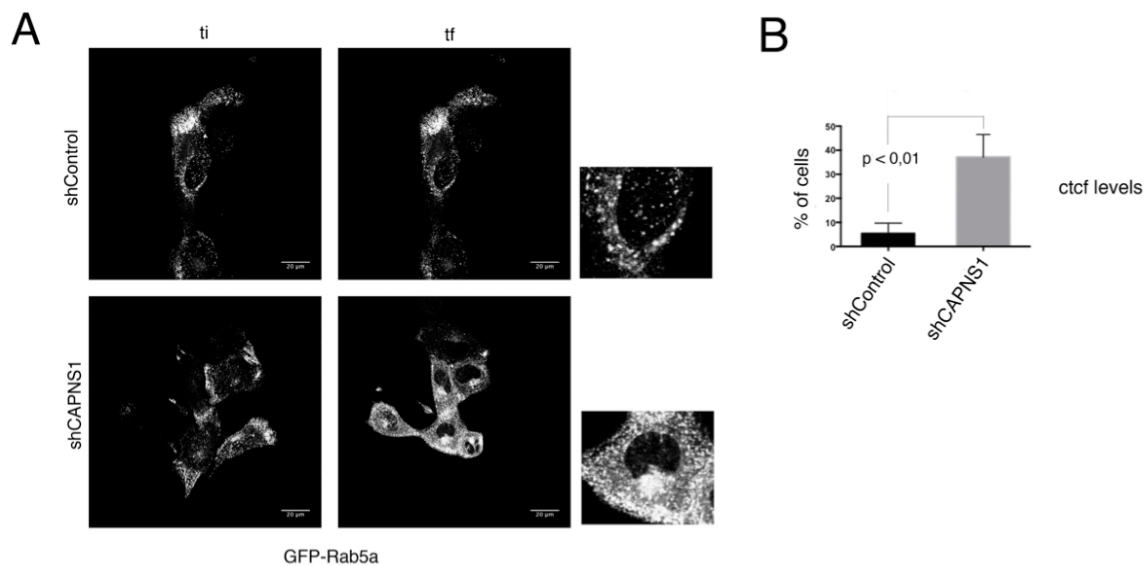

Figure 3.2: Early endosomes dynamics are impaired in CAPNS1 depleted cells: A: Control and shCAPNS1 U2OS cells were grown on petri dishes, infected with a commercial baculovirus expressing GFP-Rab5a protein and 12 hours after transfection, were analyzed using a confocal microscope to detect the dynamics of Rab5a positive vesicles. Images were acquired every 2 min., the first (ti) and last (tf) pictures of each time lapse are shown. Scale bars correspond to 20 μM. B: Corrected total cell fluorescence (CTCF) levels of GFP-Rab5a measured on fixed control and shCAPNS1 cells. The graph indicates the percentage of cells that show a CTFC $\geq 3x10^6$; the error bars represent standard deviation of three different independent experiments, where 100 cells were analyzed; p value < 0,01.

expressing the GFP tagged early-endosome marker Rab5a. 24 hours later, a 2 hours time-lapse experiment was performed using the LSM-510 Zeiss confocal microscope. After the first 15 minutes, 100 nM thapsigargin was added to trigger calpain activation and to induce autophagy. Upon treatment, GFP-Rab5a stained endosomes accumulate in shCAPNS1 cells, in particular near the perinuclear regions (Fig. 3.2A, lower panels). This phenomenon is not observed in control cells (Fig. 3.2A, upper panels). To further verify Rab5a behaviour and to quantify this phenotype, the same experiment was repeated and the cells were analysed after fixation on a coverslips. Corrected total cell fluorescence (CTCF), was measured using

ImageJ software. As in indicated in figure 3.2B, almost 40% of CAPNS1 depleted cells are characterized by a CTCF $\geq 3 \times 10^6$, 2 hours after thapsigargin addition, showing a four fold increase in the levels of GFP-Rab5a fluorescence intensity respect to control cells, confirming the data obtained by time-lapse video microscopy. Interestingly, in control cells treated with Calpeptin, a synthetic calpain inhibitor peptide, Rab5a stained endosomes accumulate just like upon CAPNS1 depletion (Fig. 3.3). Collectively these results demonstrate that calpain deficiency affects early endosomes dynamics upon autophagy induction.
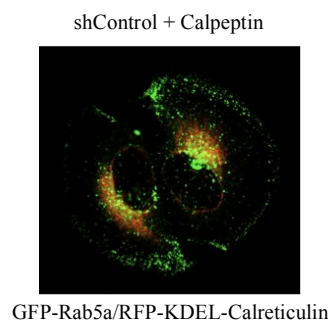
shControl + Calpeptin

GFP-Rab5a/RFP-KDEL-Calreticulin

Figure 3.3: Representative field of control U2OS cells stained with GFP-Rab5a and RFP-KDEL-calreticulin baculovirus reagents; 12 h after infection, cells were treated for 2 h with 0,5 mM Calpeptin, a calpain inhibitory peptide. Samples were then fixed and analyzed under a confocal microscope.

3.3 CAPNS1 depletion causes an accumulation of LC3-II-positive structures

We have already demonstrated that in cells lacking for calpain there is an increase in the level of expression of the lipidated LC3 (Fig. 3.1B). This form binds double lipids layer characterizing not only the matured autophagosome, but also earlier structures like the phagophore, and finally also the autolysosome. Time-lapse imagining of live cells clearly shows that CAPNS1 depletion influences early-endosomes trafficking in thapsigargin treated cells; we therefore applied the same technology to monitor RFP-GFP-LC3 behaviour, upon thapsigargin treatment. This double tagged marker stains all the structures that characterize the autophagic process; indeed, it is a pH-sensitive marker that stains in yellow the autophagosomes and earlier structures, while it stains in red autolysosomes, where the acid pH of theses vesicles bleach the GFP fluorescence.

U2OS cells were seeded and grown on coverslips for 24 hours; then RFP-GFP-LC3 baculovirus reagent was added to the cells. The day after, cells were treated with 100 nM thapsigargin for 2 hours, fixed and analysed with a confocal microscope. Figure 3.4A shows

some representative fields. The number of yellow dots was counted and graphed in figure 3.4B. CAPNS1 depletion is coupled to an increase in the amount of yellow dots as compared to control cells.
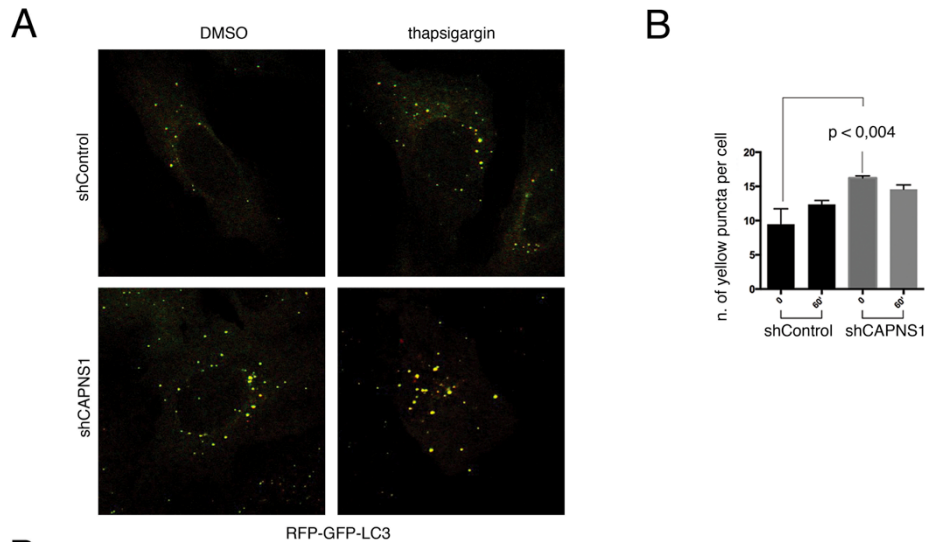

Figure 3.4: CAPNS1 depletion causes an accumulation of LC3-II-positive structures: (A) Control and CAPNS1 CAPNS1 depleted U2OS cells were treated with commercial RFP-GFP-LC3 expressing baculovirus. 12 hours later, cells were treated with 100 nM Thapsigargin or DMSO for 2 hours, and then fixed and analyzed. Representative confocal microscopy pictures of the experiments are shown. (B) Quantification of the yellow dots staining shown in panel A; error bars represent the standard deviation of the mean of three different independent experiments, where 25 cells were analysed.
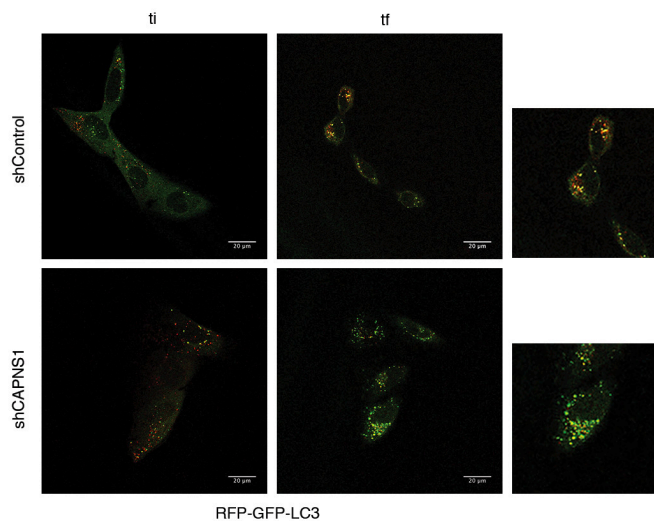

Figure 3.5: LC3 dynamics are altered in CAPNS1 depleted cells: First (ti) and last (tf) pictures of a live-cell imaging experiment, to study LC3 dynamics. Control and CAPNS1 depleted U2OS cells were treated with RFP-GFP-LC3 baculovirus reagent; 12 hours after infection, the samples were analyzed under a confcoal microscope for 2 h time-lapse experiment. After the first 15 min, 100 nM thapsigargin to induce autophagy.

To further examine LC3 dynamics, we followed its behaviour in a time-lapse experiment. In CAPN S1 depleted cells we noticed an increase in the levels of yellow dots as compared to control cells (Fig. 3.5, right panels). Taken together the increasing number of Rab5a positive

early-endosome structures, and the accumulation of LC3-II-positive structures, suggest a possible connection between calpain activity and the regulation of the early stages of autophagosome formation and maturation.

3.4 CAPNS1 depletion is coupled to Golgi redistribution

One of the major events for the nucleation of the autophagosome is the delivery of recycling membranes from different sources within the cytoplasm. Indeed the growing phagophore receives membranes from the ER-Golgi intermediate compartment, recycling endosomes, plasma membrane and also Golgi. We hypothesized that calpain could interfer at this level, regulating the delivery of membranes toward the site of autophagosome formation. In order to verify this hypothesis control, CAPNS1 depleted, and their derivative with reintroduced CAPNS1 U2OS cells were used to immunostain the endogenous cis-Golgi protein GM130.
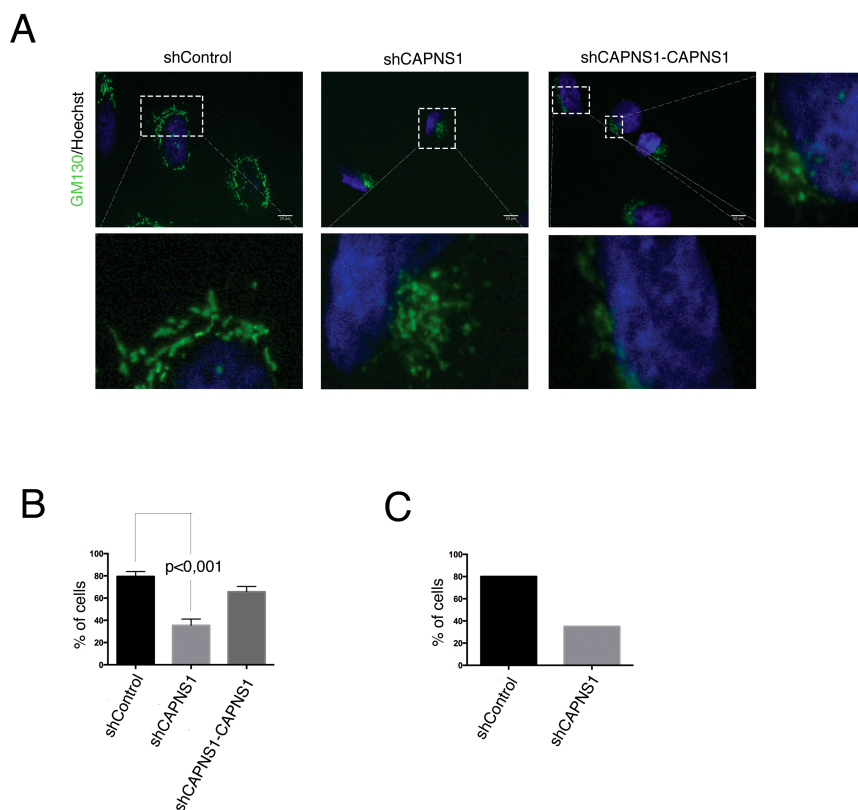

Figure 3.6: CAPNS1 depletion perturbs Golgi distribution: A: Control, CAPNS1 depleted and shCAPNS1 with the reintroduction of CAPNS1 cells were fixed and stained with GM130 antibody. Hoechst die was used to decorate nuclei. A fluorescence microscope was used to acquire pictures; scale bars represent 20 μM. B: The graph reports the quantification of % of cells with Golgi membranes surrounding the nucleus; 100 cells for each sample were considered; the error bars represent the standard deviation of three different independent experiments. C: Control and shCAPNS1 U2OS cells were analyzed by transmission electron microscopy, 20 cells for each sample were considered; the graph reports the percentage of cells with Golgi membranes surrounding the nucleus.

Fluorescence analysis reveals that in U2OS lacking CAPNS1 activity, the Golgi network preferentially localizes at one site of the nucleus, while in control cells its distribution is more scattered (Fig. 3.6A and quantification in B). To further examine the localization of the Golgi membranes we performed a transmission electron microscopy study. As expected in control cells, Golgi membranes surround the nucleus while, in cells depleted for CAPNS1 it is mainly gathered at one side of it (Fig. 3.7 and quantification in fig. 3.6C). Similar results were obtained also in mouse embryonic fibroblast (MEFs). Altogether these results indicate that calpain activity is important for Golgi distribution; a disruption of the regular localization of Golgi cisternae within the cytoplasm might have consequences also on the autophagic process.
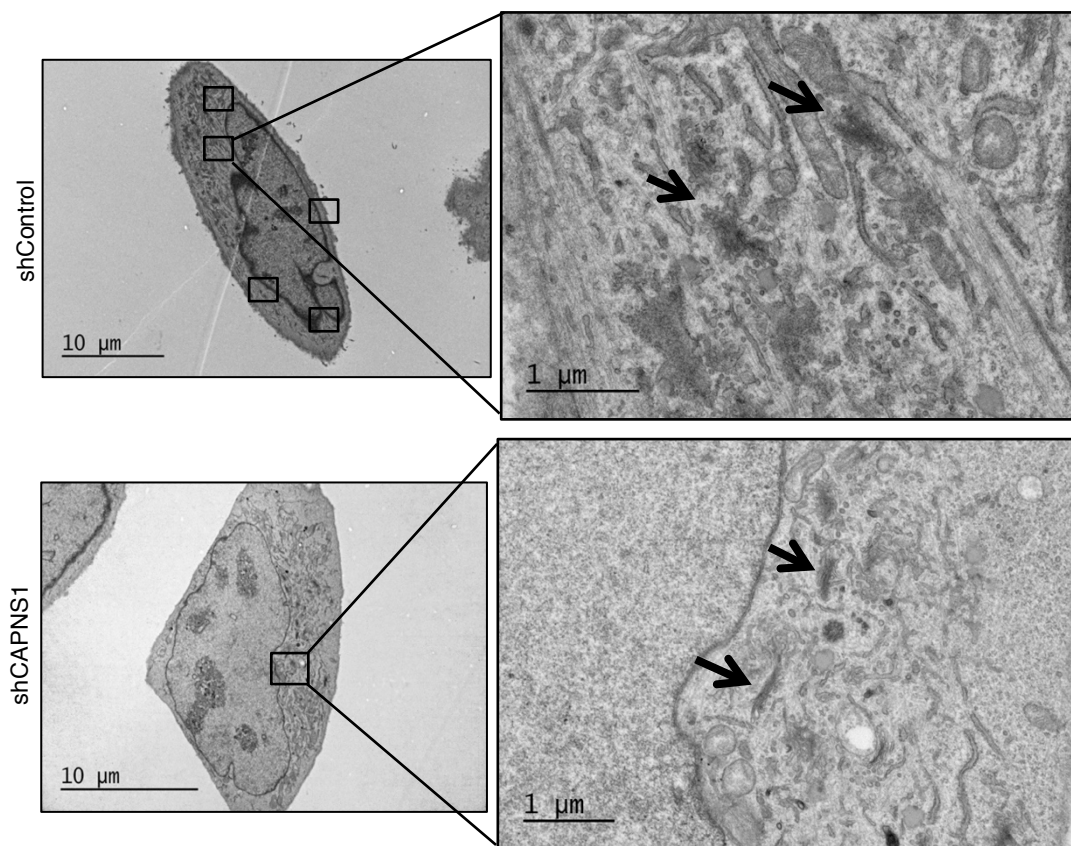

Figure 3.7: Ultrastructural analysis of Golgi membranes: Representative electron microscopy micrographs of control (upper picture) and CAPNS1 depleted (lower picture) U2OS cells that show the localization of Golgi membranes within the cytoplasm: in control cells Golgi distributes all around the nucleus; while in CAPNS1 cells it is mainly found at one side. Arrows indicate Golgi stacks.

3.5 ATG9 dynamics are altered in CAPNS1 depleted cells

The only trans-membrane protein required for the progression of the autophagic process is ATG9. This protein normally localizes on the trans-Golgi region and co-localizes with late

and early endosome markers; upon autophagy induction it co-localizes with LC3 (Young et al., 2006). Recent findings demonstrated that ATG9 is responsible for the delivery of Golgi membranes towards the site where autophagy starts (Takahshi et al., 2011). Since calpain depletion affects not only LC3-II production, but also the distribution of the Golgi membranes, we investigated ATG9 and LC3 dynamics in our U2OS cellular system. Control and shCAPNS1 U2OS cells were transiently co-transfected with GFP-ATG9 and HcRed-LC3 and 24 hours later analysed by in vivo imaging in a 2 hours time-lapse experiment. After the first 15 minutes, 100 nM thapsigargin was added to induce autophagy. In control cells, ATG9 clearly localizes in the trans-Golgi region (Fig. 3.8A shControl, left panel); after autophagy induction it co-localizes with LC3 and it is more likely presented in the peripheral cytoplasm (Fig. 3.8A shControl right panel). On the contrary, in shCAPNS1 cells, ATG9 has a different behaviour: ATG9 positive vesicles localize near LC3 positive dots; interestingly unstained vesicles appear near the nucleus (Fig. 3.78 shCAPNS1 right panel).
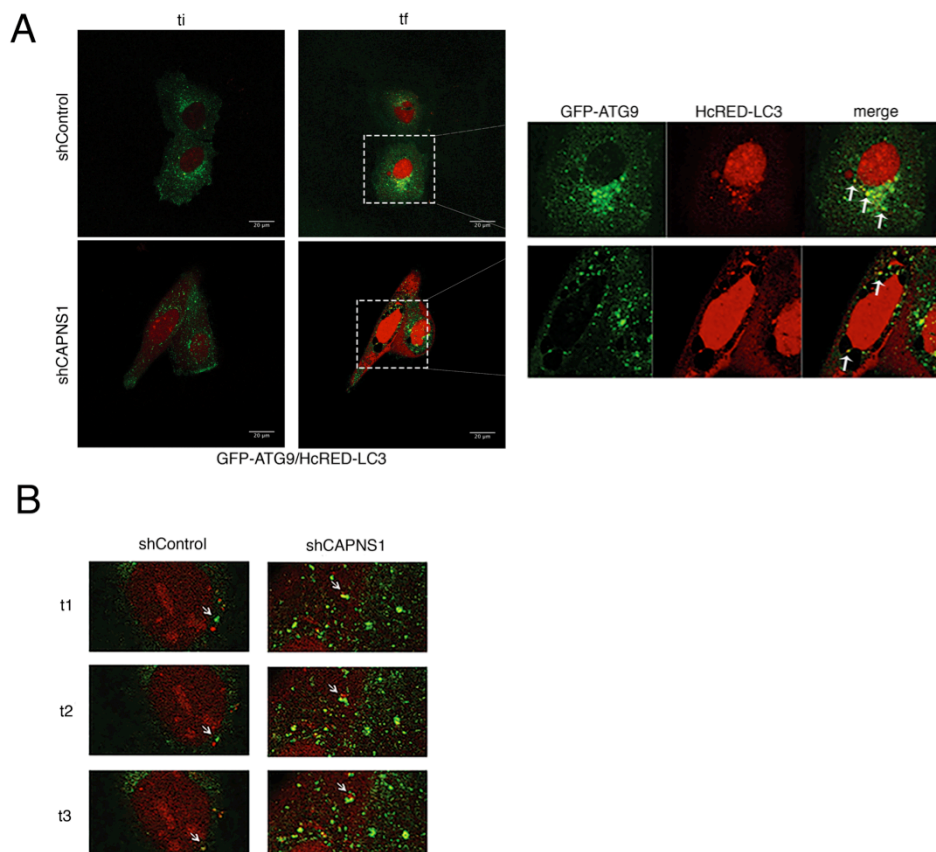

Figure 3.8: ATG9 dynamics is impaired in CAPNS1 depleted cells: A: ShCAPNS1 and control cells were co-transfected with GFP-Atg9 and HcRed-LC3. 12 hours after transfection, cells were analyzed using a confocal microscope to detect Atg9 and LC3 dynamics. Images were acquired every 2 minutes; the first (ti) and last (tf) merged pictures of the two hours time-lapse experiments are shown. Scale bars represent 20 μM. Magnifications of boxed areas are shown in right panels. B: Images sequences (t1, 2, 3) of the GFP-ATG9/HcRed-LC3 time lapse experiment made in control and CAPNS1 depleted U2OS cells. In control cells the arrow indicates one ATG9 vesicle that meets and fuses with the LC3 positive vesicle. In shCAPNS1 cells ATG9 and LC3 positive vesicles are more stationary.

Moreover, in CAPNS1 depleted cells ATG9/LC3 positive vesicles are more stationary as compared to the ones in control cells (Fig. 3.8B), suggesting the impairment in vesicles dynamics.

3.6 CAPNS1 is important for the interaction of ATG9 with its targets

To further assess the involvement of calpin in ATG9 dynamics, we investigated biochemically its interaction with reported targets: the transferrin receptor (TfR), a protein that characterizes the recycling endosomes, and Vps34 a component of the Class III PI3K complex. Flag-ATG9 was immunoprecipitated from control and CAPNS1 silenced cells and the immunoprecipitation products checked for the presence of TfR, both in basal and in autophagy induced conditions. As it was already reported, ATG9 interacts with TfR in control cells; notably CAPNS1 depletion reduced this interaction. Moreover upon autophagy induction with 100 nM thapsighargin, this is even less evident in shCAPNS1 cells (Fig.3.9).
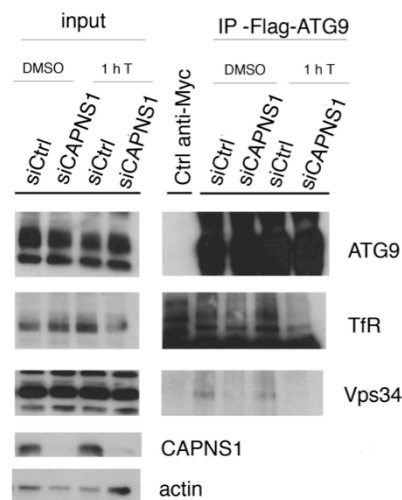

Figure 3.9: Biochemical studies of ATG9 interactors: Flag-ATG9 stably expressing U2OS cells were transfected with a CAPNS1 specific siRNA or a Control siRNA. 48 hours later the cells were treated for 1 hour with DMSO or 100 nM Thapsigargin before lysis and immunoprecipitation with an anti FLAG antibody. Western blot was performed to visualize FLAG-ATG9, endogenous TfR and Vps34.

In parallel we also checked for the interaction of ATG9 with Vps34, a component of the class III PI3K. We found that in control cells ATG9 interacts with this protein, underlying again the importance of ATG9 in the initial step of the autophagic process. Moreover, the presence

of CAPNS1 is essential for this interaction. Taken together, these data demonstrate that calpain is dispensable for the proper trafficking of ATG9.

3.7 CAPNS1 depletion prevents trafficking of ATG9 and Bif-1 containing vesicles upon induction of autophagy by thapsigargin

Endophilin B1/Bif-1 allows Golgi fission and the delivery of ATG9, upon autophagy induction. Bif-1 interacts directly to the double lipid layer of membranes thank to its N-BAR domain promoting Golgi fission (Takahashi et al., 2011). As a first approach to test any effect of calpain on Bif-1, we checked its distribution respect to LC3, in presence or absence of CAPNS1. AmCyan-Bif-1 and HcRed-LC3 constructs were transiently transfected in control and shCAPNS1 depleted cells. The day after cells were fixed and analysed with a confocal microscope. As it is shown in figure 3.10A and B, CAPNS1 depletion causes an accumulation of Bif-1 positive aggregates near the nucleus, when compared to control cells. Thus, calpain is important for Bif-1 distribution within the cytoplasm. Interestingly, in Bif-1-positive aggregates, also LC3-positive dots are visible. To study ATG9 and Bif-1 movement together and respect to the Golgi compartment, we transiently transfected Am-Cyan-Bif-1 in a U2OS cell line derivative stably expressing a Flag-ATG9 construct, after CAPNS1 depletion or treatment with a control siRNA. Before or after induction of autophagy with 100 nM thapsigargin, we analysed ATG9 and Bif-1, and endogenous GM130 by immunofluorescence staining.

We found that in control cells, Bif-1 co-localized together with ATG9 and away from the Golgi, after induction of autophagy (Fig. 3.10C, upper panels); on the contrary, in CAPNS1 depleted cells after autophagy induction, Bif-1 and ATG9 remain on the Golgi (Fig. 3.10C, lower panels; quantification in Fig. 3.10D). Collectively these data suggest that calpain regulates the delivery of Golgi derived membranes toward the site of autophagosome formation.
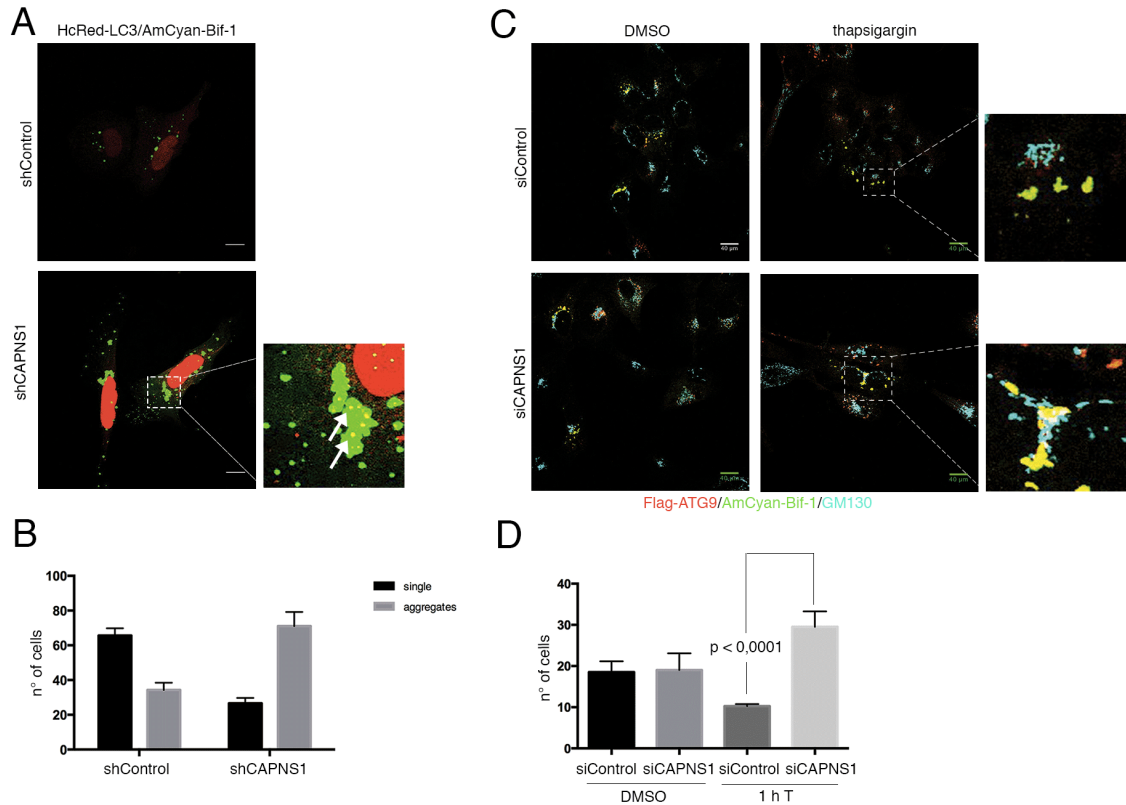
Figure 3.10: ATG9 Bif-1 trafficking from the Golgi is impaired in CAPNS1 depleted cells: A: Control and shCAPNS1 U2OS cells were transiently co-transfected with AmCyan-Bif-1 and HcRed-LC3. 16 hours later, the cells were fixed and analyzed with a confocal microscope. Scale bars represent 20 μM. B: 100 cells for each sample were considered and the number of cells where Bif-1 forms aggregates or single dots was counted. The graph represents the means and standard deviations of three independent experiments. C: U2OS cells stably expressing Flag-Atg9 were transiently silenced with a CAPNS1 specific or control siRNA and then transfected with AmCyan-Bif-1. 24 h later they were treated for 1 h with or without 100 nM thapsigargin and then fixed and analysed by Immunofluorescence to visualize endogenous GM130, Flag-Atg9 and AmCyan-Bif1. Confocal merged pictures are reported in panel C; scale bars represent 20 μM. 50 cells for each sample were considered and the n° of cells where Atg9/Bif-1 proteins remains on the Golgi membranes was counted. The graph in panel D shows the mean and standard deviation of three independent experiments.

3.8 Bif-1 as a possible substrate of calpain protease activity

The identification of a possible calpain substrate is not easy because its protease activity is not dependent on a specific aminocid sequence, but recognizes bonds between domains (Suzuki et al., 2004). In the last few years, bio-informatics tool based on the Multiple Kernel Learning algorithm, have been developed with the aim to identify putative calpain cleavage sites on an aminoacid sequence (duVerle et al, 2011; http://calpain.org/). Taking advantage of this tool, two putative calpain cleavage sites were identified on Bif-1 sequence: one after the 66th aminoacid, in the middle of the N-BAR domain, while the second one, indicates a putative cleavage site after the 253th, that represents the end of the N-BAR domain

(Fig.3.11A). To verify this prediction, we performed an in-vitro cleavage assay. Wild-type Bif-1 (Bif-1wt), Bif-1 lacking the SH3 domain (Bif-1 dSH3) and the SH3 domain alone (Bif-1 SH3) were produced as [35S]-methionine-labelled proteins by in-vitro transcription and translation.
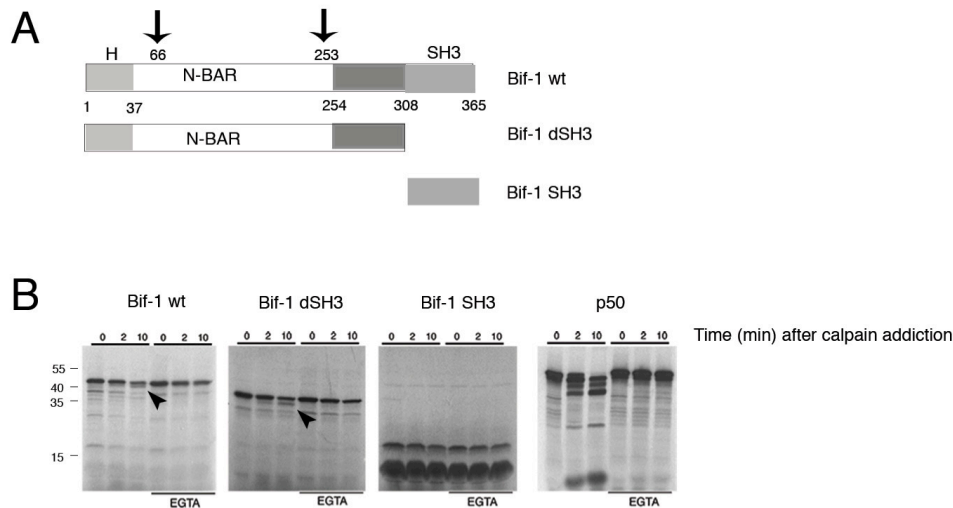

Figure 3.11: The N-terminal region of the Bif-1 protein is cleaved by calpain: A: Schematic representation of the domain structure of wild type Bif-1 and mutants. Bif-1 contains an N-BAR domain and a C-terminal SH domain. Arrows indicate 2 putative calpain cleavage sites on Bif-1. B: In vitro cleavage of Bif-1: Bif-1 wt, Bif-1 dSH, Bif-1 S or p50 NF-κB1 were produced as [35S]methionine-labelled proteins by in vitro transcription and translation and incubated for the indicated time intervals (minutes) with commercial micro-calpain, as previously described (Demarchi 2005). The reactions were then stopped in Laemmli buffer and analyzed by SDS-PAGE and autoradiography. Parallel reactions in the presence of 10 μM EGTA were carried out to prove the calcium dependency of the reactions. Arrowheads indicate the cleavage product.

NF-kB1 p50 was produced as a positive and negative control for the cleavage experiment. Radioactive products were incubated for the indicated time intervals (0, 2 and 10 min.) with commercial micro-calpain. As it is shown in figure 3.11B, a cleavage product is formed both from Bif-1 wt and for Bif-1 dSH3, but not from Bif-1 SH3, or in control samples treated with EGTA, an inhibitor of calpain proteases. These results demonstrate that micro-calpain cuts Bif-1 outside the SH3 domain.

3.9 GST-Bif-1 cleavage made by micro-calpain

To further investigate the cleavage site of calpain on Bif-1, we performed a pilot in-vitro cleavage assay using purified N-terminal GST tagged Bif-1 wilt type. For protein production, BL21de3 competent cells were transformed with pGEX4T-1-Bif-1 plasmid. GST-Bif-1 was expressed and purified with standard procedures. To better characterize the putative calpain

cleavage on Bif-1, we incubated for different times (0', 10', 20') the purified protein with micro-calpain. The cleavage products were analysed by western blot analysis, using both anti-Bif-1 and anti-GST antibodies. As it is shown in figure 3.12 (indicated by the arrows), the 70 kDa GST-Bif-1 full length band is evident in all the lanes, stained by both the antibodies, but it is less present in the samples treated with calpain; in addition a cleavage product at an apparent molecular weight slightly higher than GST alone is recognized both by the anti-GST and the anti-Bif-1 antibody (that recognizes the N-terminal region of Bif-1). This assay demonstrates therefore that the cleavage occurs near the N-terminus of Bif-1, as suggested by the invitro cleavage assay performed with 35S-labeled full length and shorter Bif-1 constructs. Further experiment, including mass spectrometry analysis have to be performed in order to establish the precise Bif-1 aminoacid cleaved by calpain.
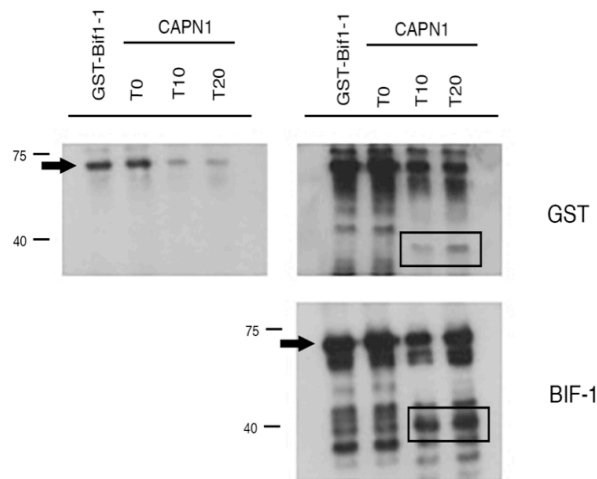

Figure 3.12: Bif-1 protein is cleaved by calpain: in vitro cleavage of GST-Bif-1 wild type: briefly, synthetic GST-Bif-1, expressed and purified from E. coli, was incubated for the indicated time (10' and 20') with purified CAPN1; the resulting products were analyzed by western blot and decorated with anti GST antibody (upper images) and with anti Bif-1 antibody (lower image). Arrows indicate the full length GST-Bif-1 while the cleavage product is indicated in the rectangular shapes.

3.10 Calpain activity coupled to mitochondrial behaviour

Calpain is important for the proper activity of Bif-1, that is a protein involved also in the mitochondrial apoptotic response through BAX. To verify if calpain activity on Bif-1 is specific for the regulation of autophagy or if affects also other processes, we investigated if the depletion of CAPNS1 affects mitochondrial dynamics. First of all, we stained mitochondria using GFP-Pyruvate-dehydrogenase baculovirus reagents and we checked the cells fixed on coverslips, with a confocal microscope. As shown in figure 3.13A, preliminary

results didn't show emerging differences in the staining. In parallel mitochondrial content was quantified using Image J software and results reported as % of mitochondrial area compared to whole cell area (Fig. 3.13B). Also in this experiment there are no significant differences in the amount of mitochondrial organelles in control and CAPNS1 depleted U2OS. Collectively both this information suggests that the lacking of CAPNS1 doesn't affect mitochondrial behaviour. To test if calpain activity on Bif-1 is important also for mitochondrial dynamics, we treated cells with 10 μM carbonyl cyanide-4-(trifluoromethoxy)phenylhydrazone (FCCP). This reagent is able to uncouple mitochondrial membranes, allowing the recruitment of Parkin and promoting mitochondrial autophagy. After 20 hours of treatment with FCCP, cells were stained with MitoTracker Orange, and analysed by FACS, detecting the fluorescence intensity (FLH2) of 10000 cells. As reported in figure 3.13C there are not significant differences in the FLH2 levels of the samples. As
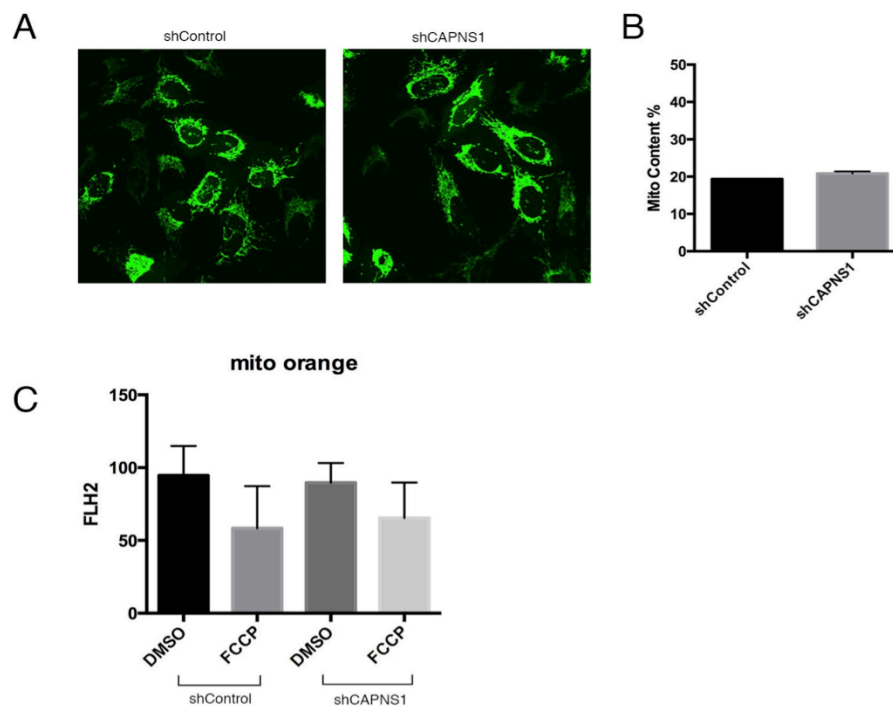

Figure 3.13: Mitochondrial behaviours in CAPNS1 depleted cells: A: Representative confocal microscopy fields of control and CAPNS1 depleted U2OS cells stained with GFP- pyruvate dehydrogenase. B: Quantification of mitochondrial content in control and shCAPSN1 cells. Error bars represent the standard deviation of the mean of three different independent experiments. C: Graph represents FACS analysis of control and CAPNS1 depleted cells stained with Mitotracker Orange, treated or not for 12 h with 10 μM FCCP.

expected, FCCP treated cells, shown a slightly lower level of FLH2, confirming that a % of mitochondria are damaged and they can't retain the staining. In parallel, we have confirmed this data, using another fluorescent probe, the tetramethylrhodamine ethyl-ester (TMRE); this

reagent stains active mitochondria and therefore measures changing in mitochondrial membrane potential (data not shown).

Collectively these preliminary results led us to hypothesis that calpain activity on Bif-1 is not important for its interaction with BAX.

CONCLUSION

Ubiquitous micro and milli-calpain are cytoplasmic proteases that require the calpain small subunit 1 for theirs proper activity (Goll et al., 2003). In this study we identified a calpain substrate that is involved in the early step of the autophagic process: the Endophilin B1/Bif-1 protein.

The controversial role of autophagy in cancer formation and progression, make this field really challenging. Indeed, the autophagic process can be activated in response to cellular stress signals, damaged organelles and increasing metabolic demand, having thus a protective role against tumour formation. On the other hand, cancer cells can exploit the autophagic machinery to escape from anti-cancer treatments, helping the progression of tumour. As we have already mentioned, the calpain system is involved in different cellular contexts connected to salvage pathways such as apoptosis and autophagy, and its overexpression was observed in different type of cancers. For these reasons the aim of this project was to dissect the role of calpain in the regulation of autophagy, in particular on macroautophagy. The cellular system choosen for this study is the U2OS cell line, where CAPNS1 is stably depleted and as a consequence also the activity of CAPN1 and CAPN2 are abrogated.

As a first approach we studied the kinetics of autophagosomes formation in our cellular system, measuring the levels of the expression of two well-known autophagic markers: p62 and LC3. Interestingly, this experiment showed us that calpain depletion is coupled to an increase in the level of lipidated LC3 expression, suggesting an alteration in the autophagic dynamics. Similar results were obtained using confocal imaging experiments. Moreover ultra-structural analysis performed with a transmission electron microscopy confirmed this data, displaying a defect in the formation of autophagosome vesicles in calpain depleted cells, upon autophagy induction. The study of the early endosome marker Rab5a, led us to identify an impairment also in the endocytic pathway, that is known to be connected at different levels with the autophagic process. The LC3-II accumulation coupled with the increase of the expression of Rab5a verified in calpain-depleted cells, suggest a possible involvement of calpain in the earlier stages of the autophagic process. Autophagosomes grow and mature as a consequence of different cellular events; one of these is the fusion with membranes derived from other organelles, such as the endoplasmic reticulum, the Golgi network, mitochondria and plasma membrane. Interestingly, in cells lacking calpain we saw a completely different

distribution of the Golgi network, as compared to control cells. Indeed, without calpain, Golgi stacks localized only at one side of the nucleus, while in control cells they surround the nucleus. This difference in the distribution of the Golgi network in calpain-depleted cells, could interfere with the process of formation of the autophagosome and partially explains the accumulation of lipidated LC3 as well as the aggregation of Rab5a positive vesicles. The only trans-membrane protein of the autophagic process, normally localized on the trans-Golgi membranes, is ATG9. One reported function of this protein is the delivery of Golgi stacks toward the site where the autophagosome forms (Takahasi et al., 2011). Upon autophagy induction it is localized together with LC3 and in peripheral cytoplasm. Time-lapse experiments evidenced that in CAPNS1 depleted cells, once autophagy is induced, the behaviour of ATG9 is completely different as compared to control cells. Moreover, biochemical studies showed that ATG9 interacts less with its targets: the TfR, marker of the recycling endosomes, and Vps34, component of the Class III PI3K complex. Taken together these data suggest that calpain is directly or indirectly necessary for the proper activity of ATG9; one possibility is that in control cells, once autophagy is active, ATG9 delivers Golgi membranes towards the phagophore, where interacts with components of the Class III PI3K; then it is recycled back thanks to recycling endosomes. On the contrary, in CAPNS1 cells, ATG9 remains on the Golgi membrane; therefore there is no interaction with its targets. Trying to explain if calpain acts directly or not on ATG9, we became interested in another protein that in the last years has acquired always more importance in the autophagy field: Bif-1. This protein is responsible of membrane dynamics of different organelles, including also the Golgi membranes. In particular, thanks to its N-BAR domain, directly binds to the lipid layers, inducing the curvature of membranes. Interestingly Bif-1 is essential for the delivery of ATG9 positive Golgi membranes, toward the site where autophagy starts. In this scenario, ubiquitous calpains could act on Bif-1 promoting its detachment from Golgi membranes once autophagosome is formed. Results obtained analysing with a confocal microscopy, ATG9, Bif-1 and Golgi dynamics together, highlights this possibility. In fact in control cells, Bif-1 co-localized together with ATG9 and away from the Golgi membranes after induction of autophagy with thapsigargin; on the opposite, in CAPNS1 depleted cells, Bif-1 and Atg9 remain on the Golgi. In parallel, taken advantages of a bio-informatics tool able to predict calpain cleavage site on an aminoacid sequence, we identified two putative cleavage sites on Bif-1. To test this prediction we performed an in-vitro cleavage assay using micro-calpain, and we identified a cleavage product of Bif-1. Micro calpain cleaves the very N-terminal of Bif-1, corresponding to the region characterized by the presence of the amphipathic helix (H)

that plays a crucial role in binding to membrane. In calpain-depleted cells Bif-1 is able to bind to Golgi membranes but it's not detached from these, possibly because calpain is not acting. This hypothesis is sustained by the imaging studies performed in this work that revealed a general dysfunction at the beginning of the autophagic process, an altered behaviours of ATG9 and Bif-1 positive structures and a different distribution of the Golgi network in absence of calpain. Interestingly, a preliminary study on mitochondria dynamics, suggests that calpain activity on Bif-1 could be specific only for macroautophagy. In fact we didn't see differences in mitochondrial behaviour in cells depleted for calpain, in terms of mitochondria content and mitophagy activation following FCCP treatment. We can therefore speculate that calpain activity on Bif-1 is not required for its interaction with Bax or we can support the hypothesis that calpain is able to cleave only Bif-1 bound to Golgi membranes. Collectively these results led us to identify a new calpain substrate, Bif-1. Calpain activity on this protein could regulate the earlier stages of autophagy, in particular the step of the delivery of Golgi membranes toward the site where a nascent autophagosomes is forming. This important information not only deepen the nowadays knowledge regarding autophagy regulation, but could also represent a starting point for the development of an anti-cancer treatment based on autophagy regulation.

REFERENCES:

Alessi, D., R., James, S., R., Downes, C., P., Holmes, A., B., Gaffney, P., R., et al. (1997). Characterization of a 3- phosphoinositide-dependent protein kinase which phosphorylates and activates protein kinase Ba. Curr Biol; 7:261–269.

Arthur, J., S., C., Elce, J., S., Hegadorn, C., Williams, K., Greer, P., (2000). Disruption of the murine Calpain Small Subunit Gene, Capn4: calpain is essential for embryonic development but not for cell growth and division. Mol Cell Biol; 20(12):4474-4481.

Averna, M., De Tullio, R., Passalacqua, M., Salamino, F., Pontremoli, S., Melloni, E. (2001). Changes in intracellular calpastatin localization are mediated by reversible phosphorylation. Biochem J; 354(Pt 1), 25-30.

Axe, E., L., Walker, S., A., Manifava, M., Chandra, P., Roderick, H., L., Habermann, A., Griffiths, G., Ktistakis, N., T., (2008). Autophagosome formation from membrane compartments enriched in phosphatidylinositol 3-phosphate and dynamically connected to the endoplasmic reticulum. J Cell Biol; 182(4):685-701.

Azam, M., Andrabi, S., S., Sahr, K., E., Kamath, L., Kuliopulos, A., Chishti, A., H., (2001). Disruption of the mouse μ-Calpain gene reveals an essential role in platelet function. Mol Cell Biol; 21(6):2213-2220.

Baghdiguian S, Martin M, Richard I, et al. (1999). Calpain 3 deficiency is associated with myonuclear apoptosis and profound perturbation of the IkappaB alpha/NF-kappaB pathway in limb-girdle muscular dystrophy type 2A. Nat Med; 5:503-511.

Baier, L., J., Permana, P., A., Yang, X., et al.(2000). A calpain-10 gene polymorphism is associated with reduced muscle mRNA levels and insulin resistance. J Clin Inves; 106:R69-R73.

Beckerle, M. C., Burridge, K., DeMartino, G. N., Croall, D. E. (1987). Colocalization of calcium-dependent protease II and one of its substrates at sites of cell adhesion. Cell; 51(4), 569-77.

Benetti, R., Del Sal, G., Monte, M., Paroni, G., Brancolini C., Schnider C., (2001). The death substrate Gas2 binds m-calpain and increases susceptibility to p53-dependent apoptosis. EMBO J; 20(11):2702-2714.

Berg, T., O., Fengsrud, M., Stromhaung, P., E., Berg, T., Seglen, P., O., (1998). Isolation and characterization of rat liver amphisomes. Evidence for fusion of autophagosomes with both early and late endosomes. J Biol Chem; 273(34):21883-21892.

Bernales, S., McDonald, K.,L., Walter, P., (20076). Autophagy counterbalances endoplasmic reticulum expansion during the unfolded protein response. PLoS Biol; 4:e423.

Bertoli, C., Copetti, T., Lam, E. W., Demarchi, F., Schneider, C. (2009). Calpain small-1 modulates Akt/FoxO3A signaling and apoptosis through PP2A. Oncogene; 28(5), 721-33.

Bialkowska K., Du Kulkarni, S., X., Goll, D., E., Saido, T., C., Fox, J., E., (2000). Evidence that beta3 integrin-induced Ras activation involves the calpain-dependent formation of integrin clusters that are distinct from the focal complexes and focal adhesions that form as Rac and RhoA become active. J Cell Biol; 151:685-696.

Bialkowska K., Saido, T., C., Fox, J., E., (2005). SH3 domain of spectrin participates in the activation of Rac in specialized calpain-induced integrin signaling complexes. J Cell Sig; 118:381-395.

Blanchard, H., Grochulski, P., Li, Y., Arthur, J.S., Davies, P.L., Elce, J.S., Cygler, M., (1997). Structure of calpain Ca(2+)-binding domain reveals a novel EF-hand and Ca(2+)-induced conformational changes. Nat. Struct. Biol. 4(7):532-8.

Boya, P., Reggiori, F., Codogno, P., (2013). Emerging regulation and functions of autophagy. Nat Cel Bio; 15:713-720.

Brancolini, C., Bottega, S., Schneider, C. (1992). Gas2, a growth arrest-specific protein, is a component of the microfilament network system. J Cell Biol; 117(6), 1251-61.

Braun, C., Engel, M., Seifert, M., Theisinger, B., Seitz, G., Zang, K. D., Welter, C. (1999). Expression of calpain I messenger RNA in human renal cell carcinoma: correlation with lymph node metastasis and histological type. Int J Cancer; 84(1), 6-9.

Budovskaya YV, Stephan JS, Reggiori F, Klionsky DJ, Herman PK (2004). The Ras/cAMP-dependent protein kinase signaling pathway regulates an early step of the autophagy process in Saccharomyces cerevisiae. J Biol Chem; 279:20663–20671.

Chan, E.Y., Longatti, A., McKnight, N.C. and Tooze, S.A. (2009). Kinase-inactivated ULK proteins inhibit autophagy via their conserved C-terminal domains using an Atg13-independent mechanism. Mol. Cell Biol; 29, 157–171.

Chan, K., T., Bennin, D., A., Huttenlocher, A., (2010). Regulation of adhesion dynamics by calpain-mediated proteolysis of focal adhesion kinase (FAK). J Biol Chem; 285(15): 11418-11426.

Chua, B. T., Guo, K., Li, P. (2000). Direct cleavage by the calcium-activated protease calpain can lead to inactivation of caspases. J Biol Chem; 275(7), 5131-5.

Colunga, A., Bollino, D., Schech, A., Aurelian, L., (2014). Calpain-dependent clearance of the autophagy protein p62/SQSTM1 is a contributor to ΔPK oncolytic activity in melanoma. Gene Ther; 21(4):371-378.

Conacci-Sorrell, M., Ngouenet, C., Eisenman, R., N. (2010). Myc-Nick: a cytoplasmic cleavage product of Myc that promotes α-tubulin acetylation and cell differentiation. Cell; 142:480-493.

Cortesio, C., L., Boateng, L., R., Piazza, T., M., Bennin, D., A., Huttenlocher, A., (2011). Calpain-mediated proteolysis of paxillin negatively regulates focal adhesion dynamics and cell migration. J Biol Chem; 286(12):9998-10006.

Cuddeback, S., M., Yamaguchi, H., Komatsu, K., Miyashita, T., Yamada, M., Wu, C., et al., (2001). Molecular cloning and characterization of Bif-1. A novel Src homology 3 domain-containing protein that associates with Bax. J Biol Chem; 276: 20559–20565.

Del Bello, B., Toscano, M., Moretti, D., Maellaro, E., (2013). Cisplatin-induced apoptosis inhibits autophagy, which acts as a pro-survival mechanism in human melanoma cells. Plos One; 8(2) e57236. Demarchi F, Bertoli, C., Copetti, T., Tanida, I., Brancolini, C., Eskelinen, E., L., Schneider, C., (2006). Calpain is required for macroautophagy in mammalian cells. J Cell Biol; 175(4):595-605.

Ding WX, Ni HM, Gao W, Hou YF, Melan MA, et al. (2007a). Differential effects of endoplasmic reticulum stress-induced autophagy on cell survival. J Biol Chem; 282:4702–4710.

Ding, W., X., Ni, H., M., Gao, W., Yoshimori, T., Stolz, D., B., et al (2007b). Linking of autophagy to ubiquitinproteasome system is important for the regulation of endoplasmic reticulum stress and cell viability. Am J Pathol; 171:513–524.

Dunn W., A., Jr. (1990). Studies on the mechanisms of autophagy: maturation of the autophagic vacuole. J Cell Biol; 110: 1935–1945.

Dusetti NJ, Jiang Y, Vaccaro MI, Tomasini R, Azizi Samir A, et al. (2002). Cloning and expression of the rat vacuole membrane protein 1 (VMP1), a new gene activated in pancreas with acute pancreatitis, which promotes vacuole formation. Biochem. Biophys. Res. Commun. 290:641–649.

Dutt, P., Croall, D., E., Arthur, J., S., C., De Veyra, T., Williams, K., Elce, J., S., Greer, P., A., (2006). M-Calpain is required for preimplantation embryonic development in mice. BMC Dev Biol; 6:3.

Eiyama, A., Okamoto, K., (2015). PINK1/Parkin-mediated mitophagy in mammalian cells. Curr Opin Cell Biol; 33:95-101.

Fahn, S., (2003). Description of Parkinson's disease as a clinical syndrome. Ann N Y Acad Sci; 991:1-14.

Fettucciari, K., Fetriconi, I., Mannucci, R., Nicoletti, I., Bartoli, A., Coaccioli, S., Marconi, P. (2006). Group B Streptococcus induces macrophage apoptosis by calpain activation. J Immunol; 176(12), 7542-56.

Franco, S., J., Rodgers, M., A., Perrin, B., J., Han, J., Bennin, D., A., Critchley, D., R., Huttenlocher, A. (2004). Calpain-mediated proteolysis of talin regulates adhesion dynamics. Nat Cel Bio,; 6(10): 977-983.

Funderburk SF, Wang QJ, Yue Z. (2010). The Beclin 1-VPS34 complex–at the crossroads of autophagy and beyond. Trends Cell Biol. 20:355–362.

Furuta, S., Hidaka. E., Ogata, A., Yokota, S., Kamata, T., (2004). Ras is involved in the negative control of autophagy through the class I PI3-kinase. Oncogene; 23:3898-3904.

Gafni, J., Cong, X., Chen, S., F., Gibson, B., W., Ellerby, L., M., (2009). Calpain-1 cleaves and activates caspase-7. J Biol Chem; 284(37): 25441-25449.

Gallop, J., L. Jao, C., C., Kent, H.,M., Butler, P.,J., Evans, P., R., Langen, R., et al. (2006). Mechanism of endophilin N-BAR domain-mediated membrane curvature. EMBO J; 25:2898–2910.

Geng, J., Klionsky, D., (2010). The Golgi as a potential membrane source for autophagy. Autophagy; 6(7):950-951.

Grynspan, F., Griffin, W., R., Cataldo, A., Katayama, S., Nixon, R., A., (1997). Active site-directed antibodies identify calpain II as an earlyappearing and pervasive component of neurofibrillary pathology in Alzheimer's disease. Brain Res; 763:145-158.

Guroff Gordon, (1964). A neutral, calcium-activated proteinase from the soluble fraction of rat brain. J. Biol. Chem. 239, 149-155.

Hailey, D., W., Rambold, A., S., Saptune-Krishnan, P., Mitra, K., Sougrat, R., Kim, P., K., Lippincott-Schwartz, J., (2010). Mitochondria supply membranes for autophagosome biogenesis during starvation. Cell; 141(4):656-667.

Hamasaki, M., Furuta, N., Matsudo, A., Nezu, A., Yamamoto, A., Fujiita, N., Oomori, H., Noda, T., Haraguchi, T., Hiraoka, Y., Amano, A., Yoshimori, T., (2013). Autophagosomes form at ER–mitochondria contact sites. Nature; 495:389-393.

Hampe, J., Franke, A., Rosenstiel, P., Till, A., Teuber, M., Huse, K., Albrecht, M., Mayr, G., De La Vega, F., M., Briggsm J., Gunter, S., Prescott, N., J., Onnie, C., M., Häsler, R., Sipos, B., Fölsch, U., R., Lengauer, T., Platzer, M., Mathew, C., G., Krawczak, M., Schreiber, S., (2006). A genome-wide association scan of nonsynonymous SNPs identifies a susceptibility variant for Crohn disease in ATG16L1. Nat Gen; 39:207-211.

Hailey, D., W., Kim, P., K., Satpute-Krishnan, P., Rambold, A., S., Mitra, K., Sougrat, R., Lippincott-Schwartz, J., (2010). Mitochondria supply membranes for autophagosome biogenesis during starvation. Cell; 141(4): 656-667.

Han, Y., Weinman, S., Boldogh, I., Walker, R. K., Brasier, A., R., (1999). Tumor Necrosis Factor-α-inducible IκBα Proteolysis Mediated by Cytosolic m-Calpain. J Biol Chem; 274:787-794.

Han, Y., Xue, X., F., Shen, H., G., Guo, X., B., Wang, X., Yuan, B., Guo, X., P., Kuang, Y., T., Zhi, Q., M., Zhao, H., (2014). Prognostic significance of Beclin-1 expression in colorectal cancer: a meta-analysis. Asian Pac J Cancer Prev; 15(11):4583-4587.

Hanna, R., A., Campbell, R., L., Davies, P., L., (2008). Calcium-bound structure of calpain and its mechanism of inhibition by calpastatin. Nature; 456:409-412.

Hayashi-Nishino, M., Fujita, N., Noda, T., Yamaguchi, A., Yoshimori, T., Yamamoto, A., (2010). Electron tomography reveals the endoplasmic reticulum as a membrane source for autophagosome formation. Autophagy; 6(2):301-303.

He, C., Klionsky, D., J., (2009). Regulation mechanisms and signaling pathways of autophagy. Annu Rev Genet. 43:67-93.

Hosfield, C.M., Elce, J.S., Davies, P.L., Jia, Z., (1999). Crystal structure of calpain reveals the structural basis for Ca(2+)-dependent protease activity and a novel mode of enzyme activation. EMBO J. 18:6880-6889.

Hosokawa N, Hara T, Kaizuka T, Kishi C, Takamura A, et al. 2009. Nutrient-dependent mTORC1 association with the ULK1-Atg13-FIP200 complex required for autophagy. Mol. Biol. Cell 20:1981–91.

Høyer-Hansen, M., Bastholm, L., Szyniarowski, P., Campanella, M., Szabadkai, G., et al. (2007). Control of macroautophagy by calcium, calmodulin-dependent kinase kinase-b, and Bcl-2. Mol Cell; 25:193–205.

Huttenlocher, A., Palecek, S., P., Lu, Q., Zhang, W., Mellgren, R., L., Lauffenburger, D., A., Ginsberg, M., H., Horwitz, A., F. (1997). Regulation of cell migration by the calcium-dependent protease calpain. J Biol Chem; 272(52): 32719-32722.

Imajoh, S., Kawasaki, H., Suzuki, K., (1986). The amino-terminal hydrophobic region of the small subunit of calcium-activated neutral protease (CANP) is essential for its activation by phosphatidylinositol. J. Biochem 99(4):1281-4.

Inoki, K., Zhu, T., Guan, K., L., (2003). TSC2 mediates cellular energy response to control cell growth and survival. Cell ; 115:577–790.

Itakura E, Kishi C, Inoue K, Mizushima N. (2008). Beclin 1 forms two distinct phosphatidylinositol 3-kinase complexes with mammalian Atg14 and UVRAG. Mol. Biol. Cell 19:5360–5372.

Itakura E, Mizushima N. (2010). Characterization of autophagosome formation site by a hierarchical analysis of mammalian Atg proteins. Autophagy 6:764–776.

Itakura, E., Kishi-Itakura, C., Mizushima, N., (2012). The hairpin-type tail-anchored snare Syntaxin 17 targets to autophagosomes for fusion with endosomes/lysosomes. Cell; 151(6): 1256-1269.

Itoh, T., Fujita, N., Kanno, E., Yamamoto, A., Yoshimori, T., Fukuda, M., (2008). Golgi-resident small GTPase Rab33B interacts with Atg16L and modulates autophagosome formation. Mol Biol Cell.; 19(7):2916-2925.

Itoh, T., Kanno, E., Uemura, T., Waguri, S., Fukuda, M., (2011). OATL1, a novel autophagosome-resident Rab33B-GAP, regulates autophagosomal maturation. J Cell Biol; 192(5):839-853.

Jahreiss, L., Menzies, F., M., Rubinsztein, D., C., (2008). The itinerary of autophagosomes: from peripheral formation to kiss-and-run fusion with lysosomes. Traffic; 9(4):574-587.

Jeffries T., R, Dove SK, Michell RH, Parker PJ. (2004). PtdIns-specific MPR pathway association of a novel WD40 repeat protein, WIPI49. Mol. Biol. Cell 15:2652–2663.

Jiang, P., Mizushima, N., (2014). Autophagy and human diseases. Cell Res; 24:69-79.

Kabeya Y, Mizushima N, Ueno T, Yamamoto A, Kirisako T, et al. (2000). LC3, a mammalian homologue of yeast Apg8p, is localized in autophagosome membranes after processing. EMBO J. 19:5720–28.

Kabeya Y, MizushimaN, YamamotoA, Oshitani-Okamoto S, OhsumiY,Yoshimori T. (2004). LC3, GABARAP and GATE16 localize to autophagosomal membrane depending on form-II formation. J. Cell Sci. 117:2805–2812.

Kageyama, S., Omori, H., Saitoh, T., Sone, T., Guan, J.-L., Akira, S., Imamoto, F., Noda, T. and Yoshimori, T. (2011). The LC3 recruitment mechanism is separate from Atg9L1-dependent membrane formation in the autophagic responseagainst Salmonella. Mol. Biol. Cell; 22:2290–2300.

Karbowski, M., Jeong, S., Y., Youle, R., J., (2004). Endophilin B1 is required for the maintenance of mitochondrial morphology. J Cell Biol 166:1027-1039.

Kimura, Y., Koga, H., Araki, N., Mugita, N., Fujita, N., Takeshima, H., Nishi, T., Yamashima, T., Saido, T. C., Yamasaki, T., Moritake, K., Saya, H., Nakao, M. (1998). The involvement of calpain-dependent proteolysis of the tumor suppressor NF2 (merlin) in schwannomas and meningiomas. Nat Med; 4(8), 915-22.

Kirisako T, Baba M, Ishihara N, Miyazawa K, Ohsumi M, et al. (1999). Formation process of autophagosome is traced with Apg8/Aut7p in yeast. J. Cell Biol. 147:435–446.

Kitada, T., Asakawa, S., Hattori, N., Matsumine, H., Yamamura, Y., Minoshima, S., Yokochi, M., Mizuno, Y., Shimizi, N., (1998). Nature; 392(6676):605-608.

Kubbutat, M., H., Vousden, K., H., (1997). Proteolytic cleavage of human p53 by calpain: a potential regulator of protein stability. Mol Cell Biol; 17(1):460-468.

Kulkarni, S., Saju, L., Farver, C., Tubbs, R, (2012). Calpain4 is required for activation of HER2 in breast cancer cells exposed to trastuzumab and its suppression decreases survival and enhances response. Int J Cancer; 131(10):2420-2432.

Kundu, M., Lindsten, T., Yang, C., Wu, J., Zhao, F., Zhang, J., Selak, M., A., Ney, P., A., Thompson, C., D., (2008). Ulk1 plays a critical role in the autophagic clearance of mitochondria and ribosomes during reticulocyte maturation. Blood; 112(4): 1493-1502.

Kuo, W., N., Ganesan, U., Davis, D., L., Walbey, D., L., (1994). Regulation of the phosphorylation of calpain II and its inhibitor. Mol Cell Biochem; 136(2):157-161.

Kusakawa, G., Saito, T., Onuki, R., Ishiguro, K., Kishimoto, T., Hisanaga, S., (2000). Calpain-dependent proteolytic cleavage of the p35 cyclin-dependent kinase 5 activator to p25. J Biol Chem; 275(22): 17166-17172.

Lang, T., Reiche, S., Straub, M., Bredschneider, M., Thumm, M., (2000). Autophagy and the cvt pathway both depend on AUT9. J Bacteriol; 182:(8):2125-2133.

Laurin, N., Brown, J., P., Morisette, J., Raymond, V., (2002). Recurrent Mutation of the Gene Encoding sequestosome 1 (SQSTM1/p62) in Paget Disease of Bone. AJHG; 70(6): 1582-1588.

Lazarou, M., Jin, S., M., Kane, L., A., Youle, R., J., (2012). Role of PINK1 binding to the TOM complex and alternate intracellular membranes in recruitment and activation of E3 ligase Parkin. Dev Cell; 22:320-333.

Lebart, M., C., Benyamin, Y., (2006). Calpain involvement in the remodeling of cytoskeletal anchorage complexes. FEBS Journal; 273:3415-3426.

Lee, S. J., Choi, Y. L., Lee, E. J., Kim, B. G., Bae, D. S., Ahn, G. H., Lee, J. H. (2007). Increased expression of calpain 6 in uterine sarcomas and carcinosarcomas: an immunohistochemical analysis. Int J Gynecol Cancer; 17(1), 248-53.

Lee, S. J., Kim, B. G., Choi, Y. L., Lee, J. W. (2008). Increased expression of calpain 6 during the progression of uterine cervical neoplasia: immunohistochemical analysis. Oncol Rep; 19(4), 859-63.

Lemasters, J., J., (2005). Selective mitochondrial autophagy, or mitophagy, as targeted defense against oxidative stress, mitochondrial dysfuntion, and aging. Rejuvenation Res; 8(1):3-5.

Liang, C., Feng, P., Ku, B., Dotan, I., Canaani, D., Oh, B., Jung, J., U., (2006). Autophagic and tumour suppressor activity of a novel Beclin1-binding protein UVRAG. Nat Cell Bio; 8:688-698.

Liang, X., H., Jackson, S., Seaman, M., Brown, K., Kempkes, B., Hibshoosh, H., Levine, B., (1999). Induction of autophagy and inhibition of tumorigenesis by beclin 1. Nature; 402(6762):672-676.

Libertini, S., J., Tepper, C., G., Rodriguez, V., Asmuth, D., M., Kung, H., J., Mudryj, M., (2007). Evidence for calpain-mediated androgen receptor cleavage as a mechanism for androgen independence. Cancer Res; 67(19):9001-9005.

Lieberman, A., P., Puertollano, R., Raben, N., Slaugenhaupt, S., Walkley, S., U., Ballabio, A., (2012). Autophagy; 8(5):719-730.

Lin, L., Ye, Y., Zakeri, Z. (2006). p53, Apaf-1, caspase-3, and -9 are dispensable for Cdk5 activation during cell death. Cell Death Differ; 13(1), 141-50.

Liou, W., Geuze, H., J., Geelen, M., J., H., Slot, J., W., (1997). The autophagic and endocytic pathways converge at the nascent autophagic vacuoles. J Cell Biol.; 136: 61–70.

Liu, T., Mendes, D., E., Berkman, C., E. (2014). Functional prostate-specific membrane antigen is enriched in exosomes from prostate cancer cells. Int J Oncol; 44(3):918-922.

Long X, Ortiz-Vega S, Lin Y, Avruch J. Rheb binding to mammalian target of rapamycin (mTOR) is regulated by amino acid sufficiency (2005). J Biol Chem; 280:23433–23436.

Longatti, A., Lamb, C., A., Razi, M., Yoshimura, S-I., Barr, F., A., Tooze, S., A., (2012). TBC1D14 regulates autophagosome formation via Rab11 and recycling endosomes. J Cell Biol; 197:659-675.

Matsunaga K, Morita E, Saitoh T, Akira S, Ktistakis NT, et al. (2010). Autophagy requires endoplasmic reticulum targeting of the PI3-kinase complex via Atg14L. J. Cell Biol. 190:511–521.

Melloni, E., Averna, M., Salamino, F., Sparatore, B., Minafra, R., Pontremoli, S., (2000). Acyl-CoA-binding protein is a potent m-calpain activator. J Biol Chem; 275(1):82-86.

Menzies, F., M., Garcia-Arencibia, M., Imarisio, S., O'Sullivan, N., C., Ricketts, T., Kent, B., A., Rao, M., V., Lam, W., Green-Thompson, Z., W., Nixon, R., A., Saksida, L., M., Bussey, T., J., O'Kane, C., J., Mizushima N., (2005).The pleiotropic role of autophagy: from protein metabolism to bactericide. Cell Death Differ; 12:1535-1541.

Melser, S., Lavie, J., Benard, G., (2015). Mitochodrial degradation and energy metabolism. Mol Cell Res.

Mizushima, N., (2007). Autophagy: process and function. Genes & Development; 21:2861-2873.

Mizishima, N., (2010). The role of the Atg1/ULK1 complex in autophagy regulation. Curr Opin Cell Biol; 22(2):132-139.

Mizushima, N., Yoshimori, T., Oshumi, Y. (2011). The role of Atg proteins in autophagosome formation. Annu. Rev. Cell. Dev. Biol.; 27:107-132.

Mochizuki, Y., Ohashi, R., Kawamura, T., Iwanari, H., Kodama, T., Naita, M., Hamakubo, T., (2013). Phosphatidylinositol 3-phosphatase myotubularin-related protein 6 (MTMR6) is regulated by small GTPase Rab1B in the early secretory and autophagic pathways. J Biol Chem.; 288(2):1009-1021.

Moldoveanu, T., Gehring, K., Green, D., R., (2008). Concerted multi-pronged attack by calpastatin to occlude the catalytic cleft of heterodimeric calpains. Nature; 456:404-408.

Molejon, M., I., Ropolo, A., Re, A., L., Boggio, V., Vaccaro, M., I., (2013). The VMP1-Beclin 1 interaction regulates autophagy induction. Sci Rep. 3:1055.

Moreau, K., Ravikumar, B., Renna, M., Puri, C., Rubinsztein, D., C., (2011). Autophagosome precursor maturation requires homotypic fusion. Cell; 146(2): 303-317.

Moretti, D., Del Bello, B., Cosci, E., Biagioli, M., Miracco, C., Maellaro, E. (2009). Novel variants of muscle calpain 3 identified in human melanoma cells: cisplatin-induced changes in vitro and differential expression in melanocytic lesions. Carcinogenesis; 30(6), 960-7.

Moretti, D., Del Bello, B., Allavena, G., Maellaro, E., (2014). Calpain and cancer: friends or enemies?. Archives of Biochemistry and Biophysics; 564:26–36.

Murthy, A., Li, Y., Peng, I., Reichelt, M., Kumar Katakam, A., Noubade, R., Roose-Girma, M., DeVoss, J., Diehl, L., Graham, R., R., van Lookeren Campagne, M., (2014). A Crohn's disease variant in Atg16l1 enhances its degradation by caspase 3. Nature; 506: 456-462.

Narendra, D., Tanaka, A., Suen, D., Youle, R., J., (2008). Parkin is recruited selectively to impaired mitochondria and promotes their autophagy. J Cell Biol 183, 5: 795-803.

Nishimo, I., Fu, J., Tanji, K., Yamada, T., Shimojo, S., Koori, T., Mora, M., Riggs, J., E., Shin, J., O., Koga, Y., Sue, C., M., Yamamoto, A., Murakami, N, Shanske, S., Byrne, E., Bonilla, E., Nonaka, I., DiMauro, S., Hirano, M., (2000). Nature; 406:906-910.

Nobukuni T, Joaquin M, Roccio M, Dann SG, Kim SY, et al. (2005). Amino acids mediate mTOR/raptor signaling through activation of class 3 phosphatidylinositol 3OH-kinase. Proc Natl Acad Sci USA; 102:14238–14243.

Noda T, Kim J,Huang W., P., Baba M., Tokunaga C., et al. (2000). Apg9p/Cvt7p is an integral membrane protein required for transport vesicle formation in the cvt and autophagy pathways. J. Cell Biol. 148:465–480.

Norman, J., M., Cohen, G., M., Bampton, E., T., W., (2010). The in vitro cleavage of the hAtg proteins by cell death proteases. Autophagy; 6(8):1042-1056.

Novak, I., Kirkin, V., McEwan, D., G., Zhang, J., Wild, P., Rozenknop, A., Rogov, V., Löhr, F., Popovic, D., Occhipinti, A., Reichert, A., S., Terzic, J., Dötsch, V., Ney, P., A., Dikic, I., (2010). Nix is a selective autophagy receptor for mitochondrial clearance. EMBO Rep; 11(1): 45-51.

Novikoff, A., B., and Essner, E., (1962). Cytolysosomes and mitochondrial degeneration. J. Cell Biol. 15:140-146.

Ogata, M., Hino, S., Saito, A., Morikawa, K., Kondo, S., et al. (2006). Autophagy is activated for cell survival after endoplasmic reticulum stress. Mol Cell Biol; 26:9220–9231.

Okatsu, K., Oka, T., Iguci, M., Imamura, K., Kosako, H., Tani, N., Kimura, M., Go, E., Koyano, F., Funayama, M., Shiba-Fukushima, K., Shiba-Fukushima K, Sato, S., Shimizu, H., Fukunaga, Y., Taniguchi, H., Komatsu, M., Hattori, N., Mihara, K., Tanaka, K., Matsuda, N., (2012). PINK1 autophosphorylation upon membrane potential dissipation is essential for Parkin recruitment to damaged mitochondria. Nat Commun; 3:1016.

Orsi, A., Razi, M., Dooley, H.C., Robinson, D., Weston, A.E., Collinson, L.M. and Tooze, S.A. (2012) Dynamic and transient interactions of Atg9 with autophagosomes, but not membrane integration, are required for autophagy. Mol. Biol. Cell; 23:1860–1873.

Pariat, M., Salvat, C., Bebien, M., Brockly, F., Altieri, E., Carillo, S., Jariel-Encontre, I., Piechaczyk, M. (2000). The sensitivity of c-Jun and c-Fos proteins to calpains depends on conformational determinants of the monomers and not on formation of dimers. Biochem J; 345 Pt 1, 129-38.

Paul, D., S., Harmon, A.,W., Winston, C.,P., Patel, Y., M.,(2003). Calpain facilitates GLUT4 vesicle translocation during insulin-stimulated glucose uptake in adipocytes. Biochem J; 376:625-632.

Pattingre, S., Tassa, A., Qu, X., Garuti, R., Liang, X., H., Mizushima, N., Packer, M., Schneider, M., D., Levine, B., (2005). Bcl-2 antiapoptotic proteins inhibit Beclin 1-dependent autophagy. Cell; 122(6): 927-939.

Pierrat, B., Simonen, M., Cueto, M., Mestan, J., Ferrigno, P., Heim, J., (2001). SH3GLB, a new endophilinrelated protein family featuring an SH3 domain. Genomics; 71: 222–234.

Polson, H.E.J., de Lartigue, J., Rigden, D.J., Reedijk, M., Urbé, S., Clague, M.J. and Tooze, S.A. (2010) Mammalian Atg18 (WIPI2) localizes to omegasomeanchored phagophores and positively regulates LC3 lipidation. Autophagy; 6:506–522.

Punnonen, E., L., Autio, S., Kaija, H., Reunanen, H., (1993). Autophagic vacuoles fuse with the prelysosomal compartment in cultured rat fibroblasts. Eur J Cell Biol.; 61(1):54-66.

Raimondi, M., Marcassa, E., Cataldo, F., Arnandis, T., Mendosa-Maldonado, R., Benstagno, M., Schneider, C., Demarchi, F., (2016). Calpain restrains the stem cells compartment in breast cancer. Cell Cycle; 15(1):106-16.

Ravikumar, B., Acevedo.-Arozena, A., Imarisio, S., Berger, Z., Vacher, C., O'Kane, C., J., Brown, S., D., M., Rubinsztein, D., C., (2005). Dynein mutations impair autophagic clearance of aggregate-prone proteins. Nat Gen; 37(7): 771-776.

Ravikumar, B., Imarisio, S., Sarkar, S., O'Kane, C., J., Rubinsztein, D., C., (2008). Rab5 modulates aggregation and toxicity of mutant huntingtin through macroautophagy in cell and fly models of Huntington disease. J Cell Sci; 121(10):1649-1660.

Ravikumar, B., Moreau, K., Jahreiss, L., Puri, C., Rubinsztein, D., C., (2010). Plasma membrane contributes to the formation of pre-autophagosomal structures. Nat Cel Biol; 12(8):747-757.

Rebecca, V., W., Amaravadi, R., K., (2015). Emerging strategies to effectively target autophagy in cancer. Oncogene; 1-11.

Ropolo A, Grasso D, Pardo R, Sacchetti ML, Archange C, et al. (2007). The pancreatitis-induced vacuole membrane protein 1 triggers autophagy in mammalian cells. J. Biol. Chem. 282:37124–37133.

Rink. J., Ghigo, E., Kalaidzidis Y., Zerial, M., (2005). Rab conversion as a mechanism of progression from early to late endosomes. Cell; 122(5): 735-749.

Rios-Doria, J., Kuefer, R., Ethier, S., P., Day, M., L., (2004). Cleavage of beta-catenin by calpain in prostate and mammary tumor cells. Cancer Res; 64(20): 7237-7240.

Rubinsztein, D., C., (2015). Calpain inhibition mediates autophagy-dependent protection against polyglutamine toxicity. Cell Death Differ; 22(3):433-444.

Saito, K., Elce, J., S., Hamos, J., E., Nixon, R., A., (1993).Widespread activation of calcium-activated neutral proteinase (calpain) in the brain in Alzheimer disease: a potential molecular basis for neuronal degeneration. Proc Natl Acad Sci U S A; 90:2628-2632.

Saitoh, T., Fujita, N., Hayashi, T., Takahara, K., Satoh, T., Lee, H., Matsunaga, K., Kageyama, S., Omori, H., Noda, T., Yamamoto, N., Kawai, T., Ishii, K., Takeuchi, O., Yoshimori, T., Akira, S., (2009). Atg9a controls dsDNA-driven dynamic translocation of STING and the innate immune response. Proc Natl Acad Sci USA 106(49): 20842-20846.

Salamino, F., De Tullio, R., Michetti, M., Mengotti, P., Melloni, E., Pontremoli, S. (1994). Modulation of calpastatin specificity in rat tissues by reversible phosphorylation and dephosphorylation. Biochem Biophys Res Commun; 199(3), 1326-32.

Salamino, F., Averna, M., Tedesco, I., De Tullio, R., Melloni, E., Pontremoli, S. (1997). Modulation of rat brain calpastatin efficiency by post-translational modifications. FEBS Lett; 412(3), 433-8.

Sancak Y, Peterson TR, Shaul YD, Lindquist RA, Thoreen CC, et al.; (2008).The Rag GTPases bind raptor nand mediate amino acid signaling to mTORC1. Science; 320:1496–1501.

Sandoval, H., Thiagarajan, P., Dasgupta, S., K., Schumacher, A., Prchal, J., T., Chen, M., Wang, J., (2008). Essential role for Nix in autophagic maturation of erythroid cells. Nature; 454(7201):232-235.

Sato, K., Hattori, S., Irie, S., Sorimachi, H., Inomata, M., Kawashima, S., (2004). Degradation of fodrin by m-calpain in fibroblasts adhering to fibrillar collagen I gel. J Biochem; 136(6): 777-85.

Scherz-Shouval, R., Shvets, E., Fass, E., Shorer, H., Gil, L., Elazar, Z., (2007). Reactive oxygen species are essential for autophagy and specifically regulate the activity of Atg4. EMBO J; 26:1749–1760.

Schmelzle T., Beck T., Martin D., E., Hall M., N., (2004). Activation of the RAS/cyclic AMP pathway suppresses a TOR deficiency in yeast. Mol Cell Biol; 24:338–351.

Schneider, C., King, R. M., Philipson, L. (1988). Genes specifically expressed at growth arrest of mammalian cells. Cell; 54(6), 787-93.

Schollmeyer, J. E. (1988). Calpain II involvement in mitosis. Science; 240(4854), 911-3.

Schweers, R., L., Zhang, J., Randall, M., S., Loyd, M., R., Li, W., Dorsey, F., C., Kundu, M., Opferman, J., T., Cleveland, J., L., Miller, J.,L., Ney, P., A., (2007). NIX is required for programmed mitochondrial clearance during reticulocyte maturation. Proc Natl Acad Sci USA; 104(49):19500-19505.

Selliah, N., Brooks, W. H., Roszman, T. L. (1996). Proteolytic cleavage of alpha-actinin by calpain in T cells stimulated with anti-CD3 monoclonal antibody. J Immunol, 156(9), 3215-21

Serrano, K. and Devine, D. V. (2004). Vinculin is proteolyzed by calpain during platelet aggregation: 95 kDa cleavage fragment associates with the platelet cytoskeleton. Cell Motil Cytoskeleton; 58(4), 242-52

Shearer, T., R., Ma, H., Shih, M., Fukiage, C., Azuma, M., (2000). Calpains in the lens and cataractogenesis. Methods Mol Biol; 144:277-285.

Shoji-Kawata, S., Sumpter, R., Leveno, M., Campbell, G., R., Zou, Z., Kinch, L., Wilkins, A., D., Sun, Q., Pallauf, K., MacDuff, D., Huerta, C., Virgin, H., W., Helms, J., B., Eerland, R., Tooze, S., A., Xavier, R., Lenschow, D., J., Yamamoto, A., King, D., Lichtarge, O., Grishin, N., V., Spector, S., A., Kaloyanova, D., V., Levine, B., (2012). Identification of a candidate therapeutic autophagy-inducing peptide. Nature; 494: 201-206.

Small, G., W., Chou, T., Y., Dand, C., V., Orlowski, R., Z. (2002). Evidence for involvement of calpain in c-Myc proteolysis in vivo. Arch. Biochem. Biophys.; 400:151–161

Sorimachi, H., Hata, S., Ono, Y. (2011). Impact of genetic insights into calpain biology. J. Biochem; 150(1):23-37.

Stokoe D., Stephens L., R., Copeland T., Gaffney P.,R., Reese C.,B., et al. (1997). Dual role of phosphatidylinositol-3,4,5-trisphosphate in the activation of protein kinase B. Science; 277:567–570.

Storr, S. J., Carragher, N. O., Frame, M. C., Parr, T., Martin, S. G. (2011). The calpain system and cancer. Nat Rev Cancer; 11(5), 364-74.

Storr, S., J., Lee1, K., W., Woolston, C., M., Safuan, S., Green, A., R., Macmillan, R., D., Benhasouna, A., Parr, T., Ellis, I., O., Martin, S., G., (2012). Calpain system protein expression in basal-like and triple-negative invasive breast cancer. Annals of Oncology; 23: 2289-2296.

Stappazzon, F., Vietri-Rudan, M., Campello, S., Nazio, F., Florenzano, F., Fimia, G., M., Piacentini, M., Levine, B., Cecconi, F., (2011). Mitochondrial BCL-2 inhibits AMBRA1-induced autophagy. EMBO J; 30(7):1195-1208.

Suzuki, H., Hata, S., Kawabata, Y., Sorimachi, H. (2004). Structure, activation and biology of calpain. Diabetes; 53 Suppl 1, S12-8.

Suzuki, K., Saido, T., C., Hirai, S., (1992). Modulation of cellular signals by calpain. Ann N Y Acad Sci; 674:218-227.

Takahashi Y, Coppola D, Matsushita N, Cualing HD, Sun M, Sato Y et al., (2007). Bif-1 interacts with Beclin 1 through UVRAG and regulates autophagy and tumorigenesis. Nat Cell Biol; 9: 1142–1151.

Takahashi, Y., Meyerkord, C.L., Hori, T., Runkle, K., Fox, T.E., Kester, M., Loughran, T.P. and Wang, H., (2011) Bif-1 regulates Atg9 trafficking by mediating the fission of Golgi membranes during autophagy. Autophagy; 7:61–73.

Takahashi, Y., Young, M., M., Serfass, J., M., Hori, T., Wang, H., (2013). *Sh3glb1/Bif-1* and mitophagy. Autophagy 9:7, 1107-1109.

Tan, Y., Dourdin, N., Wu, C., De Veyra, T., Elce, J. S., Greer, P. A. (2006b). Ubiquitous calpains promote caspase-12 and JNK activation during endoplasmic reticulum stress-induced apoptosis. J Biol Chem; 281(23), 16016-24.

Tang, H.-W., Wang, Y.-B., Wang, S.-L., Wu, M.-H., Lin, S.-Y. and Chen, G.-C. (2011) Atg1-mediated myosin II activation regulates autophagosome formation during starvation-induced autophagy. EMBO J; 30:636–651.

Tidball, J., G., Spencer, M.,J., (2000). Calpains and muscular dystrophies. Int J Biochem Cell Biol; 32:1-5.

Tooze, J., Hollinshead, M., Ludwig, T., Howell, K., Hoflack, B., Kern, H., (1990). In exocrine pancreas, the basolateral endocytic pathway converges with the autophagic pathway immediately after the early endosome. J Cell Biol; 111(2):329-345.

Tompa, P., Emori, Y., Sorimachi, H., Suzuki, K., Friedrich, P., (2001). Domain III of calpain is a Ca(2+) –regulated phospholipid-binding domain. Biochem Biophys Res Commun 9; 280(5):1333-9.

Tsukada, M., Oshumi, Y., (1993). Isofation and charact~~zation of autophagy-defective mutants of *Saccharomyces cerevisiae.* FEBS; 333(1,2):169-167.

Vaccaro, M., I., Ropolo, A., Grasso, D., Iovanna, J., L., (2008). A novel mammalian trans-membrane protein reveals an alternative initiation pathway for autophagy. Autophagy; 4(3): 388-390.

Valente, E., M., Abou-Sleiman, P., M., Caputo, V., Muqit, M.,M., Harvey, K., Gispert, S., Ali, Z., Del Turco, D., Bentivoglio, A., R., Healy, D., G., Albanese, A., Nussbaum, R., González-Maldonado, R., Deller, T., Salvi, S., Cortelli, P., Gilks, W.,P., Latchman, D., S., Harvey, R., J., Dallapiccola, B., Auburger, G., Wood, N., W., (2004). Hereditary early-onset Parkinson's disease caused by mutations in PINK1. Science; 304(5674):1158-1160.

Wang, C., W., Klionsky, D., J., (2003). The molecular mechanism of autophagy. Mol Med; 9(3-4):65-76.

Wang, D., B., Uo, T., Kinoshita, C., Sopher, B., L., Lee, R., J., Murphy, S., P., Kinoshita, Y., Garden G., A., Wang, H. Morrison, R., S., (2014). Bax Interacting Factor-1 promotes survival and mitochondrial elongation in neurons. J Neurosci, 24(7):2674-2683.

Wang, H., Guo, Z., Wu, F., Long, F., Cao, X., Liu, B., Zhu, Z., Yao, X. (2005). PKA-mediated protein phosphorylation protects ezrin from calpain I cleavage. Biochem Biophys Res Commun; 333(2), 496-501.

Wang, X. D., Rosales, J. L., Magliocco, A., Gnanakumar, R., Lee, K. Y. (2003). Cyclin E in breast tumors is cleaved into its low molecular weight forms by calpain. Oncogene; 22(5), 769-74.

Webber, J.L. and Tooze, S.A. (2010) Coordinated regulation of autophagy by p38alpha MAPK through mAtg9 and p38IP. EMBO J. 29, 27–40.

Wendt, A., Thompson, V. F., Goll, D. E. (2004). Interaction of calpastatin with calpain: a review. Biol Chem; 385(6), 465-72.

Williams, A., Sarkar, S., Cuddon, P., Ttofi, E., K., Saiki, S., Siddiqi, F., H., Jahreiss, L., Fleming, A., Pask, D., Golsmith, P., O'Kane, C., J., Andres Floto, R., Rubinsztein, D., C., (2008). Novel targets for Huntington's disease in an mTOR independent autophagy pathway. Nat Chem Bio; 4(5):295-305.

Wolter K. G., Hsu Y. T., Smith C. L., Nechushtan A., Xi X. G., Youle R. J. (1997). Movement of Bax from the Cytosol to Mitochondria during Apoptosis. J. Cell Biol; 139:1281–1292.

Wood, D. E., Thomas, A., Devi, L. A., Berman, Y., Beavis, R. C., Reed, J. C., Newcomb, E. W. (1998). Bax cleavage is mediated by calpain during drug-induced apoptosis. Oncogene; 17(9), 1069-78.

Xu, L. and Deng, X. (2006). Suppression of cancer cell migration and invasion by protein phosphatase 2A through dephosphorylation of mu- and m-calpains. J Biol Chem; 281(46), 35567-75.

Yamada, T., Carson, A., R., Caniggia, I., Umebayashi, K., Yoshimori, T., Nakabayashi, K., Scherer, S., W., (2005). Endothelial nitric-oxide synthase antisense (NOS3AS) gene encodes an autophagy-related protein (APG9-like2) highly expressed in trophoblast. J Biol Chem; 280(18)18283-18290.

Yamaguchi, R., Maki, M., Hatanaka, M., Sabe, H. (1994). Unphosphorylated and tyrosine-phosphorylated forms of a focal adhesion protein, paxillin, are substrates for calpain II in vitro: implications for the possible involvement of calpain II in mitosis-specific degradation of paxillin. FEBS Lett; 356(1), 114-6

Yamamoto, H., Kakuta, S., Watanabe, T., M., Kitamura, A., Sekito, T., Kondo-Kakuta, C., Ichikawa, R., Kinjo, M., Oshumi, Y., (2012). Atg9 vesicles are an important membrane source during early steps of autophagosome formation. J Cell Biol. 198(2):219-233.

Yang, J., Zhang, L., Lee, S., Y., Gad, H., Luini, A., Hsu, V., W., (2006). Key components of the fission machinery are interchangeable. Nat Cell Biol; 8:1376-1382.

Ylä-Anttila, P., Vihinene, H., Jokitalo, E., Eskelinen, E., L., (2009). 3D tomography reveals connections between the phagophore and endoplasmic reticulum. Autophagy; 5(8):1180-1185.

Yoshikawa, Y., Mukai, H., Hino, F., Asada, K., Kato, I. (2000). Isolation of two novel genes, down-regulated in gastric cancer. Jpn J Cancer Res; 91(5), 459-63.

Yousefi, S., Perozzo, R., Schmid, I., Ziemiecki, A., Schaffner, T., Scapozza, L., Brunner, T., Simon, H. U. (2006). Calpain-mediated cleavage of Atg5 switches autophagy to apoptosis. Nat Cell Biol; 8(10), 1124-32.

Zhang, H., Bosch-Marce, M., Shimoda, L., A., Tan, Y., S., Baek J., H., et al. (2008). Mitochondrial autophagy is an HIF-1-dependent adaptive metabolic response to hypoxia. J Biol Chem; 283:10892–10903.

Zatz, M., De Paula, F., Starling, A., Vainzof, M., (2003). The 10 autosomal recessive limb-girdle muscular dystrophies. Neuromuscul Disord; 13:532-544.

Zatz, M. and Starling, A. (2005). Calpains and disease. N Engl J Med; 352(23), 2413-23.

Zhong Y,Wang QJ, Li X, Yan Y, Backer JM, et al. (2009). Distinct regulation of autophagic activity by Atg14L and Rubicon associated with Beclin 1-phosphatidylinositol-3-kinase complex. Nat. Cell Biol. 11:468–76.

ACKNOWLEDGEMENTS

Taylor & Francis
Taylor & Francis Group

REPORT

Calpain restrains the stem cells compartment in breast cancer

M. Raimondi[a,†], E. Marcassa[a,†], F. Cataldo[a], T. Arnandis[a,$], R. Mendoza-Maldonado[a], M. Bestagno[c], C. Schneider[a,b,†], and F. Demarchi[a,†]

[a]L.N.C.I.B., Laboratorio Nazionale Consorzio Interuniversitario Biotecnologie AREA Science Park – Padriciano 99, Trieste, Italy; [b]Dipartimento di Scienze e Tecnologie Biomediche, Universita' degli Studi di Udine, Udine, Italy; [c]International Centre for Genetic Engineering and Biotechnology, AREA Science Park – Padriciano 99, Trieste, Italy

ABSTRACT

CAPNS1 is essential for the stability and function of ubiquitous CAPN1 and CAPN2. Calpain modulates by proteolytic cleavage many cellular substrates and its activity is often deregulated in cancer cells, therefore calpain inhibition has been proposed as a therapeutical strategy for a number of malignancies. Here we show that CAPNS1 depletion is coupled to impairment of MCF7 and MCF10AT cell lines growth on plate and defective architecture of mammary acini derived from MCF10A cells. In soft agar CAPNS1 depletion leads to cell growth increase in MCF7, and decrease in MCF10AT cells. In both MCF7 and MCF10AT, CAPNS1 depletion leads to the enlargement of the stem cell compartment, as demonstrated by mammosphere formation assays and evaluation of stem cell markers by means of FACS and western blot analysis. Accordingly, activation of calpain by thapsigargin treatment leads to a decrease in the stem cell reservoir. The expansion of the cancer stem cell population in CAPNS1 depleted cells is coupled to a defective shift from symmetric to asymmetric division during mammosphere growth coupled to a decrease in NUMB protein level.

Introduction

CAPNS1 regulatory subunit is essential for the stability and function of ubiquitous calpain-1, CAPN1 and calpain-2, CAPN2.[14] Both CAPN1 and CAPN2 are generally overexpressed upon transformation.[15] CAPN1 expression is associated with relapse-free survival in breast tumors from patients treated with trastuzumab following adjuvant chemotherapy.[16] Conversely, high expression of CAPN2 in basal-like or triple-negative disease was associated with adverse breast cancer-specific survival.[17] We reported that CAPNS1 interferes with PP2A-Akt interaction, consequently affecting FoxO3A-dependent cell death in mouse embryonic fibroblasts and human MCF7 cells. We therefore suggested that ubiquitous Calpain inhibition might be exploited as a tool to induce apoptosis in tumors sensitive to FoxO activation.[1] In accordance with our findings, CAPN2 regulates proliferation, survival, migration, and tumorigenesis of breast cancer cells in mouse models, via the PP2A-Akt-FoxO-p27Kip1 signaling axis.[6] CAPN1 stabilizes USP1 deubiquitinating enzyme during the G1 phase of the cell cycle in human osteosarcoma cells and fibroblasts, indeed calpain inhibits USP1 proteasomal degradation, acting as a break on the CDK5/APC/C^{cdh1} axis.[2] USP1 belongs to the class of Fanconi anemia proteins that are required for DNA repair of interstrand crosslinks and consequently for genome stability maintenance. FANCD1/BRCA2, another essential protein of the Fanconi anemia repair pathway, also plays a key role in the BRCA repair pathway, a safeguard against breast cancer, suggesting the existence of functional overlapping between the 2 machineries. USP1 stabilizes the inhibitor of differentiation ID2 and consequently preserves cellular stemness in undifferentiated osteosarcomas[19] therefore represents suitable targets for differentiation therapy of specific tumors.[3] Notably, a recent study reported that the expression of the USP1 target ID2 was directly associated with the Nottingham Prognostic Index, worsening clinical outcome and with worse disease-free and overall survival in human breast cancer.[18] In this study we unveiled a multifacet effect of CAPNS1 depletion in breast cancer biology, including a destabilizing effect of NUMB protein, a well known protein switch from symmetric to asymmetric cellular division.[13,10,8,12]

Results

CAPNS1 depletion in MCF7 and MCF10AT cells perturbs both anchorage dependent and independent growth

In order to investigate the effect of CAPNS1 depletion on anchorage dependent and independent growth of breast cancer cells, colony assays and soft agar assays were performed using both luminal type MCF7 and basal like MCF10AT cell line. CAPNS1 depleted MCF7 and MCF10AT cells and respective wild type controls were seeded on tissue culture plates and 2

weeks later the number of colonies was counted after staining with crystal violet. As it is shown in the representative pictures and in the graphs of Figure 1A and B, CAPNS1 depletion is coupled to a reduction of cellular growth on tissue culture plates. The effect of calpain on anchorage dependent growth of breast cancer cells confirms a previous study that demonstrated

an essential role for this protease in cell adhesion mediated by paxillin cleavage.[4]

Next, CAPNS1 depleted MCF7 and MCF10AT cells and respective controls were employed for soft agar assays according to standard procedures. Three weeks after cells seeding, pictures were taken and analyzed by Image J software. Typical
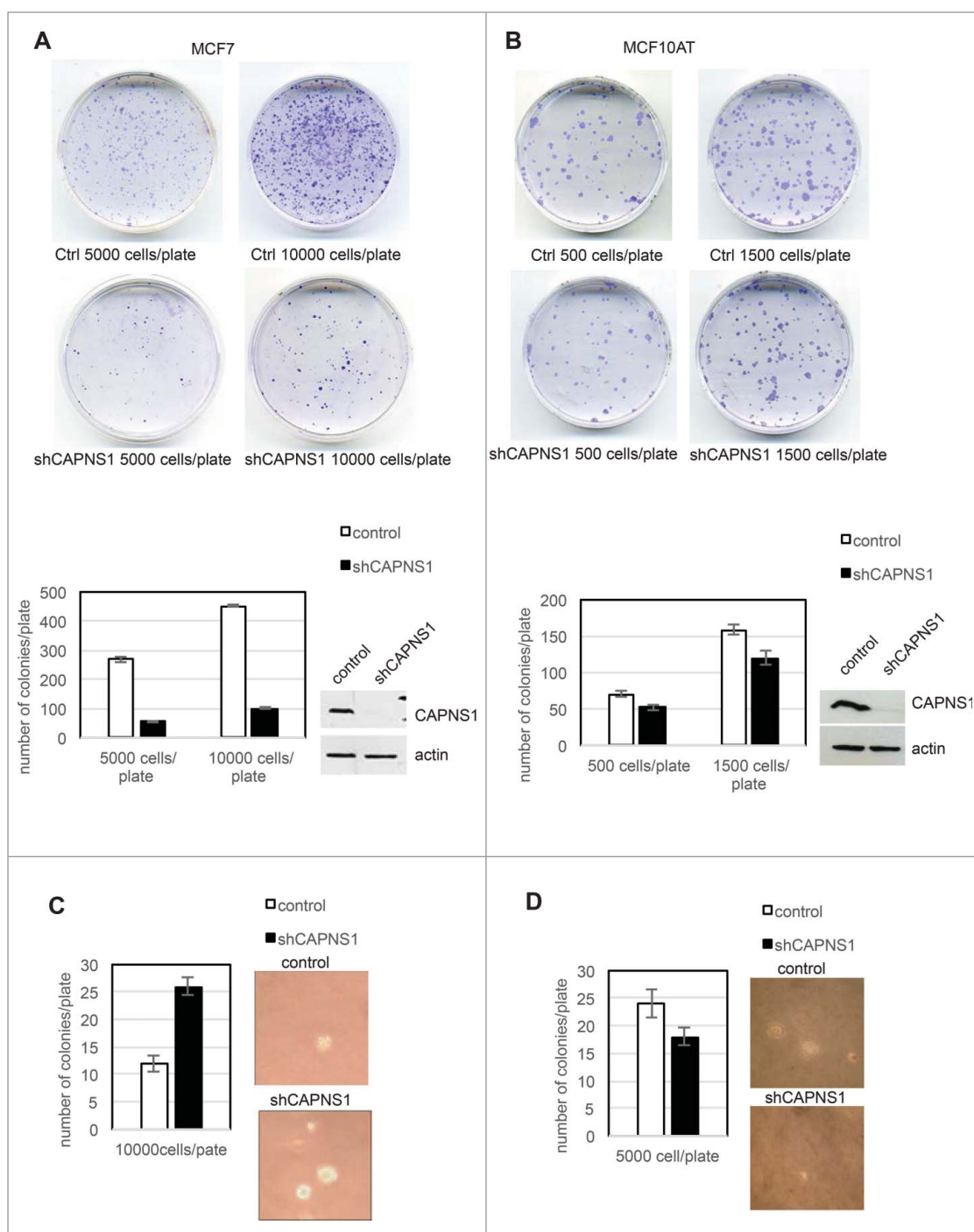

Figure 1. CAPNS1 depletion alters breast cancer cells growth on plate and in soft agar. Control and CAPNS1 depleted MCF7 cells (1A) or MCF10AT (1B) were plated on 6 cm dishes at the indicated concentration. Two weeks later, the cells were stained with crystal violet and images were acquired by Epson scanner. Images of representative experiments are shown. Colonies were counted using image J software; the graph reports the average of 3 independent experiments (p values <0.01). Control and CAPNS1 depleted MCF7 cells (1C) or MCF10AT (1D) were resuspended in 0.3 % agar and the indicated number of cells was plated on 1% agar according to standard procedures. Three weeks later colonies were counted. The graphs report the average number of colonies counted in 3 independent experiments (p values <0.01). Representative pictures are shown next to the graphs.

colonies are shown in Figure 1C, 1D, and the average number of colonies counted in 3 independent experiments are indicated in the graphs. CAPNS1 depletion enhances the growth of MCF7 in soft agar, while its loss impairs the growth of MCF10AT cells in the same semisolid medium. A similar outcome of CAPNS1 depletion on cell growth both on plates and in soft agar was reported for the highly metastatic AC2M2 mouse mammary cells.[6] It is not surprising that interfering with essential enzymes like calpain may produce opposite effects not only in different genetic settings, but also in alternative growing environments.

Calpain modulates mammary acini formation

To assess whether calpain may play a role in the maturation of mammary acini, we performed 3D studies using MCF-10A cells, a widely used model system for understanding epithelial cell biology. When plated in a mixture of collagen and laminin MCF10A cells form 3D structures that resemble acini structures of the human breast. The size of the acini is sharply reduced in CAPNS1 depleted cells as compared to control ones (Fig. 2A, C), although the number of acini is not affected (Fig. 2B). Staining with GM130, β-catenin and E-cadherin specific antibodies (Fig. 2D) revealed that the architecture of acini derived from CAPNS1 depleted cells is perturbed. These data suggest that calpain is required for the correct formation of the basic unit of breast epithelium and may play an important role in the initiation of the differentiation process in this system.

The same type of analysis was performed in MCF10AT cells, the Ras[v12] transformed derivative of MCF10A cells. In this system the differences between control and CAPNS1 depleted cells appear less evident, since also control cells have lost the capacity to form acini with well defined cavities, as already reported by others (Supplementary 1A, 1B).

To address the role of CAPNS1 in stem cell maintenance and differentiation in a more general context, we employed mice embryonic stem (ES) cells. CAPNS1 was knocked out by siRNA in mice ES cells prior the induction of differentiation and the kinetics of disappearance of stem cell markers was investigated by real time PCR. CAPNS1 depletion does not alter the kinetics of disappearance of stem cell markers, indicating that its depletion is not sufficient to affect differentiation in this system. However, CAPNS1 mRNA levels clearly decrease upon differentiation, just as the standard stem cell markers, OCT4 and SOX2 and NANOG (Fig. 2E). A similar behavior is observed for USP1 that is involved in a calpain-modulated axis in osteosarcoma and MEFs.[2]

Calpain modulates breast cancer stem cells compartment

Cancer stem cells are considered the fuel of cancer recurrence and therefore, a satisfactory chemotherapy must be effective also against this cancer reservoir. The assay of choice to assess the role of specific genes/pathways in stem cell maintenance/growth in vitro is the mammospheres formation assay. We first applied this methodology to MCF7 cells where CAPNS1 depletion is linked to a decrease of growth in 2D, but an increase of growth in soft agar. In this system CAPNS1 depletion is linked to an increase in mammosphere formation efficiency (Fig. 3B),
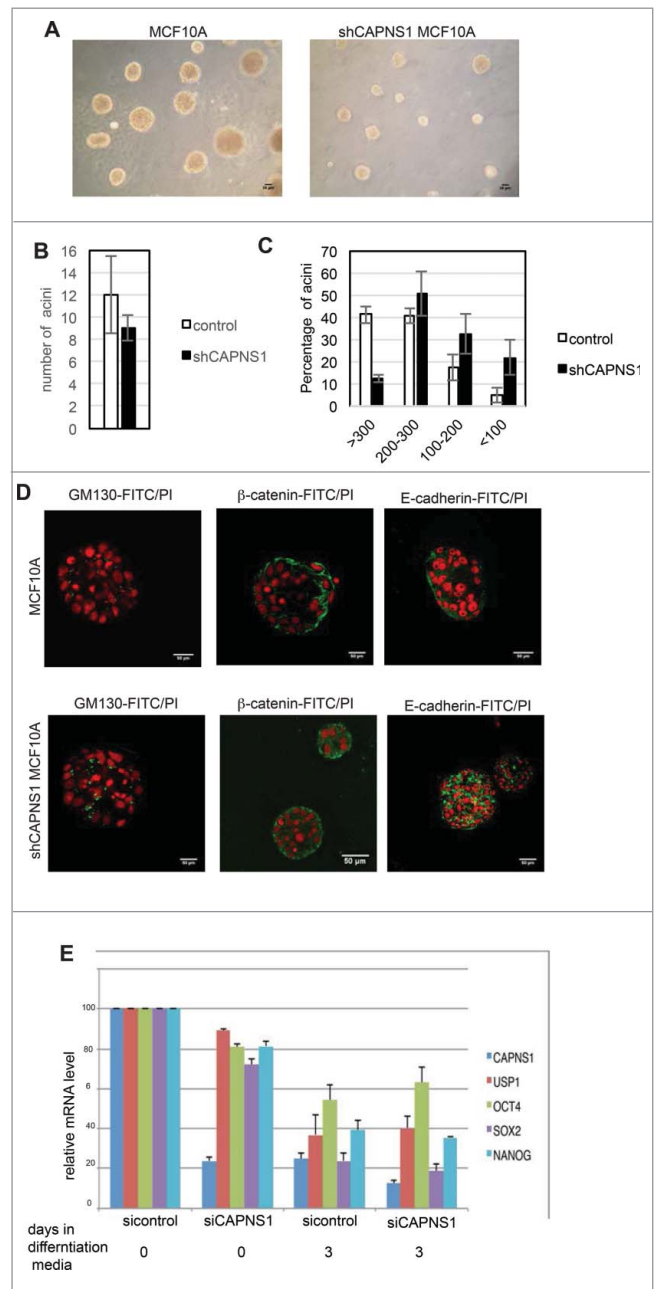

Figure 2. CAPNS1 depletion does not affect mammary acini number, but is involved in mammary acini growth and architecture. (A) Representative bright field pictures of control (left panel) and shCAPNS1 (right panel) MCF10A cells grown in 3D. Scale bar corresponds to 50 μm. (B) Average number of acini counted in 3 independent experiments (p value = 0.2). (C) Percentage of acini of different dimensions as indicated. The graph represent mean values obtained in 3 independent experiments (p values <0.01). (D) Representative immunofluorescence pictures of control (upper panels) and shCAPNS1 (lower panels) MCF10A cells grown in 3D, stained with the indicated antibodies. Scale bar corresponds to 50 μm. (E) Mouse embryonic stem cells were silenced with control siRNA or CAPNS1 specific siRNA and grown in differentiation media. The graph indicates the quantification of mRNA expression of the indicated transcripts by real time PCR analysis (p values <0.01).

and to an alteration of mammospheres shape that is less spheric respect to control (Fig. 3A).

Next, we applied mammosphere assay to MCF10AT cells where calpain depletion is coupled to a decrease of both anchorage dependent and independent growth. The shape of
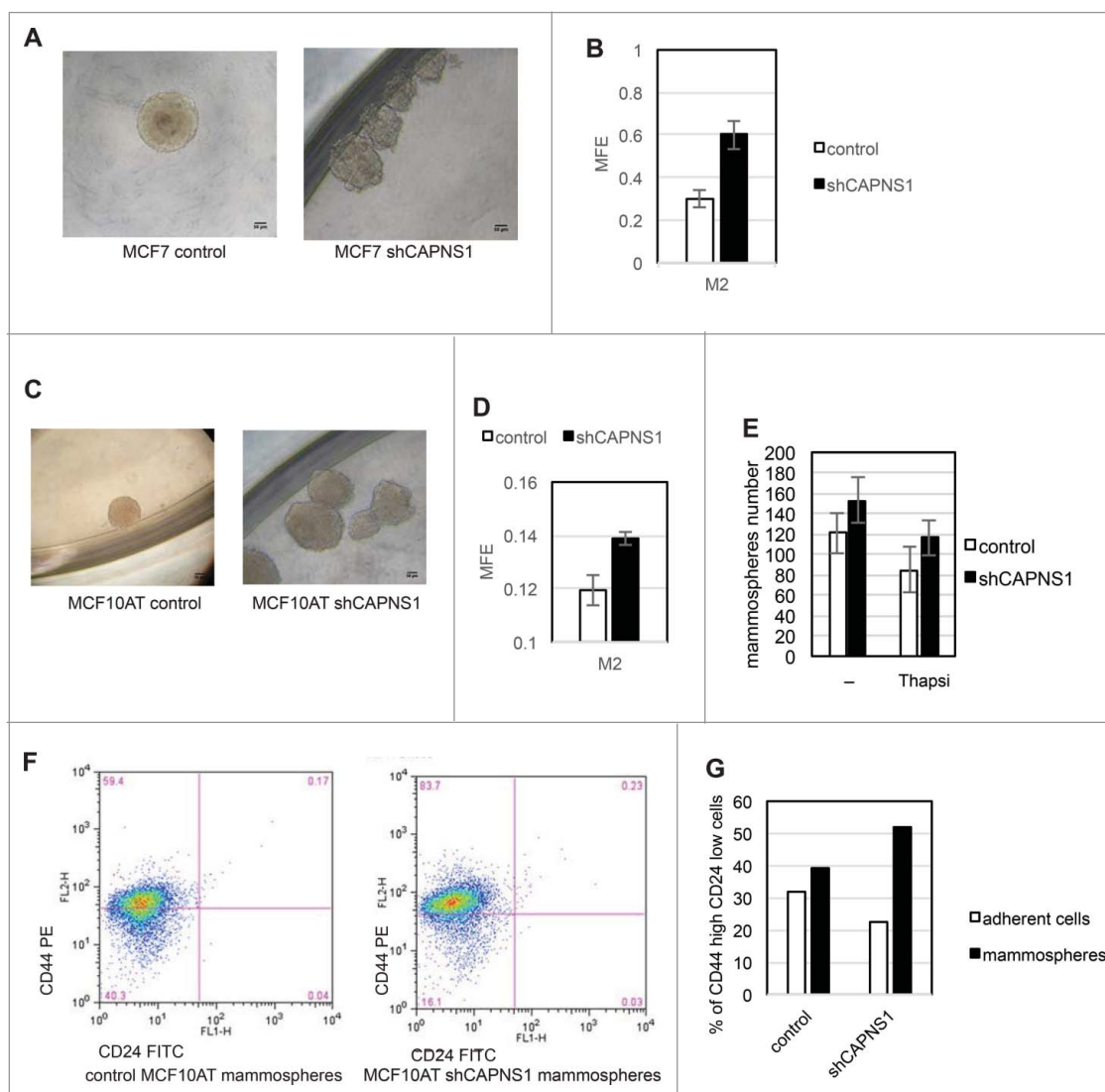
Figure 3. Calpain affects mammosphere forming efficiency. Control and CAPNS1 depleted MCF7 and MCF10AT cells were plated in 96 wells multiwell plates (1000 cells/well) in mammosphere specific medium. After ten days, the mammospheres were collected and disaggregated. Mammospheres derived cells were counted and plated as for the first generation and 7 d later picture were taken. (A) typical MCF7 mammospheres. Scale bar corresponds to 50 μm. (B) reports the average number of second generation MCF7 mammospheres obtained in 3 independent experiments (p values <0.01). (C) typical MCF10AT mammospheres. Scale bar corresponds to 50 μm. (D) reports the average number of second generation MCF10AT mammospheres obtained in 3 independent experiments (p values <0.01). (E) shows the average number of mammospheres counted in 3 independent experiments in control and shCAPNS1 MCF10AT treated or not treated with thapsigargin (p values<005). Briefly, control and CAPNS1 depleted MCF10AT cells were plated on 96 wells multiwells (1000 cells/well) in mammosphere specific medium. After 7 days, the mammospheres were incubated or not with 100 nM thapsigargin for 6 hours. Mammospheres derived cells were counted and plated as for the first generation and 7 d later the number of second generation mammospheres was counted. Control and CAPNS1 depleted MCF10AT cells derived from second generation mammospheres were stained with anti CD44 and anti CD24 antibodies and analyzed by FACS. Adherent cells were analyzed in parallel. The dot plot (F) and the graph (G) are the results of a typical FACS analysis.

mammospheres derived from CAPNS1 depleted cells is more irregular as compared to the shape of control mammospheres, as it is the case for MCF7 cells (Fig. 3C). Also in this system, CAPNS1 depletion is coupled to an increase in mammospheres formation efficiency (Fig. 3D). On the basis of these findings we hypothesized that calpain activation could hamper the expansion of the stem cell population. To verify this hypothesis, 100 nM thapsigargin was added for 6 hours to the first generation mammospheres to induce calcium release from the endoplasmic reticulum and activate calpain. Such treatment does not significantly affect cell viability, as monitored by a cell viability assay and FACS analysis performed 48 hours after treatment (Data not shown). Control and CAPNS1 depleted

MCF10AT cells were employed for a standard mammosphere formation assay. After counting the mammospheres of the first generation M1, the cells were either treated or not with 100 nM thapsigargin to activate calpain. Six hours later, the mammospheres number was counted again before harvesting and disaggregation. Afterwards, equal amounts of cells were seeded in mammosphere specific medium. The number of mammospheres in the subsequent generation, M2, decreases in thapsigargin treated cells, and the entity of the reduction in control cells is almost twice the reduction occurring in CAPNS1 depleted cells (Fig. 3E). Notably, calpain activation by ionomycin has the same effect of thapsigargin on mammosphere forming efficiency, and the calcium chelator BAPTA prevents such

effect (data not shown). These results show that transient calpain activation may limit stem cell expansion.

In order to further verify the increase of stem cell population in CAPNS1 depleted cells, parental adherent cells and mammospheres derived cells were collected and analyzed by FACS to evaluate the surface expression of the widely recognized staminality markers CD44 and CD24. Cells derived from mammospheres originated from CAPNS1 depleted cells are clearly more enriched in the CD24 low/CD44 high population as compared to control cells (Fig. 3F, G).

CAPNS1, a novel marker of breast cancer stem cells and mouse embryonic stem cells

CAPNS1 depleted MCF10AT cells and respective controls were sorted by FACS in order to isolate the CD44 high/CD24 low population from each cell line. An aliquot of sorted cells was utilized for nuclear/cytoplasmic fractionation and western blot analysis, and the remaining cells were employed for mammosphere formation assays. As expected, E-cadherin protein level is lower in sorted cells as shown in Figure 4A, indicating that epithelial-mesenchymal transition is taking place in CD44 high/CD24 low MCF10AT cells. Notably, as already observed for osteosarcomas and MEFs, full length USP1 (indicated by an arrow) decreases in CAPNS1 depleted cells. Interestingly, both calpain and USP1 are more abundant in the sorted CD44 high/CD24 low cell population, enriched in cancer stem cells. In particular, CAPN1 is present also in the nuclear compartment and USP1 is present also in the cytoplasmic compartment in the cancer stem cells enriched population. Our findings suggest that calpain and USP1 may be novel markers of breast cancer stem cells.

As already observed for unsorted cells, the CD44 high/CD24 low population derived from CAPNS1 depleted cells is characterized by an increase in first generation mammosphere forming efficiency (Fig. 4B). This result is in accordance with the higher surface expression of CD44 in CAPNS1 depleted sorted cells, shown in Figure 3F, G. The number of second generation mammospheres originated from CD44 high/CD24 low MCF10AT cells is unaffected by CAPNS1 depletion possibly due to exhaustion of stem cell potential. Indeed, the size of mammospheres originated from CAPNS1 depleted cells, is significantly larger, as quantified and reported in Figure 4C.

Calpain acts as a switch from symmetric to asymmetric division

On the basis of the data reported above, we hypothesized that calpain may be involved in the switch from symmetric division to asymmetric division at the onset of differentiation of human mammary cells. In order to investigate whether calpain is involved in this switch, we followed the distribution of the vital dye PKH26 during the growth of mammosphere originated from control cells and from CAPNS1 depleted cells. Two representative pictures are shown in Figure 4D and the quantification of the percentage of the surface of the mammospheres that retains PKH26 is shown in graph 4E. Notably, the surface of

stained mammospheres, that reflects the number of stained cells, is larger when CAPNS1 is depleted.

As a first approach to understand the molecular basis of the expansion in cancer stem cells coupled to CAPNS1 depletion, the levels of key proteins in cell extracts from adherent cells and mammospheres of the first and second generation were evaluated by western blot. As it is shown in Figure 4F, comparing adherent cells to mammospheres, E-cadherin protein levels decrease, while vimentin becomes more abundant both in control and CAPNS1 depleted cells, as expected when epithelial/mesenchimal transition is taking place. Notably, active beta-catenin, that positively modulates mammary stem cells long-term expansion, is more abundant in CAPNS1 depleted adherent and M1 cells as compared to the control counterparts, in accordance with the increase in cancer stem cells characteristics reported above for CAPNS1 depleted cells. Genotoxic stress was shown to activate p21 and consequently to induce symmetric division in mammary cancer stem cells, leading to the expansion of stem cell compartment.[7] Interestingly, p21 is more abundant in mammospheres from CAPNS1 depleted cells, as compared to control cells, further supporting the expansion of the stem cell compartment in CAPNS1 depleted mammospheres.

CAPNS1 reintroduction rescues the wild type phenotype and reduces stem cells expansion

To verify whether CAPNS1 reintroduction could rescue the phenotype observed in CAPNS1 depleted mammospheres, we produced a novel set of MCF10AT cell lines: a control cell line, a CAPNS1 depleted cell line and a CAPNS1 depleted cell line, expressing a CAPNS1 mRNA resistant to CAPNS1 silencing (Fig. 5A). Mammosphere formation assay was performed, confirming an increase in mammosphere formation efficiency in CAPNS1 depleted cells. Notably, CAPNS1 reintroduction is coupled to a reduction of mammosphere forming efficiency, further confirming that the expansion of the stem cell compartment observed in CAPNS1 depleted cells is dependent on CAPNS1 (Fig. 5B).

The three cell lines were further employed for mammosphere formation and staining with PKH26. Pictures were taken at subsequent time points, namely 3, 5, 7, 10 d after staining and seeding. Typical pictures are shown in Figure 5D. In order to quantify the number of PKH26 positive cells, FACS analysis was performed 9 days after staining (Fig. 5C). These novel sets of experiments further confirm that the number of cells retaining the PKH26 die negatively correlates with CAPNS1 protein level.

NUMB protein level is lower in CAPNS1 depleted cells

Numb is an essential modulator of the shift between symmetric and asymmetric division, therefore we evaluated NUMB protein level in CAPNS1 depleted MCF7, MCF10A and MCF10AT cells, as compared to control cells. NUMB level is lower in CAPNS1 depleted MCF7 cells, while it is apparently unaffected by CAPNS1 depletion in MCF10A and MCF10AT cells (Fig. 6A). However, analysis of nuclear
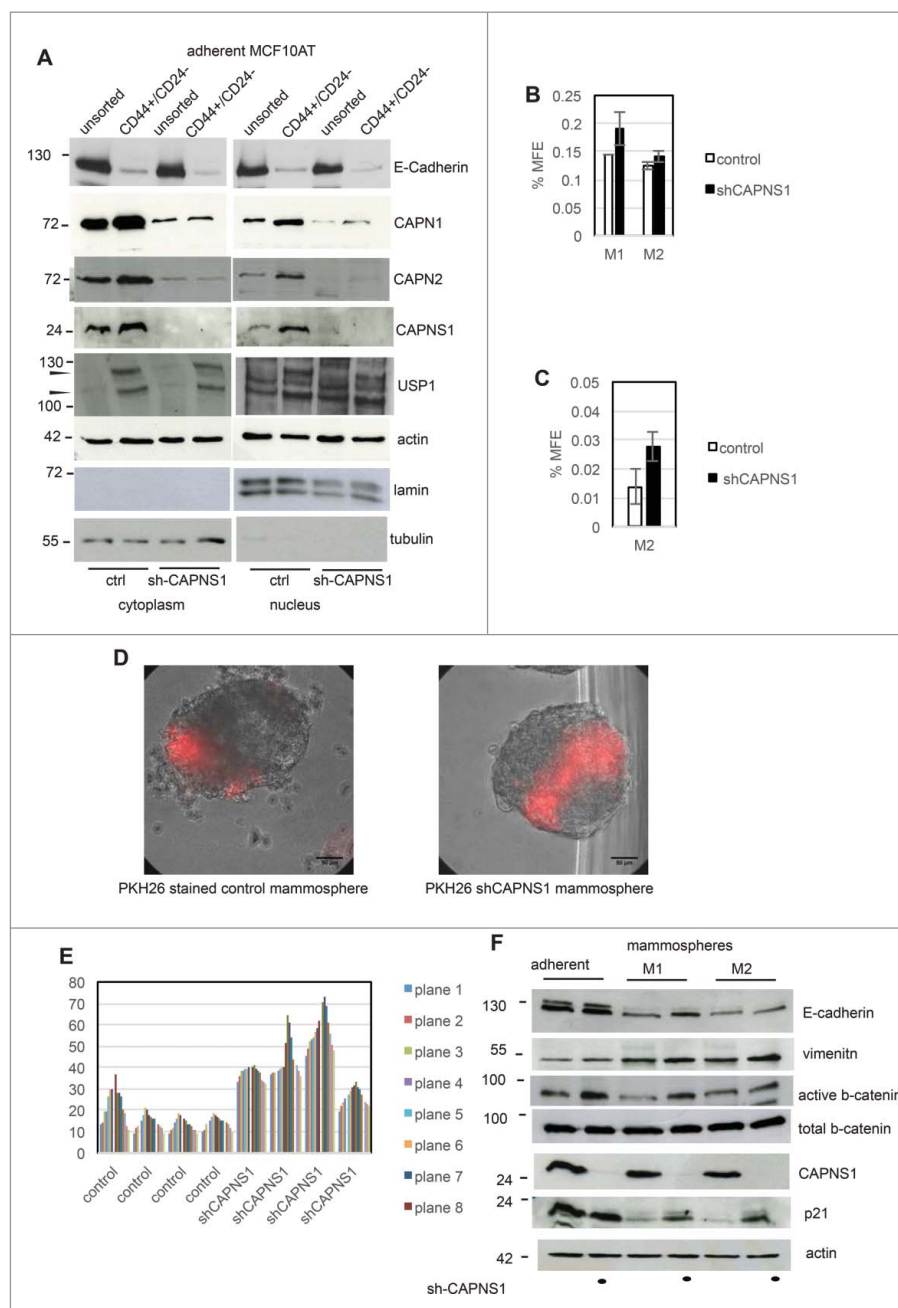
Figure 4. CAPNS1 depletion is coupled to breast cancer stem cells expansion.CD44+/CD24- population was sorted by FACS analysis from CAPNS1 depleted and control MCF10AT cells. Nuclear and cytoplasmic extracts obtained from sorted cells and analyzed by western blot with the indicated antibodies (A). In parallel, sorted CD44+/CD24- cells were utilized for mammosphere formation assay. (B) reports the average mammosphere forming efficiency for the first (M1) and second generation (M2) (p values <005). (C) reports the average MFE of second generation mammospheres with diameter larger than 250 micrometres (p values <005). (D, E) Control and shCAPNS1 MCF10AT were stained with PHK26 vital dye and after extensive washing were plated in mammosphere forming medium. Pictures were taken after 2 weeks. Scale bar corresponds to 50 μm. The percentage of PKH26 stained area of 4 planes of 4 control and 4 shCAPNS1 mammospheres was measured by Image J and is reported in the graph. (F) CAPNS1 depleted and control adherent MCF10AT cells and cells derived from first and second generation mammospheres derived from the same cells were lysed and analyzed by western blot with the indicated antibodies.

and cytoplasmic fractions of MCF10AT cells shows that NUMB protein level is lower in cytoplasms extracted from CAPNS1 depleted as compared to control ones (Fig. 6B). The decrease in NUMB protein level coupled to CAPNS1 depletion is sharper in the cytoplasms of CD44 high/CD24 low population (Fig. 6C).

Why the increase in the expansion of the stem cell compartment is sharper in MCF7 cells than in MCF10AT cells? We previously reported that CAPNS1 positively modulates

USP1 stability in osteosarcoma and MEFs. Since USP1 inhibition/depletion was shown to induce differentiation in various cellular contexts, we hypothesized that USP1 reduction might buffer the effect due to NUMB reduction.

CAPNS1 was transiently depleted in MCF10A, MCF10AT, MCF10CA1, MCF7 cells and USP1 level was evaluated by western blot. As expected, USP1 level decreases in MCF10A and MCF10AT cells, upon CAPNS1 depletion, but it is unaffected in MCF7 cells.
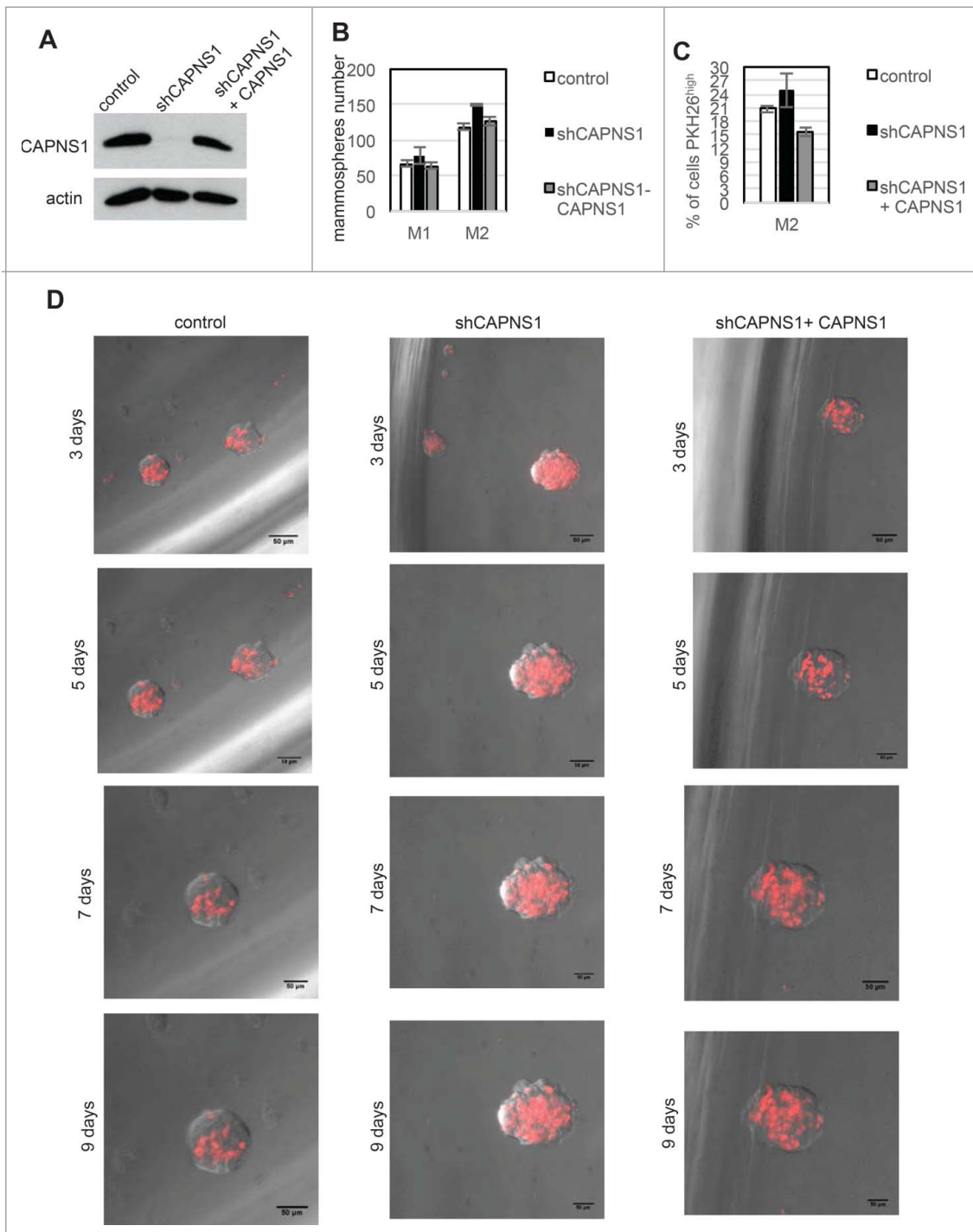
Figure 5. CAPNS1 depletion is linked to expansion of PKH26 stained cells that can be rescued upon CAPNS1 reintroduction. (A) CAPNS1 expression in MCF10AT cell lines: control MCF10AT, shCAPNS1 MCF10AT, shCAPNS1 MCF10AT stably expressing siRNA resistant CAPNS1. (B) Average number of mammosphere number obtained in 3 independent experiments with MCF10AT derived cell lines described above (p values <005). (C) Average of PKH26 stained cells in mammospheres obtained in 3 independent experiments (p values <005). (D) Subsequent pictures taken 3, 5, 7, 9 d after seeding of representative mammosphere obtained from the above described cell lines. Scale bar corresponds to 50 μm.

Discussion

CAPNS1 depletion is coupled to a reduction of growth on plates in both epithelial MCF7 and basal like MCF10AT cancer cells. On the other hand, CAPNS1 depletion has opposite effects on soft agar growth of MCF10AT and MCF7 and suggest that when cancer cells bypass the first environmental barrier and become able to grow in an anchorage independent manner, the overall role of calpain may vary in different genetic settings. The positive effect of CAPNS1 on MCF10AT cells growth in soft agar is in accordance with the previously reported negative role of APC/C^{cdh1} in the same experimental
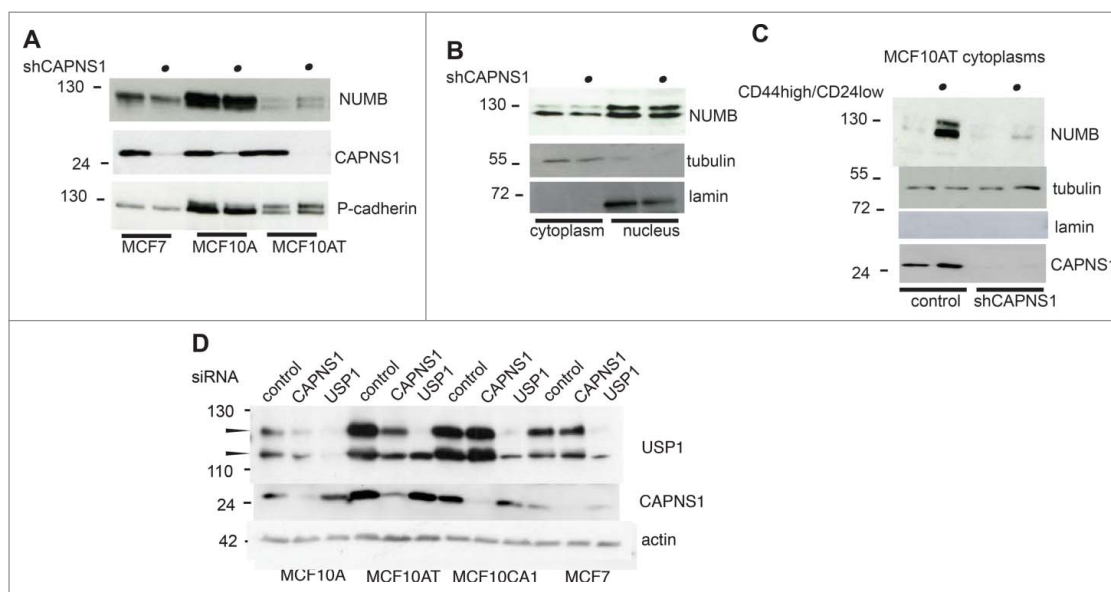
Figure 6. CAPNS1 depletion is coupled to a decrease in NUMB protein level.NUMB protein level was compared by western blot in CAPNS1 depleted versus control cells, using total cell lysates of MCF7, MCF10A and MCF10AT cells (A) nuclear and cytoplasmic extracts of MCF10AT cells (B) and cytoplasms from CD44 high/CD24 low sorted MCF10AT cells (C). (D) CAPNS1 specific, USP1 specific or a control siRNA were transfected in the indicated cell lines. 48 hours later, lysates were analyzed by western blot to monitor USP1 and CAPNS1 levels. Actin was used as loading control.

system.[5] Indeed, calpain negatively modulates APC/C^{cdh1}[2,11] and therefore in CAPNS1 depleted cells, APC/C^{cdh1} is more active and growth results impaired.

The negative effect of CAPNS1 depletion on the growth of MCF10AT cells demonstrated by colony and soft agar assays is in accordance with the results obtained by Wai Chi-Ho et al. in ACM2 cells.[6] Interestingly, they demonstrate that while CAPN2 knockout reduced tumor growth in a breast tumor engraftment model, lung metastasis was not affected by CAPN2 depletion and the percentage of mice with metastasis in the 2 reported experiments was higher when CAPN2 depleted cells were injected. This result is in agreement with our finding on the expanded cancer stem cell compartment in CAPNS1 depleted MCF7 and MCF10AT cells. Accordingly, we have shown that calpain activation reduces the expansion of this compartment in a calpain dependent manner. Cancer stem cells are resistant to standard therapies that reduce the bulk of the tumor. Thus new therapies specifically targeting this tumor reservoir are warranted.

Altogether previously published data and our findings highlight a role of calpain as a master director of cellular architecture and cell fate decision. In this study we have also demonstrated by mammosphere formation assays, western blot and FACS analysis of breast cancer stem cell markers that calpain depletion increases the amplification of the breast cancer stem cell compartment. The vital dye PKH26 used to stain the individual cancer stem cells is inherited by a larger number of daughter cells when CAPNS1 is depleted, indicating a longer persistence of symmetric division. Accordingly, NUMB protein, a master regulator of the shift between symmetric to asymmetric division that is coupled to differentiation, is reduced in CAPNS1 depleted cells.

Materials and methods

Chemicals and reagents

Thapsigargin and PKH26 were bought from Sigma-Aldrich. Lipofectamine™ RNAiMAX from Invitrogen. USP1 specific siRNA with the following sequence: AACCCUAUGUAU-GAAGGAUAU was purchased from Eurofins Mwg/Operon. RNAi oligonucleotides specific for CAPN1, Cdk5 and cdh1 were purchased from Santa Cruz Biotechnology. CAPN2 RNAi and SMARTpool for CAPNS1 silencing were purchased from DHARMACON, Inc., Dallas, TX (USA). AllStars Negative Control siRNA (Qiagen) was used as negative control.

Cell culture and transfections

MCF-7 cells were grown in Eagle' s Minimum Essential Medium supplemented with 10% fetal calf serum, 1% Penicillin/Streptomycin (Lonza) and Non essential Amino Acid Solution 100X (Sigma). MCF10A and MCF10AT cells were cultured in DMEM:F12 media (1:1) supplemented with 10μg/ml Insulin (Sigma), 20ng/ml EGF (PEPROTECH), 500ng/ml hydrocortisone (Sigma), 5% horse serum, 10U/ml Penicillin, 100μg/ml Streptomycin and 1% HEPES (Gibco). MCF10CA1 were cultured in DMEM:F12 media (1:1) supplemented with 10% foetal calf serum, 1% Penicillin/Streptomycin (Lonza). MDA-MB231 and MDA-MB468 were grown in Dulbecco's modified Eagle's Medium (DMEM) supplemented with 10% foetal calf serum, 1% Penicillin/Streptomycin (Lonza). SKBR3 cells were grown in RPMI supplemented with 10% foetal calf serum, 1% Penicillin/Streptomycin (Lonza). Mouse embryonic stem (ES) cells were cultured on 0.2% gelatin-coated plates in mESC self-renewal medium: Dulbecco's modified Eagle's

medium (DMEM) supplemented with 15% knockout serum replacement (Gibco), 1% nonessential amino acids (Gibco), 1 mM sodium pyruvate (Invitrogen), 0.1 mM ß-mercaptoethanol, 1% penicillin/streptomycin (Invitrogen), and 1,000 U/ml mouse leukemia inhibitory factor (LIF). All cells were grown in 5% CO_2 at 37°C in a humidified incubator. MCF10A, MCF10AT, MCF10CA1 (obtained from Karmanos Cancer Institute, US), MCF-7, MDA-MB-231, MDA-MB468 and SKBR3 cells at 60–80% confluence, and ES cells at low confluence were transiently oligofected using Lipofectamine RNAi-MAX (Invitrogen) according to the manufacturer's instructions.

Viral constructs

shCAPNS1 was obtained by annealing the following sense oligonucleotide: 5′- GAT CCC CGC CAC AGA ACT CAT GAA CAT TCA AGA GAT GTT CAT GAG TTC TGT GGC TTT TTA - 3′ to the following antisense oligonucleotide: 5′ - AGC TTA AAA AGC CAC AGA ACT CAT GAA CAT CTC TTG AAT GTT CAT GAG TTC TGT GGC GGG G - 3′. The annealed product was inserted by standard procedures in pRetroSuper vector, previously linearized by BglII and HindIII digestion, and checked by sequencing.

Cell infections

293GP packaging cells were transfected with the calcium-phosphate method with pRetroSuper-shCAPNS1 or vector alone, after 72 hours the supernatant was harvested, filtered and added to MCF10AT or MCF-7 cells. The infected cells were selected by the addition of puromycin and after 7 d the expression of CAPNS1 was checked by western blot.

Colony formation assay

Cells were seeded at 1000 cells/ml and 2000 cells/ml for MCF-7 and 100 cells/ml and 300 cells/ml for MCF10AT in a 21 cm^2 cell culture dish and incubate at 37°C in a humidified, 5% CO_2 atmosphere. After incubation for 15 days, cell culture plates containing colonies were gently washed with PBS twice, fixed with 4% paraformaldehyde for 20 minutes at room temperature and stained with 0.5% Crystal violet. Excess stain was removed by washing repeatedly with PBS and colonies were counted. For quantification, the colonies were analyzed using ImageJ software. Three reduplicate dishes were used from each condition.

Soft-agar assay

To evaluate anchorage-independent growth, 5×10^3 and 1×10^4 MCF-7 cells and MCF10AT were resuspended in 0.3% agarose in growth media. Cells were plated on a solidified bed of 1% agarose in growth media in 21 cm^2 plates. Plates were incubated for 3 weeks at 37°C. Bright field images of MCF-7 and MCF10AT colonies were taken using a 10× objective. The number of colonies per field was counted using ImageJ software. The experiments were conducted in triplicate.

Three dimensional culture

3D culture was carried out based on the method as already described by others.[9] Briefly, 12 mm round glass coverslips were coated with 80 μl of ice-cold rBM (Cultrex) and incubated at 37°C for 20 minutes to allow rBM to solidify. The coated coverslips were placed in a 24-well plate with the rBM facing up. Single cell suspensions containing 7000 cells/well for MCF10A and 5000 cells/well for MCF10AT, were resuspended in 250μl of complete growth medium with 2% (v/v) of Cultrex and plated on top of the rBM coated chamber slides and incubated at 37°C for 30 minutes to let the cells attach. Then 250μl of the assay medium was added per well and the cells were cultured al 37°C and 5% CO_2 for 3 weeks, with the medium being changed every 3 d.

Immunostaining and microscopy

The three-dimensional structures in rMB Cultrex were fixed in 4% paraformaldehyde at room temperature for 20 minutes, permeabilized with 1% Triton X-100 in PBS for 15 minutes and washed with 100 mM glycine in PBS, 3 times at 10 min/wash. After the 3-dimensional structures were blocked with IF (immunofluorescent) blocking buffer (0.1% BSA, 0.2% Triton X-100, 0.05% Tween 20, 7.7 mM NaN_3, in PBS) containing 10% normal goat serum for 1h and incubated overnight at 4°C with the following primary antibodies: anti-GM130 (BD Biosciences), anti-E-cadherin (Takara bio) and anti-βcatenin (Santa Cruz). Samples were then washed with IF buffer (0.1% BSA, 0.2% Triton X-100, 0.05% Tween 20, 7.7 mM NaN_3, in PBS) 3 times at 20 min/wash and stained with secondary antibody for 1h at room temperature. This was followed by 3 washes with IF buffer at 10 min each. To stain the nuclei, the slides were incubated with RNase 200μg/ml for 15 min at room temperature and then stained with Propidium Iodide 25μg/ml for 5 min at room temperature, washed 3 times with PBS and mounted on glass coverslips. Confocal microscopic images of the acinus structures were captured by the Z-stacking function for serial confocal sectioning (LSM-510 META confocal microscope) and then analyzed by ImageJ software. The experiments were conducted in triplicate.

Mammosphere cultures

To generate mammospheres, confluent monolayers cells were trypsinized, counted and plated as single suspension (1000 cells/well) in a low attachment plates (Corning) and grown in non-adherent culture conditions, as described in Dontu et al, 2003. MCF10AT cells were grown in a serum-free mammary epithelial growth medium (MEBM) (Lonza) supplemented with 2 % of B27 (Invitrogen), 20 ng/mL hEGF (PEPROTECH), 20 ng/mL bFGF (Provitro), and 4 μg/mL heparin (Sigma), 10 ng/ml hydrocortisone (Sigma) and 5 μg/ml Insulin (Sigma) and 1% Penicillin/Streptomycin (Lonza) while MCF-7 cells were grown in a serum-free mammary epithelial growth medium (MEBM) supplemented with B27 (Invitrogen), 20 ng/mL hEGF (PEPROTECH) 5 μg/ml Insulin (Sigma) and 1% Penicillin/ Streptomycin (Lonza). Primary mammospheres after 10 d were collected by gentle centrifugation (800 rpm) and dissociated enzymatically to be re-seeded to obtain

secondary mammospheres. The number of mammospheres ($\geq 250 \ \mu$m) per well was then counted and percentages of mammospheres forming efficiencies (% MFE) was calculated as a number of mammospheres divided by the plated cell number and multiplied for a hundred.

PKH26 assay

Primary mammospheres were collected and dissociated enzymatically, resuspendend in PBS and labeled with PKH26 (Sigma) 10^{-7} M for 5 min. To stop the staining, an equal volume of serum was added to the cells and incubated for 1 minute to allow binding of excess dye. Labeled cells were re-plated (1000cells/well) in ultralow attachment plates in mammospheres culture medium to obtain secondary mammospheres. After 10 days, secondary mammospheres were analyzed by confocal microscopy.

Drug treatments

Cells in 3D culture and primary mammospheres were treated with 100nM thapsigargin. For cells in 3D culture, the drug was added after a week and replaced every 3 days, while for primary mammospheres, 100nM of thapsigargin was added 6h before collection, dissociation, and re-seeding to obtain secondary mammospheres.

Flow cytometric analysis and cell sorting

Single cell suspension of adherent cells or mammospheres was stained with CD24-FITC (BD Biosciences) and CD44-PE (BD Biosciences). Appropriate isotype controls were used to set the threshold for CD44 and CD24 positive cells. Cells were incubated with the appropriate antibodies at room temperature in the dark for 30 minutes, then washed with PBS and finally resuspended in 500μL of PBS. 10,000 cells were analyzed for each condition using a FACSCalibur flow cytometer (BD Biosciences); data were analyzed using FlowJo software (Tree Star, Ashland, USA).

To separate CD44^{high}/CD24^{low} MCF10AT cells, flow cytometric cell sorting was performed on single-cell suspensions previously stained with CD44 and CD24 antibody.

Quantitative Real Time PCR (qRT-PCR) analysis of ES cells

ES cells were transiently transfected using Lipofectamine RNAiMAX (Invitrogen) according to the manufacturer's instructions, using a control siRNA (AllStars Negative Control siRNA, Qiagen) or a siRNA targeting mouse CAPNS1 (5′ - CAGGCTATATACAAACGCTTT - 3′). 72 hours later, ES cells were re-seeded and subjected to a second round of siRNA silencing, and grown for 72 hours in mESC differentiation medium: DMEM supplemented with 15% ES cell certified serum (Invitrogen), 1% non-essential amino acids (Gibco), 1 mM sodium pyruvate (Gibco), 0.1 mM ß-mercaptoethanol and 1% penicillin/streptomycin (Lonza).

For quantitative real-time PCR, total RNA from ES cells was purified using QIAzol lysis reagent (Qiagen). 1.5 μg of total RNA was treated with DNase (RQ1, Promega) and subjected to reverse transcription in the presence of random primers (Promega) or oligo dT primers using SuperScriptIII Reverse Transcriptase (Invitrogen) according to the manufacturer's suggestions. Quantitative real-time PCR was performed on StepOnePlus real-time PCR machine (Applied Biosystems), using SYBR Green Universal PCR Master Mix (Applied Biosystems) and the following oligonucleotides targeting mouse genes: CAPNS1 for TTCATCAGCTGCTTGGTCAG, rev AGC-CACTCCTGGATGTTCAC; USP1 for CATTTGAAGTGC TTTGCTGCT, rev CTTGGAAAGTCCACCACCAT; Gapdh: for TTCACCACCATGGAGAAGGC, rev CCCTTTTGGC TCCAC; Nanog for TTCTTGCTTACAAGGGTCTGC, rev AGAGGAAGGGCGAGGAGA; Oct4 for CAGGGACACCT TTCCCAGGG, rev TTTAAGAACAAAATGATGAG; Sox2 for TGCTGCCTCTTTAAGACTAGGG, rev TCGGGCTCCAAAC TTCTCT.

Quantitative RT (qRT-pCR) was performed in triplicate and relative expression levels were normalized to controls by using the comparative Ct ($\Delta\Delta$Ct) method, using Gapdh mRNA as internal control.

Western blot analysis

Western blotting was performed on cells protein lysates (50 mM Tris-HCl pH 7.5; 150 mM NaCl, 5 mM EDTA, 1% Triton X-100, 0.5 mM NaF, 1 mM Sodium orthovanadate, complete protease inhibitor cocktail Sigma-Aldrich). When specified, nuclear and cytoplasmic extracts were prepared using nuclear and cytoplasmic extraction reagents (ThermoScientific) according to manufacturer instructions. Lysates were clarified by centrifugation for 15 min at 4°C and protein concentrations were assessed using Bradford protein assay (BioRad Laboratories). Samples containing equal amounts of protein were boiled in SDS sample buffer, resolved using SDS-PAGE (15-20 μg protein per lane) and transferred to nitrocellulose membranes. The blots were then probed with the following antibodies: anti-β-catenin active (Abcam), anti-E-cadherin (Takara bio), anti-Capns1, anti-Capn2, anti-sβ-catenin, anti-α Actin (Sigma-Aldrich), anti-Capn1, anti-p21, anti-p53, anti-β-catenin, anti-Cdc27, anti-Cdc6 (Santa Cruz), anti-cdh1 (Calbiochem), anti-USP1 (Bethyl Laboratories) and anti-vimentin (BD Biosciences), overnight at 4°C, then washed, incubated with horseradish peroxidase-conjugated secondary antibodies (Sigma), and analyzed by enhanced chemiluminescence

Statistical analysis

Results are expressed as means $\pm$ standard deviations of at least 3 independent experiments. Statistical analysis was performed using Student's t test with the level of significance set at $P < 0.05$.

Disclosure of potential conflicts of interest

No potential conflicts of interest were disclosed.

References

1. Bertoli C, Copetti T, Lam EW, Demarchi F, Schneider C. Calpain small-1 modulates Akt/FoxO3A signaling and apoptosis through PP2A. Oncogene 2009; 28:721–33; PMID:19029949; http://dx.doi.org/10.1038/onc.2008.425

2. Cataldo F, Peche LY, Klaric E, Brancolini C, Myers MP, Demarchi F, Schneider C. CAPNS1 regulates USP1 stability and maintenance of genome integrity. Mol Cell Biol 2013; 33:2485–96; PMID:23589330; http://dx.doi.org/10.1128/MCB.01406-12

3. Chen J, Dexheimer TS, Ai Y, Liang Q, Villamil MA, Inglese J, Maloney DJ, Jadhav A, Simeonov A, Zhuang Z, Selective and cell-active inhibitors of the USP1/ UAF1 deubiquitinase complex reverse cisplatin resistance in non-small cell lung cancer cells. Chem Biol 2011; 18:1390–400; PMID:22118673; http://dx.doi.org/10.1016/j.chembiol.2011.08.014

4.. Cortesio CL, Boateng LR, Piazza TM, Bennin DA, Huttenlocher A. Calpain-mediated proteolysis of paxillin negatively regulates focal adhesion dynamics and cell migration. J Biol Chem 2011; 286:9998–10006; PMID:21270128; http://dx.doi.org/10.1074/jbc.M110.187294

5.. Fujita T, Liu W, Doihara H, Date H, Wan Y. Dissection of the APCCdh1-Skp2 cascade in breast cancer. Clin Cancer Res: An Off J Am Assoc Cancer Res 2008; 14:1966–75; PMID:18381934; http://dx.doi.org/10.1158/1078-0432.CCR-07-1585

6.. Ho WC, Pikor L, Gao Y, Elliott BE, Greer PA. Calpain 2 regulates Akt-FoxO-p27(Kip1) protein signaling pathway in mammary carcinoma. J Biol Chem 2012; 287:15458–65; PMID:22427650; http://dx.doi.org/10.1074/jbc.M112.349308

7.. Insinga A, Cicalese A, Faretta M, Gallo B, Albano L, Ronzoni S, Furia L, Viale A, Pelicci PG. DNA damage in stem cells activates p21, inhibits p53, and induces symmetric self-renewing divisions. Proc Natl Acad Sci U S A 2013; 110:3931–6; PMID:23417300; http://dx.doi.org/10.1073/pnas.1213394110

8.. Kechad A, Jolicoeur C, Tufford A, Mattar P, Chow RW, Harris WA, Cayouette M. Numb is required for the production of terminal asymmetric cell divisions in the developing mouse retina. J Neurosci: Off J Soc Neurosci 2012; 32:17197–210; PMID:23197712; http://dx.doi.org/10.1523/JNEUROSCI.4127-12.2012

9.. Lee GY, Kenny PA, Lee EH, Bissell MJ. Three-dimensional culture models of normal and malignant breast epithelial cells. Nat Methods 2007; 4:359–65; PMID:17396127; http://dx.doi.org/10.1038/nmeth1015

10. Lerner RG, Petritsch C. A microRNA-operated switch of asymmetric-to-symmetric cancer stem cell divisions. Nat Cell Biol 2014; 16:212–4; PMID:24576899; http://dx.doi.org/10.1038/ncb2924

11. Maestre C, Delgado-Esteban M, Gomez-Sanchez JC, Bolanos JP, Almeida A. Cdk5 phosphorylates Cdh1 and modulates cyclin B1 stability in excitotoxicity. EMBO J 2008; 27:2736–45; PMID:18818692; http://dx.doi.org/10.1038/emboj.2008.195

12. Rennstam K, McMichael N, Berglund P, Honeth G, Hegardt C, Ryden L, Luts L, Bendahl PO, Hedenfalk I. Numb protein expression correlates with a basal-like phenotype and cancer stem cell markers in primary breast cancer. Breast Cancer Res Treat 2010; 122:315–24; PMID:19795205; http://dx.doi.org/10.1007/s10549-009-0568-x

13. Shen Q, Zhong W, Jan YN, Temple S. Asymmetric Numb distribution is critical for asymmetric cell division of mouse cerebral cortical stem cells and neuroblasts. Development 2002; 129:4843–53; PMID:12361975

14. Sorimachi H, Hata S, Ono Y. Expanding members and roles of the calpain superfamily and their genetically modified animals. Exp Anim 2010; 59:549–66; PMID:21030783; http://dx.doi.org/10.1538/expanim.59.549

15. Storr SJ, Carragher NO, Frame MC, Parr T, Martin SG. The calpain system and cancer. Nat Rev Cancer 2011a; 11:364–74; PMID:21508973; http://dx.doi.org/10.1038/nrc3050

16. Storr SJ, Woolston CM, Barros FF, Green AR, Shehata M, Chan SY, Ellis IO, Martin SG. Calpain-1 expression is associated with relapse-free survival in breast cancer patients treated with trastuzumab following adjuvant chemotherapy. Int J Cancer. J Int du Cancer 2011b; 129:1773–80; PMID:21140455; http://dx.doi.org/10.1002/ijc.25832

17. Storr SJ, Lee KW, Woolston CM, Safuan S, Green AR, Macmillan RD, Benhasouna A, Parr T, Ellis IO, Martin SG. Calpain system protein expression in basal-like and triple-negative invasive breast cancer. Ann Oncol: Off J Euro Soc Med Oncol/ESMO 2012; 23:2289–96; PMID: 22745213; http://dx.doi.org/10.1093/annonc/mds176

18. Wazir U, Jiang WG, Sharma AK, Newbold RF, Mokbel K. The mRNA expression of inhibitors of DNA binding-1 and -2 is associated with advanced tumour stage and adverse clinical outcome in human breast cancer. Anticancer Res 2013; 33:2179–83; PMID:23645773

19. Williams SA, Maecker HL, French DM, Liu J, Gregg A, Silverstein LB, Cao TC, Carano RA, Dixit VM. USP1 deubiquitinates ID proteins to preserve a mesenchymal stem cell program in osteosarcoma. Cell 2011; 146:918–30; PMID:21925315; http://dx.doi.org/10.1016/j.cell.2011.07.040